AN ABSTRACT OF THE DISSERTATION OF

Yong Zhang for the degree of Doctor of Philosophy in Molecular and Cellular Biology presented on November 29, 2007.
Title: Some Potential Mechanisms for Finely-tuned Regulation of Phospholipase C-β Isozymes: Studies of Dimerization and Phosphatidylinositol 3,4,5-Trisphosphate Activation

Abstract approved: _____
Theresa M. Filtz

Phospholipase C-β (PLC-β) isozymes are key effectors in G protein-coupled signaling pathways. Prior research suggested that some isoforms of PLC-β may exist and function as dimers, but little is known about dimerization of PLC-β. Data from co-immunoprecipitation assays of differentially-tagged PLC-β constructs and size-exclusion chromatography of native PLC-β support homodimerization of PLC-β3 and PLC-β1 isozymes, but not heterodimerization of these isozymes. Size-exclusion chromatography data also suggest that PLC-β3 and PLC-β1 form higher affinity homodimers than PLC-β2. Evidence supportive of limited PLC-β monomer-homodimer equilibrium appears at 100 nM and lower. Further assessment of homodimerization status by co-immunoprecipitation assays with differentially-tagged PLC-β3 fragments demonstrated that at least two subdomains of PLC-β3 are involved in dimer formation, one in the catalytic X and Y domains, and the other in the G protein-regulated carboxy-terminal domain. Additionally, microscopic fluorescence

resonance energy transfer assays provide evidence consistent with the existence of PLC-β homodimers in a whole cell context.

Phosphatidylinositol 3,4,5-trisphosphate (PIP_3) has been proposed as a second messenger that affects a variety of cellular responses. Previously, we had shown that PLC-β1 and PLC-β3 bound immobilized PIP_3. In this study, PIP_3 was found to potentiate Ca^{2+}-stimulated PLC-β activities using an *in vitro* reconstitution assay. LY294002, a specific PI 3-kinase inhibitor, significantly inhibited 10 minutes agonist-stimulated total IP accumulation. Both LY294002 and wortmannin inhibited 90 seconds agonist-stimulated IP_3 accumulation in intact cells. Moreover, transfected p110CAAX, a constitutively activated PI 3-Kinase catalytic subunit, increased 90 seconds oxytocin-stimulated IP_3 accumulation. Receptor-ligand binding assays indicated that LY294002 did not affect G protein-coupled receptors directly, suggesting a physiological role for PIP_3 in directly potentiating PLC-β activity. When co-expressed with p110CAAX, fluorescence-tagged PLC-β3 was increasingly localized to the plasma membrane. Conversely, a greater proportion of PLC-β3 associated with cytosolic fraction following H9c2 cells treatment with LY294002. Additional observations suggest that the C-tail domain of PLC-β1 and β3, not the PH or catalytic XY domain, is important for membrane association.

Some Potential Mechanisms for Finely-tuned Regulation of Phospholipase C-β Isozymes: Studies of Dimerization and Phosphatidylinositol 3,4,5-Trisphosphate Activation

by
Yong Zhang

A DISSERTATION

submitted to

Oregon State University

in partial fulfillment of
the requirements for the
degree of

Doctor of Philosophy

Presented November 29, 2007
Commencement June 2008

Doctor of Philosophy dissertation of Yong Zhang presented on November 29, 2007.

APPROVED:

Major Professor, representing Molecular and Cellular Biology

Director of the Molecular and Cellular Biology Program

Dean of the Graduate School

I understand that my dissertation will become part of the permanent collection of Oregon State University libraries. My signature below authorizes release of my dissertation to any reader upon request.

Yong Zhang, Author

ACKNOWLEDGEMENTS

First and foremost, I would like to thank Dr. Theresa M. Filtz for being my advisor and role-model. From her, I learned how to be a scientist, a teacher and parent, which will be extremely important for my future career and life. Emphatic thanks to the rest of my committee, Dr. Jeffrey Greenwood, Dr. Mark Leid, Dr. Michael Schimerlik, Dr. Paul Murtaugh, Dr. Claudia Maier and Dr. Lan Xue for their invaluable support and feedback during this process.

I would like to express my sincere appreciation to Dr. Walter K. Vogel, Dr. Jeniffer S. McCullar, Dr. Shannon Long, Kristi Crofoot and Sun Hyung Kwon for their technical assistance and discussion.

A special thanks to College of Pharmacy and the Molecular and Cellular Biology office staff who keep things running and standing behind their students, especially Debra Peters, Rosa Hill and Gail Millimaki.

This work was supported by the Pharmaceutical Research and Manufacturer's Association Foundation (to TMF), and the National Institutes of Health grant R01-GM61244 (to TMF). I also appreciate the support of Oregon Sports Lottery Scholarship to my study.

And last, but certainly not least, I would like to thank my wonderful wife and parents. Without their selfless love and great encouragement throughout these years, I could not finish this long journey.

CONTRIBUTION OF AUTHORS

Dr. Theresa M. Filtz discussed all experimental analysis, and reviewed all manuscripts. Dr. Jeffrey A. Greenwood helped with the FRET experiments (chapter 2). Dr. Walter K. Vogel did the size-exclusion chromatography analysis (chapter 2) and purified PLC-β (Chapter 2 and 3). Sun Hyung Kwon characterized H9c2 cell line and helped with OptiPrep density gradient centrifugation (Chapter 3).

TABLE OF CONTENTS

LIST OF FIGURES

LIST OF TABLES

Chapter 1: Introduction

It is well-established that the metabolism of phosphoinositides plays a crucial role in numerous cellular processes. The hydrolysis of a minor phosphoinositide, phosphatidylinositol 4,5-bisphosphate ($PI(4,5)P_2$) by phosphoinositide-specific phospholipase C (PI-PLC) into inositol 1,4,5-triphosphate (IP_3) and diacylglycerol (DAG), is one of the earliest key events to trigger the further intracellular signal transduction pathways (Berridge, 1993). Both IP_3 and DAG are well-known second messengers which subsequently initiate Ca^{2+} release from intracellular stores and activate protein kinase C. Both increased intracellular Ca^{2+} and activated PKC will regulate a wide variety of downstream effectors, such as calmodulin, calmodulin kinase, and MAP kinase (mitogen-activated protein kinase).

$PI(4,5)P_2$ is a precursor not only of IP_3 and DAG, but also of phosphatidylinositol 3,4,5-trisphosphate (PIP_3), which is generated by phosphatidylinositol 3-kinase (PI 3-kinase). PIP_3 has been shown to affect a great variety of cellular responses, including exocytosis, cytoskeleton remodeling, chemotaxis and regulation of ion channels, and has been proposed as a second messenger (Blazer-Yost and Nofziger, 2005). Given the important role of $PI(4,5)P_2$ and its derivatives in cell signaling, the conversion of $PI(4,5)P_2$ into IP_3 and DAG is stringently controlled. The PLC isozymes, along with PI 3-kinase, PTEN (phosphatase and tensin homolog deleted in chromosome 10), phospholipase D and inositol phosphatases, are involved in the regulation and metabolism of $PI(4,5)P_2$.

Currently, thirteen identified mammalian PLC isozymes have been classified by sequence homology into six families, PLC-β, PLC-γ, PLC-δ, PLC-ε, PLC-ζ and PLC-

η (Harden and Sondek, 2006). In this review, I will mainly focus on PLC-β, the unique PLC isozymes that are regulated by heterotrimeric G proteins. To better understand PLC-β, we require a detailed description of different PLC-β isozymes, their functional analysis and involvement in diseases, structural domains, post-translational modifications and regulatory proteins and lipids, which are described in the following pages.

Members in PLC-β family

Lower eukaryotes such as yeast contain only PLC-δ (Flick and Thorner, 1993; Yoko-o et al., 1993), suggesting that PLC-β in higher eukaryotes evolved from the archetypal PLC-δ. PI-PLC similar to mammalian PLC-β isozymes have been found in invertebrates such as *Drosophila* (Bloomquist et al., 1988; Shortridge et al., 1991), and other vertebrates including *Danio rerio* (Walker et al., 2007), *Xenopus* (Ma et al., 1993), and turkey (Morris et al., 1990a). In *Drosophila*, *norpA*, an ortholog of PLC-β4, is involved in phototransduction (Bloomquist et al., 1988) whereas the function of *plc-21*, another *Drosophila* ortholog of PLC-β, has not been clearly defined yet (Shortridge et al., 1991). *Schmerle*, a zebrafish ortholog of PLC-β3, is required for endothelin1 regulation of pharyngeal arch patterning (Walker et al., 2007). *Xenopus* PLC, which is closest to PLC-β3, is involved in the receptor stimulation of Ca^{2+}-activated Cl^- current in *Xenopus* oocytes (Choi et al., 2001; Ma et al., 1993). Turkey PLC-β (PLC-βT), most similar to PLC-β2, was first purified in erythrocytes and

shown to be subject to the regulation by G protein (Morris et al., 1990a; Morris et al., 1990b).

To date, the mammalian PLC-β family exists as four identified isozymes, β1 – β4 (Jhon et al., 1993a; Lee et al., 1993; Park et al., 1992a; Suh et al., 1988). Among them, PLC-β1 and β3 are ubiquitously expressed in a variety of tissues, including brain, liver, uterus, parotid gland, lung, platelets and heart *(Hansen et al., 1995; Jhon et al., 1993a).* Interestingly, PLC-β1 is expressed at highest level in the cerebral cortex and hippocampus (Homma et al., 1989; Kim et al., 1997b), indicating the crucial roles of PLC-β1 in the brain. In contrast, PLC-β2 and PLC-β4 have limited tissue distribution; expression of PLC-β2 is restricted to hematopoietic cells, such as spleen, thymus and bone marrow (Jhon et al., 1993a; Jiang et al., 1997; Park et al., 1992a) and taste receptor cells (Rossler et al., 1998), and PLC-β4 are expressed in the retina (Lee et al., 1993) and certain neuronal cells in the cerebellum (Kim et al., 1997b).

It is worth noting that PLC-β1 and PLC-β4 each exist as two splice variants, which are alternatively spliced in the carboxyl-terminal (C-tail) domain. In PLC-β1, 75 amino acids at the C-tail (residues 1142-1216) of PLC-β1a is replaced by 32 amino acids (residues 1142-1173) of PLC-β1b (Bahk et al., 1994; Peruzzi et al., 2002). In PLC-β4, the C-tail sequence of 162 amino acids (residues 1015-1176) of PLC-β4a is replaced by 10 amino acids (residues 1015-1024) of PLC-β4b (Kim et al., 1998). Although two PLC-β1 bands (~150 kD and 140 kD) can be detected by Western blot in many cases (Jhon et al., 1993a), the smaller band might be either a proteolytic

fragment of 150 kD PLC-β1a or the alternative splice variant. Recently, Lanzafame et al. reported that PLC-β1b is detectable in neonatal rat cadiomyocytes but not in adult rat heart (Lanzafame et al., 2006), suggesting we need to appreciate differential expression and potential regulation of splice variants of PLC-β.

Functional analysis of PLC-β

Coupling receptors

Why do mammals have four PLC-β isozymes? One possible reason is for redundancy of function in critically important pathways. Alternatively, each isoform may couple to different receptors and perform specific functions. G protein-coupled receptors (GPCR) that activate PLC-β include angiotensin receptors, histamine receptors, oxytocin receptors, muscarinic receptors, α1-adrenergic receptor, vasopressin receptors and endothelin receptors, among many others (Rhee, 2001). Here, I will summarize some reported specific receptor/PLC-β couplings.

Incubation of permeabilized vascular smooth muscle cells with anti-PLC-β1 or anti-$G\alpha_q$ antibodies inhibited angiotensin II-dependent inositol polyphosphate (IP) formation (Schelling et al., 1997). These data are consistent with another study showing that angiotensin II type 1 receptors sequentially couple to PLC-β1 via heterotrimeric G proteins in vascular smooth muscle cells (Ushio-Fukai et al., 1998). Both studies suggest that PLC-β1 is the isoform that is critical to angiotensin II - regulated PLC signaling in these cells. By infecting neonatal rat cardiomyocytes with different PLC-β adenoviruses, the [^{3}H]IP response to 100 μM norepinephrine, an

agonist for α1-adrenergic receptor, was enhanced when PLC-β1 but not PLC-β3 was over-expressed. In contrast, the [^{3}H]IP response to 100 μM ATP was enhanced in PLC-β3 over-expressed neonatal rat cardiomyocytes (Arthur et al., 2001), implying that α1-adrenergic receptor selectively couples to PLC-β1 and $P2Y_2$ receptor couples to PLC-β3.

By taking advantage of siRNA technology, Kim et al. suggested that the bradykinin-induced transient Ca^{2+} rise is mediated by PLC-β1 but not PLC-β3 in myoblast cells (Kim et al., 2006). Over-expressed lysophosphatidic acid receptor 2 has been shown to couple to PLC-β3 in Hela cells (Oh et al., 2004).

PLC-β in smooth muscle contraction

Smooth muscle contraction is one of the physiological effects of activation of PLC-β. Since a PLC-β isozyme specific inhibitor is not available, most of the following studies used PLC-β isozyme specific antibodies in permeabilized cells as inhibitors. These studies not only suggest the crucial role of PLC-β isozyme in smooth muscle contraction, but also indicate that different receptors couple to different signaling pathways.

In rat and human myometrial membranes, oxytocin consistently stimulates PLC activity, and this stimulation is attenuated almost completely by $G\alpha_{q/11}$-specific antibodies (Ku et al., 1995); PLC-β isozyme specific coupling to oxytocin receptor was not studied. Cholecystokinin-stimulated contraction (through CCK receptor) was selectively blocked by PLC-β1- and $G\alpha_{q/11}$-specific antibodies in permeabilized intestinal muscle cells (Murthy and Makhlouf, 1995a), and CCK (cholecystokinin)-8-

induced contraction in permeabilized intestinal circular muscle cells was also selectively inhibited by PLC-β1 antibody (76%), PLC-β3 antibody (24%), and $G\alpha_{q/11}$antibody (86%)(Murthy and Makhlouf, 1995c) , indicating CCK receptor is mainly coupled to PLC-β1.

Adenosine-stimulated contraction (through A1 receptor) in permeabilized intestinal muscle cells was selectively blocked by $G\alpha_{i3}$-, Gβ-, and PLC-β3-specific antibodies, which is consistent with another report in which $G\alpha_{i2}$ and PLC-β3 antibody inhibited R-PIA (the selective A1 receptor agonist)-induced contraction in permeabilized esophageal muscle cells (Shim et al., 2002). DPDPE (a δ opioid receptor agonist)-stimulated IP_3 formation, Ca^{2+} release, and contraction in permeabilized intestinal muscle cells were selectively blocked by Gβ antibody and PLC-β3 antibody. Both Gβ antibody and PLC-β3 antibody also block the contractions stimulated by DAMGO, a μ opioid receptor agonist, and U-69593, a κ opioid receptor agonist (Murthy and Makhlouf, 1996). In permeabilized intestinal smooth muscle cells that express somatostatin 3 receptors, IP_3 formation, Ca^{2+} release, and contraction were inhibited (approximately 80%) by pretreatment with antibodies to PLC-β3 but not other PLC-β isozymes (Murthy et al., 1996). The $G\alpha_{i3}$, Gβ or PLC-β3 antibodies also inhibited endothelin-1 (ET-1)-induced contraction in cat esophageal circular muscle cells (Shin et al., 2002). Recent study showed that $G\alpha_{i3}$ or PLC-β3 antibody inhibits bombesin-induced contraction in permeabilized esophageal circular muscle cells (Park et al., 2006). These data implicate that PLC-β3 couples to A1 receptors,

opioid receptors, somatostatin receptors, endothelin-1 receptors and bombesin receptors.

However, this is only a partial list of PLC-β physiologic functions in contraction of most smooth muscle. PLC-β isozymes are also involved other physiological processes, as indicated in the PLC-β knockout studies and clinically-related studies discussed below.

PLC-β Knockout studies

Prior PLC-β knockout mouse studies suggest PLC-β isozymes are involved in numerous physiological processes. PLC-β1$^{-/-}$ mice fail to form the cortical barrel in the mouse somatosensory cortex (Hannan et al., 2001) which leads to death due to epilepsy-like seizures. In PLC-β1$^{-/-}$ mice, PLC activation by muscarinic agonist is substantially decreased (Kim et al., 1997b), suggesting muscarinic receptors couple to PLC-β1 in the cerebral cortex and hippocampus. PLC-β2 is essential for sweet, amino acid and bitter taste response (Zhang et al., 2003). It was surprising that the absence of PLC-β2 enhances, instead of inhibits, chemotaxis of different leukocyte populations and the *in vivo* response to bacteria and viruses (Jiang et al., 1997), suggesting alternative pathway (s) involved in chemotaxis in leukocytes.

PLC-β3 knockout mice demonstrate a 10-fold-increase in sensitivity to morphine, a selective μ opioid receptor agonist, in antinociceptive tests (Xie et al., 1999), suggesting that PLC-β3 may modulate the analgesic effect of morphine. PLC-β3 knockout mice also have significant defects in scratching behaviors induced by histamine (Han et al., 2006), suggesting PLC-β3 specifically couples to the histamine

H1 receptors in dorsal root ganglia neurons. PLC-β4$^{-/-}$ mice showed a motor defect, broadly defined as ataxia. In PLC-β4$^{-/-}$ mice, phosphoinositide hydrolysis induced by muscarinic agonists and metabotropic glutamate receptors agonist is decreased in cerebellum (Kim et al., 1997b). In addition to ataxia, PLC-β4$^{-/-}$ mice have impaired visual processing ability, expected for this retina specific isoform. While the behavioral and electroreniographic results indicate that PLC-β4 plays a significant role in visual signal processing, isolated rod recording shows little or no apparent deficit, suggesting that the effect of PLC-β4 deficiency on the rod signaling pathway occurs at some stage after the initial phototransduction cascade (Jiang et al., 1996b).

Double knockout mice lacking PLC-β2 and PLC-β3 (PLC-β2/β3$^{-/-}$) were first reported in 2000. The study of those mice reveals that PLC-β2 and PLC-β3 are critical to chemoattractant-mediated response in neutrophils, such as superoxide production and regulation of protein kinases, but not required for chemtaxis of neutrophils (Li et al., 2000). Those mice also have defects in platelet activation, such as agonist-stimulated calcium release, platelet ATP secretion and platelet actin assembly (Lian et al., 2005). Recent study shows loss-of-function mutations in PLC-β2 and PLC-β3 impair T cell, but not granulocyte, chemotaxis, and that process is calcium-dependent (Bach et al., 2007), suggesting a fundamental difference between the chemotactic signaling pathways in T cells and granulocytes.

Germline gene knockout studies are subject to confounding effects from protein redundancies or functional substitution within isoenzyme families. To our knowledge,

double knockout of the two most abundant PLC-β isoforms, PLC-β1 and PLC-β3, and a conditional knockout of PLC-β have not been reported.

PLC-β involvement in disease

Former studies suggest PLC-β isozymes are also involved in pathological processes. PLC-β1 is involved in heart disease and emotion. In failing heart, the specific binding of phosphatidic acid (PA) to PLC-γ1 and PLC-δ1 isoenzymes was decreased, whereas binding to PLC-β1 was absent (Tappia et al., 2001). Considering that PA promotes PLC-β1 activity, lower PLC-β1 activity may be associated with heart failure. In addition, teenage suicide subjects also had significantly lower PLC activity and lower expression of PLC-β1 in the prefrontal cortex whereas no significant difference in the expression of PLC-γ1 and PLC-δ was found (Pandey et al., 1999).

PLC-β isozymes are associated with different tumors. PLC-β2, virtually absent in untreated NB4 cells, an *in vitro* model for the study of acute promyelocytic leukemia, was strongly up-regulated after ATRA (all trans-retinoic acid)-induced granulocytic differentiation (Bertagnolo et al., 2002), indicating PLC-β2 represents a sensitive and reliable marker of neutrophil maturation of normal and malignant myeloid progenitors. PLC-β2 has also been proposed as a molecular marker for breast cancer since its expression levels appears to correlate with malignancy of breast cancer (Bertagnolo et al., 2006; Bertagnolo et al., 2002). In five endocrine tumor samples, no transcript of PLC-β3 was detected (Weber et al., 1994). Moreover, the

growth of three neuroendocrine tumor cell lines were suppressed when PLC-β3 was transfected into these cells (Stålberg et al., 1999), implying an essential role for PLC-β3 in suppression of neuroendocrine tumorigenesis.

Platelets from a patient with a mild inherited bleeding disorder and abnormal platelet aggregation and secretion contain approximately 1/3 the amount of PLC-β2, whereas PLC-β4 was increased threefold (Lee et al., 1996). This study is consistent with data from double knockout mice (PLC-β2/β3$^{-/-}$) which have defects in platelet secretion and aggregation (Lian et al., 2005).

Domain structure of PLC-β

All PLC isozymes contain conserved catalytic X and Y domains as well as various regulatory domains. PLC-δ, a prototype PLC, is composed of a PH (pleckstrin homology) domain, four EF-hand domains, a catalytic XY domain and a C2 domain, which are conserved among the PLCs (with exception of PLC-ζ which does not have PH domain). In addition to these feature domains, PLC-β have a unique long C-tail domain (~ 400 amino acids) and a PDZ (PSD-95, DLG, and ZO-1)-binding domain at the end of C-tail (Rhee, 2001) except for PLC-β1b which lacks the a PDZ-binding domain. We will discuss these domains in detail in the following part.

PH domain

The PH domain was first identified as ~120 residues in pleckstrin (Haslam et al., 1993), and represents the 11th most common domain in the human proteome (Letunic et al., 2006). PH domains share an almost identical core β-sandwich structure

which consists of two nearly orthogonal β-sheets (β1-β4 and β5-β7) with a long C-terminal α-helix and 3 variable loops (VL1, VL2 and VL3), although the primary sequence identity among PH domains is very low (Lemmon et al., 2002). Functionally, PH domains, such as PLC-δ-PH, are best-known for their ability to bind phosphoinositides with high affinity and specificity and to recruit their host proteins to the membrane; although it is now clear that only a small fraction of PH domains fall into this category (Yu et al., 2004).

PLC-β has a PH domain at its amino terminus. In contrast to the PLC-δ PH domain which specifically binds $PI(4,5)P_2$ (Garcia et al., 1995), binding of $Ins(1,4,5)P_3$, the polar head group of $PI(4,5)P_2$, to PLC-β1, -β2, or -β3 was not detected (Tall et al., 1997). Although PH domains of the PLC-β1 and β2, like their full length PLC-β (Runnels et al., 1996), bind to artificial membranes composed of zwitterionic phosphatidylcholine with moderate affinity, these bindings are relatively insensitive to the presence of $PI(4,5)P_2$ or phosphatidylserine (Wang et al., 1999c). In addition, the structure of PLC-β2 (Jezyk et al., 2006), as well as homology models of PLC-β isozymes (Singh and Murray, 2003), indicate that PLC-β's PH domains are not in contact with the plasma membrane and lack the electrostatic potentials of the PLC-δ PH domain required to specifically bind phosphoinositide. Nevertheless, one group has reported that the PLC-β1 PH domain translocates rapidly but transiently to the plasma membrane upon stimulation of cells with serum or lysophosphatidic acid, and the PLC-β1 PH domain appears to bind PI-3P *in vitro* (Razzini et al., 2000).

Besides lipid binding, the PH domain also has been proposed as an important protein-protein interaction domain. Since PLC-β are effectors of Gβγ (with the exception of β4), the interaction between Gβγ and PLC-β PH domain has been intensively studied. Using fluorescence resonance energy transfer assay, Wang et al showed that Gβγ binds to PLC-β PH domains in the following order: PH-β2>PH-β1>PH-δ1 (Wang et al., 1999c). Furthermore, replacing the PH domain of PLC-δ1 for PH-β2 not only changes the membrane-binding properties of chimera (PH-β2-PLC-δ1) to become similar to those of PLC-β2, but also results in a Gβγ regulated chimeric enzyme. Thus, PH domains are important regulatory signals to the host protein (Wang et al., 2000). Of great interest, biochemical, cell-biological and structural studies indicate that the PH domains of PLC-β2 and β3 are the major binding determinant for Rho-family GTPases (Illenberger et al., 2003b; Jezyk et al., 2006; Snyder et al., 2003).

EF-hand domain

EF-hand domains are normally Ca^{2+}-binding units and play essential roles in Ca^{2+}-related cellular signaling. Named after a Ca^{2+}-binding motif formed by helices E and F in the crystal structure of parvalbumin, the EF-hand motif is defined by a typical helix-loop-helix structural unit: two α-helices bridged by a Ca^{2+}-chelation loop (Gifford et al., 2007). An EF-hand domain is a pair of EF-hand motifs that form a stable four-helix bundle domain. The pairing of EF-hands enables positive cooperativity in the binding of Ca^{2+}, which is important considering the relatively modest change of Ca^{2+} concentration in cells. Upon binding Ca^{2+}, EF-hand domains undergo a conformational change from the apo state (calcium-free state) to a Ca^{2+}-

bound state. Calmodulin, the archetypal EF-hand calcium sensor, is the great example of this structure change.

There are four EF-hand motifs in PLC-β located between the PH and XY domains. Although no report about PLC-β1 EF-hand, we can gain some insight from EF-hand of other PLC isoforms. In mammalian PLC-δ1, the enzyme activity was decreased to 15-20% by deletion of the EF-hand motif (amino acids 144-172), but the mutant catalytic activity was still Ca^{2+}-dependent (Nakashima et al., 1995). Similar results were reported in *Dictyostelium discoideum* (cellular slime molds) PLC (Drayer et al., 1995), indicating that the EF-hand region may not play a role in regulation of Ca^{2+}-sensitivity of PLC, but is important for its activity. Controversially, another study showed that the binding of Ca^{2+} to the EF-hand motifs can modulate binding to $PI(4,5)P_2$ mediated by the PH domain of PLC-δ1 (Yamamoto et al., 1999). EF-hand motifs in PLC-ζ are shown to be important for its activity and high Ca^{2+} sensitivity (Kouchi et al., 2005; Nomikos et al., 2005).

Catalytic XY domain and XY linker

The catalytic XY domains of PLC family enzymes share a very similar overall topology from bacteria to human (Heinz et al., 1998). The domain is composed of X (~ 179 amino acids) and Y regions (~ 260 amino acids), which are highly conserved among mammalian PLC, and a divergent linker sequence. The crystal structure of rat PLC-δ1 showed that the X and Y domains form two halves of a distorted but closed $(\beta\alpha)_8$-like TIM (Triosephosphate isomerase) barrel, with the active site located on the C-terminal end of the barrel (Essen et al., 1996). Point mutation analysis demonstrates

the crucial role of PLC-δ1 His311 and His356, which are conserved in mammalian PLC, for the catalytic process (Ellis et al., 1998).

Despite the highly conserved XY domain, mammalian PLCs exhibit a high variable linker sequence. Strikingly, there is a long stretch of negatively charged residues (Aspartic acid and Glutamic acid) in the XY linker of all PLC-β isozymes. Early studies found that proteolytic cleavage or removal of the XY linker of PLC-β2 stimulated its catalytic activity (Schnabel and Camps, 1998; Zhang and Neer, 2001). In line with these data, structural study suggests that the active site in PLC-β2 is occluded by the XY linker (Jezyk et al., 2006). It has been hypothesized that the inhibition mechanism of steric occlusion by the XY linker in PLC-β2 might be common to all PLC isozymes (Jezyk et al., 2006). The interaction between PLC-β and G protein activators may result in rearrangement of the XY linker and make the catalytic domain more accessible to substrates.

C2 domain

The C2 domain (PKC conserved 2), ~ 130 residues in length, was first discovered as one of two conserved regulatory domains (C1 and C2) in Ca^{2+}-dependent protein kinase C (PKC). Structure analyses indicate that C2 domains share a common fold of eight antiparallel β-strands arranged as a β-sandwich, with the Ca^{2+}-binding sites located at one side of the domain (Cho and Stahelin, 2006). Besides Ca^{2+}-binding, the C2 domain is reported as a lipid-binding module although C2 domains have neither a well-defined lipid-binding pocket nor a conserved cationic

patch. Recently, one group reported that the C2 domain of PKCδ is also a phosphotyrosine binding domain (Benes et al., 2005).

Historically, C2 domains of PLC were considered as an extended Y domain since it was originally thought to be part of TIM barrel. With elucidation of the PLC-δ structure (Essen et al., 1996), the C2 domain is referred separately now. There are 3 Ca^{2+}-binding regions in PLC-δ1 C2 domain (Essen et al., 1997; Grobler et al., 1996), and C2 plays a key role in the activation of PLC-δ1 by forming the C2-Ca^{2+}-phosphatidylserine (PS) ternary complex (Lomasney et al., 1999). In the resting state, PLC-δ1-C2-EGFP and PLC-δ3-C2-EGFP are evenly dispersed in the cytoplasm. However, when the cells were activated by ionomycin, the Ca^{2+}-ionophore, these C2 domains rapidly (within 5 minutes) translocated to the plasma membrane, presumably through binding PS in the inner plasma membrane (Ananthanarayanan et al., 2002). Those data support the "tether and fix" model (Essen et al., 1996); the PH domain of PLC-δ tethers the enzyme to the membrane by higher affinity binding to PIP_2 and then the C2 domain fixes the catalytic domain to the membrane through the low affinity binding to PS.

Although Ca^{2+}-binding regions in PLC-δ C2 domain are well conserved (Essen et al., 1997), the key residues involved in Ca^{2+}-binding in PLC-β C2 domain are not conserved, indicating that the C2 domain of PLC-β may not bind Ca^{2+} (Nalefski and Falke, 1996). PLC-β1-C2 and PLC-β2-C2 do not bind the artificial membrane bilayers, and addition of 10 mM free Ca^{2+} does not influence the binding. However, PLC-β1-C2 and PLC-β2-C2 associate strongly and specifically to activated GTP[γS]-bound

Gαq subunits, and that binding is independent of Ca^{2+}. The C2 domain of PLC-β1 effectively suppresses the activation of the intact isozyme by GTP[γS]-bound-Gαq, indicating that the C2-Gαq interaction may be physiologically relevant (Wang et al., 1999a).

C-tail domain

PLC-β isozymes are distinguished by a structurally unique C-tail domain (approximately 400 amino acids), which contains a marked enrichment in positively charged amino acids (Kim et al., 1996a). Cleavage of PLC-β1 by calpain, which separates the C-tail domain from the catalytic domains, had no significant effect on Ca^{2+}-stimulated catalytic activity but completely abrogated Gαq-stimulated activity *in vitro*, indicating the C-tail is important for Gαq stimulation (Park et al., 1993b). By transfecting different truncated mutants of PLC-β1 into COS-7 cells, Wu et al. found that the region of C-tail domain required for $G\alpha_q$ activation corresponds to residues 903-1142 of PLC-β1 (Wu et al., 1993b). In human small cell lung cancer cells stably transfected with PLC-β1 C-tail, muscarinic receptor-mediated inositol phosphate release and intracellular Ca^{2+} mobilization were significantly inhibited (Beekman et al., 1998), indicating the crucial role of C-tail in the G protein activation of PLC-β. Point mutation analysis demonstrated that the basic amino acids in region 1 (residues 911-928) and region 2 of PLC-β1 (residues 1055-1072) are important for the activation by $G\alpha_q$ (Kim et al., 1996a), consistent with the former study (Wu et al., 1993a). Deletion of the C-tail domain of PLC-β1 and β2 also dramatically reduced their affinity for

phospholipids (Jenco et al., 1997), suggesting a role of PLC-β C-tail in membrane association. Crystallization of the isolated C-tail domain of a turkey PLC-β revealed a structure of three α helices forming a coiled-coil which associates as an antiparallel homodimer along its long axis *(*Singer et al., *2002)*. Importantly, the structure of C-tail of PLC-β is highly electrostatically polarized (Singer et al., 2002), with a large positive charged surface hypothesized to interact with membrane phospholipid.

One group has reported that the C-tail of PLC-β1 has intrinsic GTPase-activating protein (GAP) activity toward $G\alpha_q$ (Paulssen et al., 1996), hypothesizing a function for direct negative feedback of the G protein by its effector. We will discuss more about GAP activity later. Additionally, C-tail domain appears to harbor a nuclear localization signal sequences. A PLC-β1 M2b mutant in which lysine 1056, 1063 and 1070 were replaced with isoleucine, has less expression in nuclei and increased cytosolic localization (Kim et al., 1996a).

PDZ-binding domain

At the very C terminus of PLC-β C-tail domain is a PDZ-binding domain. The PDZ domain was originally identified from three proteins; PSD-95, DLG, and ZO-1. It consists of ~ 90 amino acids and mediates protein-protein interactions by binding to a short carboxyl-terminal peptide sequence of an (S/T)-X-Y motif (where X is any amino acid and Y is hydrophobic amino acids), which is called PDZ-binding domain.

The first evidence of PDZ domain-mediated PLC-β/protein interaction was from *Drosophlia* retina. *Drosophlia norpA*, an ortholog of PLC-β4, interacts with a PDZ-containing protein, *INAD*, and forms a protein complex involved in phototransduction

(Tsunoda et al., 1997). Using PLC-β's PDZ-binding motif as the bait in yeast two-hybrid assay, several PDZ-containing proteins, such as NHERF and Shank2, were identified as PLC-β interacting proteins (Hwang et al., 2000; Hwang et al., 2005). We will discuss these interactions in detail below.

Post-translation modification and dimerization of PLC-β

Post-translation modifications of PLC-β, such as phosphorylation, play important roles in the regulation of PLC-β activity. In the following section, we will discuss phosphorylation, degradation, and glycosylation of PLC-β and their relevant effects on PLC-β activity.

Phosphorylation

Phosphorylation is a well-characterized PLC-β modification. Several protein kinases, including protein kinase A (PKA), protein kinase C (PKC), protein kinase G (PKG) and CaMK (Camodulin kinase), have been reported to phosphorylate PLC-β and regulate its activity.

By transfecting plasmids containing kinases and PLC-β2 into COS-7 cells and assaying for inositol phosphate accumulation, Liu et al found that PKA, but not PKC, inhibits Gβγ-stimulated PLC-β2 activity. Cotransfection of PKA catalytic subunit has little effect on the expression of PLC-β2, but increases the phosphorylation of PLC-β2. *In vitro* phosphorylation assay demonstrated that PKA rapidly phosphorylates PLC-β2 (Liu and Simon, 1996). The following study suggested that fMLP (formylated peptide, n-formyl-Met-Leu-Phe) and cpt-cAMP (a membrane-permeable cAMP

analog), both of which activate PKA, stimulate PLC-β3 phosphorylation in intact RBL cells. Pre-treatment of cells with fMLP and cpt-cAMP results in a substantial inhibition of subsequently isolated PLC-β3 phosphorylation by PKA *in vitro* (Ali et al., 1998), suggesting that the endogenous PKA has blocked the same phosphorylation site(s) in PLC-β3 as *in vitro*. Later, PKA was shown to phosphorylate PLC-β3 at Serine1105 and inhibit $G\alpha_q$-stimulated PLC-β3 activity in COSM6 cells (Yue et al., 1998). Since Serine1105 is at C-tail, a region important for $G\alpha_q$ stimulation, the authors hypothesized that phosphorylation by PKA at Serine1105 may perturb the association of PLC-β3 with $G\alpha_q$ (Yue et al., 1998). It is known that fMLP activates PLC-β3 through the release of Gβγ. Thus the PKA-mediated PLC-β3 phosphorylation may block its activation by Gβγ (Ali et al., 1998). This idea was supported by a group who found PKA inhibits Gβγ-stimulated PLC-β3 activity by mechanisms that do not involve Ser1105 (Yue et al., 2000), implying the existence of other PKA site(s) in PLC-β3.

PKC is another intensively studied kinase which phosphorylates PLC-β. Since PKC activation is one of the downstream effects of activation of PLC-β, PLC-β phosphorylation of by PKC represents a logical negative feedback pathway in PLC-β regulation. In 1997, Ali et al. reported that platelet-activating factor (1-*O*-Alkyl-2-Acetyl-*sn*-Glycero-3-Phosphocholine, PAF, agonist of PAFR) or 5' phorbol 12-myristate 13-acetate (PMA, a PKC activator) pre-treatment inhibits wild type PAFR-induced PLC-mediated Ca^{2+} mobilization by approximately 90% in RBL-2H3 cells.

PAF and PMA, as well as cpt-cAMP, stimulated phosphorylation of PLC-β3. BIM, a PKC inhibitor, blocks phosphorylation of PLC-β3 stimulated by PAF and PMA, but not by cpt-cAMP, in RBL-2H3 cells, suggesting that both PKC and PKA can phosphorylate PLC-β3 (Ali et al., 1997). PLC-β phosphorylation by PKC was also suggested by the observation that opioid-mediated IP_3 response is potentiated by calphostin C, an inhibitor of PKC, and was abolished by PMA in NG108-15 cells. Moreover, challenging NG108-15 cells with [D-Pen2, D- Pen5]enkephalin (DPDPE), the δ-opioid receptor selective agonist, results in a rapid increase of PLC-β3 but not PLC-β1 phosphorylation (Strassheim et al., 1998). Although the above studies suggested that PKC affects PLC-β3 in intact cells, they did not distinguish a mechanism for PLC-β inhibition. *In vitro* activity assays suggested that turkey PLC-β phosphorylation by PKC inhibits both Ca^{2+}- and $G\alpha_q$- or $G\alpha_{11}$-stimulated activity, but not Gβγ-stimulated activity (Cunningham et al., 1999; Filtz et al., 1999). Serine1105, which is also phosphorylated by PKA, was identified as the predominant PKC phosphorylation site of PLC-β3. Like PKA, phosphorylation of Serine1105 by PKC inhibits $G\alpha_q$- stimulated PLC-β3 (Yue et al., 2000), PKC also inhibits Gβγ-stimulated PLC-β3 activity (Yue et al., 2000), and that inhibition is not dependent on Serine1105 or Serine26, implying other PKC site(s) in PLC-β3. Using PKA and PKC agonists and inhibitors, Yue et al. found that both PKC and PKA phosphorylate PLC-β3 in PHM1-41 cells expressing oxytocin receptor, but their inhibitory effects are independent of each other (Yue et al., 2000). However, conflicting data suggest that PKC, rather than PKA, mediates the G protein-coupled receptor ($P2Y_2$ receptors or

M3 muscarinic receptor)-induced phosphorylation of PLC-β3, but not PLC-β1 in CHO cells (Strassheim and Williams, 2000). It is undefined whether differences in receptor coupling (P2Y2 receptors vs. M3 muscarinic receptor vs. oxytocin receptor) or differences among cell lines (CHO cells vs. PHM1-41 cells vs. RBL-2H3 cells) cause varying effects of PLC-β3 phosphorylation on activity. Tissue studies in guinea pig suggest chronic morphine treatment (5 days) substantially augments the phosphorylation of PLC-β3, presumably by PKC, but significantly reduces the phosphorylation of PLC-β1 (Chakrabarti et al., 2003; Liu et al., 2004). In contrast to chronic morphine treatment, acute morphine treatment (5 minutes) of opioid naive longitudinal muscle myenteric plexus tissue attenuates PLC-β3 phosphorylation (Chakrabarti et al., 2003), indicating that PLC-β phosphorylation is dynamically regulated and system dependent.

Besides PKA and PKC, PKG directly phosphorylates PLC-β2 and PLC-β3 *in vitro* with purified proteins and *in vivo* with metabolic labeling. Phosphorylation by PKG leads to the inhibition of both $G\alpha_q$- and Gβγ-stimulated PLC-β3 activity by 50-70% in COS-7 cell transfection assays. Mutation experiments suggest Serine26 and Serine1105 are two key phosphorylation sites for the regulation of PLC-β3 by PKG (Xia et al., 2001). Furthermore, CaM kinase II has also been reported to phosphorylate PLC-β3 but not PLC-β1 *in vitro*. Serine537 in the X-Y linker region of PLC-β3 was proposed as a phosphorylation site. However, mutation of Ser537 to Glu had no effect on inhibition of $G\alpha_q$- or Gβγ-stimulated PLC-β3 activity by KN-93, an inhibitor of CaMK II (Yue and Sanborn, 2001).

PLC-β1 phosphorylation studies have been mainly focused on the nuclear PLC−β1. Nuclear PLC-β1, in particular the PLC-β1b subtype, was found to be phosphorylated on serine residues in response to insulin treatment of NIH 3T3 cells (Martelli et al., 2000). Stimulation of Swiss 3T3 cells with insulin-like growth factor I (IGF-I) causes rapid nuclear translocation of activated ERK and concurrently induces phosphorylation of nuclear PLC-β1, which was completely blocked by the MEK inhibitor PD98059. Activated ERK, but not PKA, efficiently phosphorylates recombinant PLC-β1 *in vitro*; the ERK phosphorylation site was mapped to Serine982 (Xu et al., 2001a). A recent study showed an increase in the serine-phosphorylation of PLC-β1b is detected in the nuclei of HL-60 cells isolated at 1 and 8.5 h after nocodazole block, which arrests over 90% cells in G2/M phase. The presence of MEK-inhibitor PD98059 completely inhibited the serine phosphorylation (Lukinovic-Skudar et al., 2005), most likely through ERK.

Xu et al. also found PKCα promotes phosphorylation of PLC-β1 at Serine887 in the nucleus of IGF-I-treated Swiss 3T3 cells (Xu et al., 2001b). Point mutation analysis suggested that ERK-evoked phosphorylation in PLC-β1 activates the nuclear phosphoinositol cycle while phosphorylation of PLC-β1 by PKCα terminates IGF-stimulated IP_3 release in nuclei, suggesting that phosphorylation of PLC-β1 is important for regulating its activity in the nuclei (Xu et al., 2001a; Xu et al., 2001b).

Degradation

PLC isozymes are frequently isolated from cells as proteolytic fragments. Historically, putative PLC-α was a separate PLC type, but now it is clear that PLC-α

was just proteolytic catalytic fragment derived from PLC-β, -γ and –δ. Moriyama et al. found that incubating platelet PLC in the presence of Ca^{2+} resulted in conversion of high mass forms (250-440 kD) into lower mass forms (70-100 kD), suggesting the conversion was due to a Ca^{2+}–dependent protease (Moriyama et al., 1990). In the purification of PLC-β1 from bovine brain, three related proteins with molecular sizes of 140 kD (presumably PLC-β1b), 100 kD and 45 kD were co-purified. The Ca^{2+}–dependent protease calpain appears to be responsible for the cleavage of PLC-β1 *in vitro* (Park et al., 1993b). Banno et al. also found truncated 100 kD and 45 kD forms when purifying PLC-β1 from human platelets. Interestingly, the 100 kDa PLC-β1 was found to be activated to a greater extent by brain Gβγ subunits compared to the intact 150 kDa enzyme (Banno et al., 1994). By treating human platelets with calpain activators (A23187 and dibucaine) and calpain inhibitor (calpeptin), Banno et al. proposed that PLC-β3 is cleaved by endogenous calpain in human platelets (Banno et al., 1995). To date, only calpain has been reported to cleave PLC-β endogenously. The physiological consequence of PLC-β proteolysis, whether as a step in ubiquitin-mediated degradation, or a manner of increasing preference for activation by Gβγ, or of inhibiting PLC-β activity by reducing membrane association in the presence of high levels of calcium, remains unknown.

Glycosylation

A single publication has documented that *O*-GlcNAc (O-linked β-N-acetylglucosamine) modification of PLC-β1 in C2C12 cells in response to increases in the level of cellular *O*-GlcNAc. Glycosylation does not change the expression level of

PLC-β, but inhibits its activation as measured by production of IP_3 and Ca^{2+} in response to bradykinin (Kim et al., 2006). Thirteen potential *O*-GlcNAc sites in PLC-β1 were predicted.

Dimerization

Early studies of PLC isozymes suggested the existence of protein dimers. In 1986, molecular weights of purified bovine PLC-I and PLC-II, determined by SDS-PAGE, were 150 kD and 145 kD, respectively. However, under non-denaturing conditions (PAGE), purified PLC-I migrated consistent with a dimer while PLC-II remained mainly at 145 kD (Ryu et al., 1986), indicating that different PLC-β-like enzymes have different dimer affinities. Two types of cytosolic PLC from human platelets purified as a trimer (PLC-I) and a dimer (PLC-II) of 146 kD protein. Importantly, both enzymes hydrolyzed PIP_2 in a Ca^{2+}-dependent manner (Moriyama et al., 1990), implying the PLC-β-like dimers are active enzymes. Size exclusion chromatography of 150 kD PLC-β eluted at 290 kD and was catalytically active (Banno et al., 1994), suggesting that a dimer form of PLC-β is active.

In a PLC-β1 C-tail fragments study, Paulssen et al. found that several tails fragments inhibit the Ca^{2+}-stimulated PLC-β1 activity (Paulssen et al., 1996). One explanation for the inhibition is that C-tail may bind to lipid vesicles. Another possible reason is that the C-tail fragments may bind PLC-β1 directly and this hypothesis is consistent with the crystal structure of C-tail dimer (Singer et al., 2002). The crystal structure of the C-tail from an avian PLC-β reveals that C-tail is composed of three long helices forming a coiled-coil that dimerizes along its long axis in an antiparallel

orientation (Singer et al., 2002). PLC-δ1, which lacks the C-tail motif of PLC-β isoenzymes, also purifies as a dimer (Ellis et al., 1993; Ryu et al., 1987), although the crystal structure of truncated PLC-δ1 suggests it is monomer (Essen et al., 1996; Ferguson et al., 1995). *Bacillus thuringiensis* phosphatidylinositol-specific phospholipase C (PI-PLC), a bacterial PLC ortholog containing only the catalytic XY domain of PLC, also forms a dimer (Shao et al., 2007; Zhang et al., 2004), reinforcing the idea that the catalytic domains may participate in the dimer association. In addition, PLC-β2 can strongly bind to PLC-δ1 and inhibits its catalytic activity (Guo et al., 2005). Considering that PLC-δ1 lacks a C-tail domain, perhaps PLC-β2/PLC-δ1 association occurs through the catalytic domains. All of above data are consistent with a model that the catalytic XY domain and the C-tail domain are important in PLC dimer formation.

An important issue of PLC-β dimer is the significance of the dimerization of PLC-β. Ilkaeva *et al*. reported that most PLC-β1 mutations that altered either $G\alpha_q$ response or GAP activity map at the long interface of C-tail dimer (Ilkaeva et al., 2002), suggesting that the GAP activity and $G\alpha_q$ activation of PLC-β1 may depend on the dimerization of the C tail domain. Since the catalytic domains of PLC-β are involved dimer formation, PLC-β dimers may be cooperative for substrate binding. PLC-β isoenzymes display steep concentration dependence curves for G protein activation (Boyer et al., 1992a; Paterson et al., 1995), and Hill coefficients of PLC-β1 and PLC-β2 for substrate hydrolysis were found to be 1.8 ± 0.01 (PLC-β1) and 1.4 ± 0.1 (PLC-β2) (James et al., 1995), supporting a cooperative homodimer model.

Moreover, Ca^{2+}-stimulated PLC-β1 activity increases markedly with increasing enzyme concentration up to 50 pM (Ross et al., 2006), suggesting PLC-β1 monomers may form more active dimers at higher concentration. Robert et al. have proposed a "dual-phospholipid" model in which one subunit of the dimer is responsible for binding to the phospholipid while the other hydrolyses an accessible phospholipid (Roberts et al., 1977), which is consistent with the dual-substrate binding model predicted in PLC-δ1 (Wang et al., 1996).

Dimerization may be a common structural feature of phospholipases. Deems *et al.* observed a concentration-dependent aggregation of phospholipase A2 from cobra venom (Deems and Dennis, 1975). And Kam *et al.* reported that phospholipase D isozymes could form homodimers (PLD1/PLD1) and heterodimers (PLD1/PLD2) (Kam and Exton, 2002).

Proteins interacting with PLC-β

Protein-protein interactions are very important in signal transduction since they provide specificity in signaling networks. A few proteins listed below are known to interact with PLC-β. However, considering the central role of PLC-β to G protein-coupled receptors activation, we expect that more proteins may interact with and regulate PLC-β**.**

<u>Gα subunit</u>

G protein-coupled receptor (GPCR) mediated activation of PLC-β through heterotrimeric G protein is the classic model for PLC-β regulation. Heterotrimeric G

proteins consist of α, β, and γ subunits that are associated in the inactive, GDP bound state. When an agonist stimulates its GPCR, the activated receptor induces the exchange of GDP for GTP on Gα subunit and subsequently releases it from the tightly associated Gβγ dimer. Both GTP bound Gα subunit and Gβγ can regulate PLC-β activity (Rhee, 2001).

Based on the sequence homology, Gα subunits have been divided into four subfamilies: $G\alpha_{i/O}$, $G\alpha_s$, $G\alpha_q$, and $G\alpha_{12}$. Among them, $G\alpha_q$ subfamily members, which include $G\alpha_q$, $G\alpha_{11}$, $G\alpha_{14}$, and $G\alpha_{15/16}$, can activate PLC-β isozymes. $G\alpha_q$ and $G\alpha_{11}$ are ubiquitously expressed in nearly all tissues, whereas the distribution of $G\alpha_{14}$ and $G\alpha_{15/16}$ are more limited (Hubbard and Hepler, 2006). Interestingly, both $G\alpha_{15/16}$ and PLC-β2 are restricted to cells of hematopoeitic origin. Functionally, $G\alpha_{16}$ most effectively activates PLC-β2 whereas $G\alpha_{q/11}$ most efficiently stimulates PLC-β1 (Lee et al., 1992), suggesting each $G\alpha_q$ subfamily member has tissue-specific or receptor-specific signaling functions.

Three GTPγS-activated $G\alpha_q$ members ($G\alpha_q$, $G\alpha_{11}$ and $G\alpha_{16}$) stimulate PIP_2 hydrolysis by PLC-β with a order of activation PLC-β1≥ PLC-β3>> PLC-β2 (Hepler et al., 1993; Jhon et al., 1993b; Kozasa et al., 1993; Smrcka and Sternweis, 1993). All $G\alpha_q$ members can also stimulate PLC-β4 in transfected cell assays (Jiang et al., 1994). However, PLC-β4 is selectively inhibited by ribonucleotides, including GTPγS (Lee et al., 1994), making it difficult to compare PLC-β4 to other PLC-β isozymes *in vitro*. As discussed above, activated $G\alpha_q$ interacts with the C2 and C-tail domains of PLC-

β (Kim et al., 1996a; Park et al., 1993b; Wang et al., 1999a; Wu et al., 1993b), which is different from Gβγ binding sites.

Strikingly, Berstein et al. illustrated that PLC-β1 acts as a GAP (GTPase-activating protein) for $G\alpha_{q/11}$, its physiological regulator, *in vitro*. PLC-β1 markedly enhances GTP hydrolysis by the $G\alpha_{q/11}$ subunit and accelerates the termination of its own activation (Berstein et al., 1992). C-tail domain of PLC-β1 is important for GAP activity (Paulssen et al., 1996) and this $G\alpha_q$ GAP activity of PLC–β1 is inhibited by Gβγ (Chidiac and Ross, 1999; Tang et al., 2006). By taking advantage of different *Drosophila* mutants, Cook et al. showed PLC-β amount is proportional to $G\alpha_q$ GAP activity and light response termination (Cook et al., 2000), the first evidence that suggested PLC-β is a $G\alpha_q$ GAP *in vivo*. The reciprocal regulation between PLC-β and $G\alpha_q$ represents the fine-tuning control in the G protein-coupled receptor signaling pathway. Using an effector itself (PLC-β) as GAP is a parsimonious mechanism because cells do not need another protein. Moreover, this attractive mechanism allows effector-specific feedback regulation of signaling. Indeed, Elliott Ross's unpublished data suggest that all the PLC-β isozymes display GAP activity towards $G\alpha_q$, $G\alpha_{11}$ and $G\alpha_{16}$ (Chidiac and Ross, 1999), indicating that effectors act as GAPs in G protein-coupled receptor signaling may be a common mechanism.

Gβγ subunit

According to current knowledge, seven genes encode for Gβ- and twelve genes encode for Gγ-subunits (Rhee, 2001). Initially, Gβγ was thought to bind inactivated

Gα subunit and hasten the return of the heterotrimic G proteins to the plasma membrane. Today, Gβγ is known to interact with several effectors, including PLC-β, potentially explaining a mechanism whereby stimulation of many $G\alpha_i$-coupled receptors (pertussis toxin-sensitive receptors) also activate PLC-β (Jiang et al., 1996a).

In vitro data suggest that Gβγ activates PLC-β with the order of PLC-β3≥ PLC-β2>> PLC-β1 (Park et al., 1993a), which is different from the order for $G\alpha_q$ stimulation. However, direct binding experiments indicate that Gβγ binds PLC-β2 with the highest affinity among three PLC-β tested (Runnels and Scarlata, 1999); PLC-β4 is completely insensitive to Gβγ (Lee et al., 1994).

The region of PLC-β that interacts with $G\alpha_q$ (the C-tail domain) is different from that associating with Gβγ. The C-tail domain truncated PLC-β2 mutant is insensitive to $G\alpha_q$ but has no defect in Gβγ stimulation (Schnabel et al., 1993). Further experiments suggest a region in catalytic Y domain of PLC-β2 is important for Gβγ interaction (Kuang et al., 1996; Sankaran et al., 1998). Moreover, other evidence indicates the PH domain of PLC-β is another binding site for Gβγ (Barr et al., 2000; Wang et al., 1999c).

Rho family GTPases

Rho GTPases constitute a distinct family with the superfamily of Ras-related small GTPases and are found in all eukaryotic cells. Rho GTPases were first characterized as regulators of actin dynamics. Subsequence studies have revealed that they affect a variety of other processes, including regulation of enzymatic activities, cell cycle, and cell migration (Jaffe and Hall, 2005). Most studies have focused on 3 of

22 Rho isoforms: RhoA, Rac1 and cdc42. However, other members in the family, such as Rac2, are also important and have more specialized functions.

Direct regulation of PLC-β by Rho family GTPases is one of the exciting findings in the field. The groundbreaking work of Illenberger and colleagues suggested low-molecular-mass GTP-binding proteins (23 kD and 26 kD), which are distinct from $G\alpha_q$, are involved in the isozyme-specific activation of PLC-β2 (Illenberger et al., 1997). These two low-molecular-mass GTP-binding proteins were identified as CDC42Hs and Rac1, members of the Rho GTPases family, as novel regulators of PLC-β2 (Illenberger et al., 1998). Rho GTPases stimulate PLC-β2 with a rank order of potency of Rac2 ≥ Rac1 > Cdc42Hs (Illenberger et al., 1998; Snyder et al., 2003). Rac2 activates PLC-β isozymes with the rank order of PLC-β2 > PLC-β3 ≥ PLC-β1 (Illenberger et al., 2003a). The removal of the C-tail domain of PLC-β2 enhances Rac2 mediated-, but not $G\beta_1\gamma_1$-mediated, stimulation (Illenberger et al., 2003a), suggesting that the C-tail domain may inhibit the interaction between PLC-β2 and Rac2. Constitutively active Rac2(12V) stimulates the activity of GFP-PLC-β2 in live cells and enhances PLC-β2 membrane association (Illenberger et al., 2003b). The PH domain of PLC-β2 is absolutely required for Rac2-mediated stimulation (Illenberger et al., 2003a; Illenberger et al., 2003b; Snyder et al., 2003), which is consistent with a crystal structure demonstrating that contacts between Rac1 and PLC-β2 occur entirely through the PH domain of PLC-β2 (Jezyk et al., 2006). Both PLC-β2 and Rac2 are expressed in myeloid cells (Heyworth et al., 1994; Park et al., 1992b) and both of them are activated in the response to stimulation of

chemoattractant receptors. Thus, it is logic to propose that the interaction between PLC-β2 and Rac2 may be critically involved in chemoattractant-induced responses in intact cells (Illenberger et al., 2003a).

Among PLC-β isozymes, PLC-β2 is the least responsive to $G\alpha_q$ stimulation but most sensitive to Gβγ and Rac2 stimulation. *In vitro* assay data showed that the stimulation of PLC-β2 by Rac2 and $G\beta_5\gamma_2$ was additive (Illenberger et al., 2003a). This raises the question as to whether PLC-β2 is regulated by Rho GTPases and Gβγ simultaneously. Substitution of Glu52 with alanine in PLC-β2 greatly diminishes activation of PLC-β2 by Rac1 but has no effect on $G\beta_1\gamma_2$-stimulated activity in transfected COS-7 cells (Jezyk et al., 2006), indicating the binding sites for Rac1 and $G\beta_1\gamma_2$ within the PH domain of PLC-β2 are distinct.

Scaffolding protein

NorpA, a *Drosophila* ortholog of PLC-β4, interacts with *INAD*, a scaffolding protein consisting of 5 PDZ domains which forms a protein complex with TRP channel (transient receptor potential) and PKC in retina. In $inaD^1$ null mutant fly retina, *NorpA* is completely mislocated from rhabdomeres, dense retinal membranes, to the cytoplasm and is not stable (less than 10% of wile-type levels 10 days post-eclosion) (Tsunoda et al., 1997). *INAD* directly binds to *NorpA* via two regions; the C-terminus of *NorpA* and the G box-homology region (a putative G protein-interacting site). The *NorpA* proteins lacking PDZ binding sites, which display normal basal PLC catalytic activity, can no longer associate with *INAD in vivo* and these truncates fail to express in rhabdomeres (van Huizen et al., 1998), consistent with the explanation that *INAD* is

required to hold *NorpA* at the rhadomere for highly efficient light signal transduction and rapid inactivation of transduction.

Using a yeast two-hybrid assay system, NHERF2 (Na^+/H^+ exchanger regulatory factor 2) was identified as a protein that specifically interacted with a C-terminal heptapeptide (QEENTQL) of PLC-β3. Importantly, NHERF2 potentiates the PLC-β activation induced by carbachol in COS7 and HeLa cells, while mutant NHERF2, lacking the second PDZ domain, has no such effect (Hwang et al., 2000). NHERF2 was found to indirectly link LPA (Lysophosphatidic acid) receptor 2 to PLC-β3 to form a complex, indicating that NHERF2 may act as a scaffolding protein which couples PLC-β3 in the protein complex to increase its activity (Oh et al., 2004). Another group reported association of TRP4 channel and PLC-β1 with NHERF in adult mouse brain (Tang et al., 2000), which is similar to *NorpA* colocalization with TRP channel in *Drosophila* retina (Tsunoda et al., 1997). Both NHERF1 and NHERF2 were reported to assemble a signaling complex containing PTH1R (The parathyroid hormone 1 receptor) and PLC-β1 (Mahon et al., 2002; Mahon and Segre, 2004). Data regarding the binding specificity of NHERF for PLC-β are somewhat conflicting. Suh and coworkers reported that NHERF2, but not NHERF1, specifically binds to PLC-β3, not other PLC-β isozymes (Hwang et al., 2000; Oh et al., 2004), whereas Segre group demonstrated the existence of NHERF2-PLC-β1 complex (Mahon et al., 2002), NHERF1-PLC-β1 complex, and NHERF1-PLC-β3 complex (Mahon and Segre, 2004). These differences may result from different methods (co-immunoprecipitation vs. GST pull-down). The physiologic consequence of NHERF

scaffolding of PLC-β proteins, whether on the time course of activation or desensitization or receptor-specific interaction in mammalian cells remains unknown.

In addition to NHERF, Shank2, a PDZ domain-containing protein in postsynaptic density, interacts with PLC-β3 and mediates the association of PLC-β3 and Homer 1b (Hwang et al., 2005). Furthermore, PLC-β4 forms complexes with mGluR1 (metabotropic glutamate receptor type 1) and Homer 1 (Nakamura et al., 2004). Interestingly, Homer 2 preferentially binds to PLC-β in pancreatic and brain extracts and stimulated PLC-β GAP activity by ~140% in an *in vitro* reconstitution system (Shin et al., 2003). The molecular mechanisms of Homer 2 control of PLC-β GAP activity remains to be determined. However, it suggests that scaffolding is important for desensitization, similar to *Drosophila* retina. Recently, cell polarity proteins Par3 and Par6 (Par: partition-defective), PDZ domain-containing proteins, were identified to interact with PLC-β1 and β3. The PLC-β3-Par complex modestly increases Gβγ-stimulated PLC-β3 activity, and PLC-β1-Par complex significantly stimulates the transcriptional activity of Lef (lymphoid enhancer factor), a transcriptional factor involved in the Wnt pathway (Cai et al., 2005).

From our experience, we found a c-tail fragment of PLC-β1 and β3 (last 50 amino acids) bound to PDZ domains of CAL and PDZK1 *in vitro*, but we could not verify those interactions by co- immunoprecipitation assay (data not shown). Thus, interaction data must be verified by several means and ideally functional relevance established.

Tubulin

Tubulin is a main component of microtubules and mitotic spindle fibers, which are composed of α- and β-tubulin heterodimers in all eukaryotic cells. Tubulin has been shown to regulate PLC-β activity in a unique biphasic pattern. Low concentrations of tubulin with guanine nucleotide (GppNHp) bound activate PLC-β1, whereas higher concentrations of tubulin inhibit its activity. Interaction of tubulin with both $G\alpha_q$ and PLC-β1 accompanied by guanine nucleotide transfer from tubulin to $G\alpha_q$ is suggested as a mechanism for enzyme activation. On the other hand, $PI(4,5)P_2$, the substrate of PLC-β1, binds to tubulin, which may be a mechanism for the inhibition of PLC-β1 by tubulin, since high tubulin concentrations might prevent access of PLC-β1 to its substrate (Popova et al., 1997). In SK-N-SH neuroblastoma cells, muscarinic receptor activation induces a rapid and transient translocation of tubulin to the plasma membrane (Popova and Rasenick, 2000), and PIP_2 augments this process. Similar data is obtained in Sf9 cells, containing a recombinant PLC-β1 pathway (Popova et al., 2002). Moreover, the same group reported that Gβγ inhibits carbachol-evoked membrane translocation of tubulin by promoting tubulin polymerization (Popova and Rasenick, 2003). In contrast to the preferential association of $G\alpha_q$ with the GTPγS-bound tubulin (Popova and Rasenick, 2000), $G\beta_1\gamma_2$ preferentially interact with the tubulin-GDP which is engaged in the microtubule polymerization (Popova and Rasenick, 2003). Thus G protein-coupled receptors might evoke Gα and Gβγ to orchestrate regulation of PLC-β signaling by tubulin dimers and control of cell shape by microtubules.

In addition, β-tubulin was recently identified as a binding protein of PLC-γ1 through its PH domains (PH1 and nPH2). In the presence of purified tubulin, PLC-γ1 activity is substantially increased *in vitro*, suggesting that β-tubulin activates PLC-γ1. PLC-γ1 reciprocally modulates microtubule assembly by β-tubulin (Chang et al., 2005).

Besides microtubule assembly, PLC isozymes are also important in cytokinesis (Naito et al., 2006; Wong et al., 2007). At least three GFP tagged mammalian PLC izozymes, PLC-δ1, PLC-δ1 and PLC-β1a, are localized to the cleavage furrow during cytokinesis. Treatment of NIH3T3 cells with U73122 and ET-18-OCH3, two different PLC inhibitors, significantly increases the number of paired cells, an indication of incomplete cell division (Naito et al., 2006). Similarly, U73122 and ET-18-OCH3 cause the relocalization of F-actin and cleavage furrow regression in crane-fly and *Drosophila* spermatocytes (Wong et al., 2007). These results are consistent with a model in which PLC isozymes control the contractile ring consisting of actin and myosin during cytokinesis.

Calmodulin

Calmodulin (CaM) is the prototypical example of the EF-hand family of Ca^{2+}-sensing proteins. It is expressed in all eukaryotic cells where it participates in signaling pathways that regulate many crucial processes such as growth, proliferation and movement (Chin and Means, 2000). Using a yeast two-hybrid assay method, our lab has identified CaM as a PLC-β interacting protein which binds the amino-terminus of PLC-β3. CaM inhibitors reduce M1-muscarinic receptor stimulation of inositol

phospholipid hydrolysis in whole cell assay, suggesting its physiological role in potentiating PLC-β activity (McCullar et al., 2003). *In vitro* assay showed CaM increases Gβγ-stimulated PLC-β3 activity, but not Ca^{2+}- and $G\alpha_q$-stimulated activity (McCullar et al., 2007). Interestingly, CaM also binds to PLC-δ1 at an IQ motif, a classic CaM binding motif, within the XY linker region of PLC-δ1. This binding inhibits PLC-δ1 activity, while addition of Ral, another PLC-δ1 binding protein, reverses the inhibition (Sidhu et al., 2005).

The mechanism of how CaM regulates PLC-β remains elusive although our lab demonstrate direct binding. Gβγ also binds CaM, and thus CaM may serve to link Gβγ more strongly to PLC-β for increased activation.

PLC-β in the nucleus

So far, we have mainly focused on the response of PLC-β to receptor activation at the plasma membrane and cytoplasm. However, the existence of nuclear phospholipids, such as $PI(4,5)P_2$, is now widely recognized, suggesting a distinct phosphoinositol signaling pathway in nuclei (Bunce et al., 2006).

Although several PLC isozymes have been detected in the nucleus (Crljen et al., 2004), the most intensively investigated isozyme is PLC-β1. In 1992, PLC-β1 was found in the nucleus of Swiss 3T3 cells and IGF-1 treatment exclusively stimulates the activity of nuclear PLC (Martelli et al., 1992). Interestingly, PLC-β1b was found predominantly in the nuclei of C6Bu-1 cells, rat glioma cells (Bahk et al., 1998). As discussed above, nuclear PLC-β1 can be phosphorylated by ERK and PKCα upon the

stimulation by IGF in Swiss 3T3 cells. PLC-β1 phosphorylation appears to be important for regulating PIP_2 hydrolysis in the nuclei and the mitogenic effect of IGF (Xu et al., 2001a; Xu et al., 2001b).

Friend erythroleukemia cells over-expressing PLC-β1 (both a and b variants) shows a higher level of cyclin D3/CDK4 complex and phosphorylation of retinoblastoma protein (Rb), both important for G1/S progression, in the serum-starved state. Moreover, cell lines over-expressing PLC-β1 have more cells in S phase in the absence of serum, compared with wild type cells or cells expressing the M2b cytoplasmic mutant (Faenza et al., 2000). These data suggest that PLC-β1 could partially replace serum as a mitogenic signal in cell cycle control. When C2C12 myoblast cells differentiate into myotube cells upon stimulation by insulin, nuclear PLC-β1a and PLC-β1b expression level significantly increase (Faenza et al., 2003; Faenza et al., 2004). Further experiments show overexpressed PLC-β1 and PLC-γ1are able to mimic insulin induction of both cyclin D3 and muscle differentiation in C2C12 cells by affecting specific regions of the cyclin D3 promoter (Faenza et al., 2007), indicating cyclin D3 as a target of nuclear PLC-β1 during myogenic differentiation. Besides cyclin D3, CD24, an antigen involved in differentiation and hematopoiesis, was identified as a PLC-β1 target by microarray. And PLC-β1 dependent up-regulation of CD24 is mediated, at least partially, at the transcriptional level since PLC-β1 affects CD24 promoter activity (Fiume et al., 2005).

Taken together, nuclear PLC-β, especially PLC-β1, have important roles in differentiation, mitogenesis and cell cycle progression. However, there are many open

questions in this field. What controls PLC-β transportation into the nucleus? How does PLC-β1 regulate gene expression? Why is PLC-β1b predominantly in the nuclei of certain cells?

Regulatory Lipids

Phosphatidic acid (PA)

Phosphatidic acid (PA) is a novel signaling phospholipid that has been implicated in regulation of multiple cell functions. It can be generated by hydrolysis of phosphatidylcholine through phospholipase D or phosphorylation of DAG by diacylglycerol kinase (Stace and Ktistakis, 2006).

PA has been demonstrated to increase PLC-γ1 activity (Jones and Carpenter, 1993). PA, but not PS (phosphatidylserine), binds PLC-β1 and increases Ca^{2+}-stimulated activity *in vitro* (Litosch, 2000). In addition, PA increases basal and G protein stimulated PLC-β1 activity in rat cerebral cortical membranes (Litosch, 2002). As compared to PLC-β1, PLC-β3 is less sensitive to PA (Litosch, 2003). The C-tail of PLC-β1 has been shown important for PA stimulation (Litosch, 2000), and further investigation identified that a region that includes the αA helix and flexible loop of the $G\alpha_q$-binding domain as necessary for PA regulation (Ross et al., 2006). Interestingly, these data also suggest PA may have an effect on dimerization of PLC-β1 (Ross et al., 2006).

Phosphatidylinositol 3,4,5-trisphosphate (PIP_3)

$PI(4,5)P_2$ and PIP_3 represent less than 1% of the total phospholipid in eukaryotic cell membranes (Czech, 2000). $PI(4,5)P_2$ has been found to be a large and relatively static pool, whereas PIP_3 comprises only a small fraction of the total phosphoinositol pool (Blazer-Yost and Nofziger, 2005), implicating that PIP_3 is strictly regulated and important in signal transduction. PIP_3 is generated by phosphorylating $PI(4,5)P_2$ at its 3-postion of the inositol ring through class I phosphatidylinositol 3-kinases (PI 3-kinases). There are at least eight mammalian PI 3-kinases which are divided into three classes according to their structure and substrate specificity. Of particular interest are the class 1 PI 3-kinases, the only class that produces PIP_3 and comprises a p110 catalytic subunit and a separate regulatory subunit. class 1 PI 3-kinases are further subdivided into class 1A (p110α, p110β, p110δ), which are activated by receptor tyrosine kinases, and class 1B (p110γ), which is uniquely activated by heterotrimeric G proteins (Foster et al., 2003). Recent studies suggest type I phosphatidylinositol phosphate kinase (PIP kinase) can also generate PIP_3 by phosphorylating $PI(3,4)P_2$ (Hinchliffe, 2001). Furthermore, PIP_3 is dynamically metabolized by two other enzymes: PTEN (phosphatase and tensin homolog deleted in chromosome 10) and SHIP (SH2-containing inositol 5'-phospatease) which produce $PI(4,5)P_2$ and $PI(3,4)P_2$, respectively.

PIP_3 has been proposed as a second messenger that affects numerous cellular responses, including autoimmunity (Kashiwada et al., 2007), chemotaxis (Charest and Firtel, 2006), cytokinesis (Janetopoulos and Devreotes, 2006), regulation of ion channels (Pochynyuk et al., 2007), exocytosis (Ishiki and Klip, 2005), and

cytoskeleton remodeling (Hilpela et al., 2004), which will not be discussed in this review.

Extracellular stimuli, such as growth factors, activate PI 3-kinase and generate local pools of PIP_3 which act as membrane-bound second messengers by recruiting signaling proteins with PH domains (Rameh and Cantley, 1999a). Akt/PKB (protein kinase B), a key mediator of cell proliferation and survival**,** is one well-characterized example. PIP_3 binds the PH domain of Akt (Frech et al., 1997) and may induce a conformation change of Akt which facilities phosphorylation by PDK1 (3-phosphoinositide-dependent protein kinase-1) which also binds PIP_3 through PH domain (Alessi and Cohen, 1998; Stephens et al., 1998). Similarly, Btk (Bruton's tyrosine kinase), a member of the TEC family of tyrosine kinases that are important for B cell and T cell function, has a PH domain that binds to PIP_3 (Salim et al., 1996) and controls its plasma membrane localization (Bolland et al., 1998; Varnai et al., 1999). PIP_3 binding also induces Btk autophosphorylation, presumably through relieving the inhibitory effect of the PH domain (Saito et al., 2001). DAPP1 (dual adaptor for phosphotyrosine and 3-phosphoinositides), specifically interact with PIP_3 and $PI(3,4)P_2$ (Dowler et al., 1999), and its membrane translocation is dependent on both PI 3-kinase activity and an intact DAPP1 PH domain (Anderson et al., 2000).

Small GTPases, such as Rho, Rac and ARF (ADP-ribosylation factor), are stimulated by the relevant guanine nucleotide exchange factors (GEF) which characteristically contain a PH domain. GRP1 (general receptor for phosphoinositides-1), a GEF for ARF, specifically binds to PIP_3 through its PH domain with high affinity

(Klarlund et al., 1997; Klarlund et al., 1998; Klarlund et al., 2000). ARNO (ARF nucleotide-binding-site opener), a GRP1 related protein, also binds to PIP_3 by PH domain and its translocation to the plasmas membrane is dependent on PI 3-kinase (Klarlund et al., 2000; Venkateswarlu et al., 1998). Vav, a GEF for Rho/Rac GTPase, binds PIP_3 by PH domain and this binding enhances Vav's phosphorylation by Lck tyrosine kinase and its GEF activity (Han et al., 1998). Importantly, NGF (nerve growth factor) stimulation in PC12 cells results in the translocation of Vav2/3 to plasma membrane and this translocation is abolished by pretreatment with LY294002 (Aoki et al., 2005), suggesting that local PIP_3 accumulation recruits Vav2/3 to plasma membrane.

Besides PH domains, other domains such as SH2 (Src homology 2) domain and polybasic clusters can also bind PIP_3. It has been shown that PIP_3 binds PLC-γ through its PH and SH2 domains to enhance PLC-γ's activity (Bae et al., 1998; Falasca et al., 1998). Heo et al. proposed that polybasic amino acid clusters bind negatively charged PIP_2 and PIP_3 to target proteins to the plasma membrane (Heo et al., 2006), which is consistent with regulation of ARNO (Macia et al., 2000) and WAVE2 (Oikawa et al., 2004). DOCK180, a specific GEF for Rac, lacks a PH domain and relies on DHR-1 (DOCK homology region) to interact with PIP_3 and relocate to the membrane (Cote et al., 2005).

There are several lines of evidence pointing to a PIP_3 effect on PLC-β enzymes. LY294002, a PI 3-kinase inhibitor, diminishes serotonin (5-HT)-induced inositol phosphate formation in primary cultures of rat smooth muscle cells (Tolloczko

et al., 2004). A PI3Kγ knockout study indicates that PI3Kγ makes a small but significant contribution to thrombin-stimulated calcium response in platelets. Importantly, LY294002 impairs the thrombin-induced rise in cytosolic calcium by a larger extent, suggesting other PI3K isoforms in platelets also contribute to this PLC-β mediated process (Lian et al., 2005). Interestingly, PI 3-kinase has been reported to mediate agonist-stimulated smooth muscle contraction (Northcott et al., 2005; Su et al., 2004), which is one of important physiological effects of PLC-β activation (Murthy and Makhlouf, 1995a). In aortic strips from normal Wistar-Kyoto rats, LY294002 inhibits norepinephrine-induced contraction (Northcott et al., 2005). Similarly, using intact medial strips of the swine carotid artery, histamine-stimulated contraction was significantly decreased in the presence of LY294002 (Su et al., 2004). Those data support a PIP_3 effect on PLC-β at both molecule and organ levels.

Although these phenomena are intriguing, the related molecular mechanisms have not been clearly defined. Our laboratory recently showed PLC-β directly binds PIP_3 (McCullar et al., 2007), implying PIP_3 could be an important regulator of PLC-β activity.

Chapter 2: Phospholipase C-β3 and -β1 form homodimers, but not heterodimers, through catalytic and carboxy-terminal domains

Yong Zhang, Walter K. Vogel, Jennifer S. McCullar, Jeffrey A. Greenwood, and Theresa M. Filtz

Molecular Pharmacology

c/o The American Society for Pharmacology and Experimental Therapeutics

9650 Rockville Pike

Bethesda, MD 20814-3995

70(3): 860-868

Abstract

Phospholipase C-β (PLC-β) isoenzymes are key effectors in G protein-coupled signaling pathways. Prior research suggested that some isoforms of PLC-β may exist and function as dimers. Using co-immunoprecipitation assays of differentially-tagged PLC-β constructs and size-exclusion chromatography of native PLC-β, we observed homodimerization of PLC-β3 and PLC-β1 isoenzymes, but failed to detect heterodimerization of these isoenzymes. Size-exclusion chromatography data suggest that PLC-β3 and PLC-β1 form higher affinity homodimers than PLC-β2. Evidence supportive of limited PLC-β monomer-homodimer equilibrium appears at 100 nM and lower. Further assessment of homodimerization status by co-immunoprecipitation assays with differentially-tagged PLC-β3 fragments demonstrated that at least two subdomains of PLC-β3 are involved in dimer formation, one in the catalytic X and Y domains, and the other in the G protein-regulated carboxy-terminal domain. Additionally, we provide evidence consistent with the existence of PLC-β homodimers in a whole cell context, using fluorescent protein-tagged constructs and microscopic fluorescence resonance energy transfer assays.

Introduction

Phospholipase C (PLC) is a key effector enzyme in multiple cellular signaling pathways, hydrolyzing phosphatidylinositol 4,5-bisphosphate (PtdIns(4,5)P) to inositol 1,4,5-triphosphate and diacylglycerol, second messengers which subsequently regulate Ca^{2+} release from intracellular stores and protein kinase C activation. PLC isozymes are grouped into five families based on structure and regulatory mechanism: PLC-β, PLC-γ, PLC-δ, PLC-ε, and PLC-ζ. The PLC-β family exists as four known homologues in mammals, β1-β4, all of which are involved in G protein-coupled receptor-mediated signaling cascades *(Rhee, 2001; Saunders et al., 2002)*. Of the four isoenzymes, PLC-β1 and PLC-β3 are widely distributed and and are often found co-expressed in a variety of tissues including brain, liver, uterus, parotid gland, lung, platelets, and heart *(Fukami, 2002; Hansen et al., 1995).*

PLC-β isoenzymes contain sequences with homology to several characterized protein structural motifs commonly found in membrane associated, Ca^{2+} and lipid binding proteins. These structural domains include PH (pleckstrin homology), EF hand, and C2 homology regions, as well as a PDZ-binding domain at the C terminus. Highly conserved among PLC family members are two domains required for catalytic activity, designated X and Y, which structurally form a TIM barrel to create the catalytic pocket in the crystal form of PLC-δ *(Rhee, 2001).*

Unique among PLC family members, PLC-β isoenzymes contain a carboxy-terminal (C-tail) domain of approximately 400 amino acids that is involved in membrane association and regulation by G protein αq (Gαq) subunits. Crystallization

of the isolated C-tail domain of a turkey PLC-β revealed a structure of three α helices forming a coiled-coil that associates as an antiparallel homodimer along its long axis *(Singer et al., 2002)*. Size-exclusion chromatography data suggested that purified, concentrated, full-length rat PLC-β1 and turkey PLC-β migrated consistent with protein dimerization *(Singer et al., 2002)*. However, crystallographic data on any full-length PLC-β isozyme is not yet available.

PLC-β isoenzymes are both activated by Gαq subunits and have inhibitory GTPase-activating protein (GAP) activity towards Gαq subunits. Studies of regulated and regulatory activities of some PLC-β isoenzymes support a hypothesis that dimerization is involved in the active state of the enzymes *(Paterson et al., 1995; Paulssen et al., 1996)*. However, purified PLC-β2 is reported to fractionate by size-exclusion chromatography (SEC) consistent with a monomeric species *(Guo et al., 2005)*, suggesting that different PLC-β isoenzymes have different homomeric affinities.

All previous studies of PLC-β assessed oligomerization status following purification and concentration. Using co-immunoprecipitation assays of differentially-tagged full-length PLC-β3 and fragments thereof, we demonstrate that PLC-β3 exists as a dimer in dilute cell lysates in the presence of detergent. Additionally, we observe that the catalytic domain of PLC-β3 dimerizes independent of the C-tail domain of PLC-β3, suggesting that at least two separate domains are involved in the formation of PLC-β3 dimers. We also demonstrate fluorescence resonance energy transfer (FRET)

between fluorescently-tagged PLC-β3 constructs in a whole cell microscopy assay consistent with PLC-β homodimerization *in situ*.

Materials and Methods

Materials. Minimum essential medium (MEM) and Dulbecco's modified Eagle's medium (DMEM) were purchased from Mediatech Cellgro (Herden, VA) and fetal bovine serum was purchased from Hyclone (Logan, UT). Antibodies purchased from Santa Cruz Biotechnology (Santa Cruz, CA) included anti-hexahistidine antibody (H-15), PLC-β-selective polyclonal antibodies (PLC-β1, G-12; PLC-β3, H-84), anti-green fluorescent protein (GFP)/cyan fluorescent protein (CFP) polyclonal antibody (FL), horseradish peroxidase-conjugated goat anti-rabbit secondary antibody and horseradish peroxidase-conjugated goat anti-mouse secondary antibody. Anti-FLAG epitope (M5) monoclonal antibody was purchased from Sigma (Dallas, TX) and anti-c-Myc epitope tag monoclonal antibody (Ab-1) was purchased from Oncogene (La Jolla, CA). SuperSignal West Pico chemiluminescent substrate was from Pierce (Rockford, IL). All restriction endonucleases were purchased from Promega (Madison, WI). High-Five insect (*Trichoplusia ni)* cells, Express Five SFM media, DNA polymerase Platinum *Pfx* and pCDNA3.1 (+) vector were obtained from Invitrogen (Carlsbad, CA). pCMV-Myc and pECFP-C1 vectors were from Clontech (Palo Alto, CA). Protein A-Sepharose, size-exclusion chromatophaphy molecular weight standards and all chromatographic media were purchased from GE Healthcare (Piscataway, NJ), except CHT, which was from Bio-Rad (Hercules, CA). Vectors

containing human PLC-β3 and human PLC-β1a cDNA sequences were gifts from Dr. Günther Weber (Karolinska Institutet, Sweden) and Dr. Lucio Cocco (University of Bologna, Italy) respectively. Baculovirus expression vectors containing cDNA sequence for rat PLC-β1, human PLC-β2, and amino-terminally hexahistidine-tagged human PLC-β3 were provided by Dr. T. Kendall Harden and Dr. John Sondek, respectively (University of North Carolina at Chapel Hill School of Medicine).

Plasmid construction. Sequence for the FLAG tag epitope DYKDDDDK *(Chubet and Brizzard, 1996)* was inserted into the multiple cloning site of the mammalian expression vector pCDNA3.1(+) using two complementary oligonucleotides. The resultant vector, pDNA3.1 (+)-FLAG, allows for in-frame addition of a FLAG epitope tag to the amino terminus of an inserted sequence. YFP fragment was amplified by PCR and inserted into pDNA3.1(+) for construction of the pDNA3.1 (+)-YFP vector. The mammalian expression plasmids pDNA3.1(+)-FLAG, pCMV-Myc, pDNA3.1(+)-YFP and pECFP-C2 will express Flag tag, Myc tag, YFP or CFP, respectively, at the amino terminus of an in-frame inserted sequence.

Full-length PLC-β3 cDNA sequence was subcloned into pCMV-Myc, pDNA3.1 (+)-YFP and pCDNA3.1(+)-FLAG plasmids using *Eco*R I and *Xho* I restriction sites, creating the vectors pCMV-Myc-PLC-β3, pCDNA3.1(+)-YFP-PLC-β3 and pCDNA3.1(+)-FLAG-PLC-β3. Full-length PLC-β3 cDNA sequence was subcloned into pECFP-C2 using *Eco*R I and *Hin*d III restriction sites, creating the vector pECFP-C2-PLC-β3, which expresses CFP fused to the amino terminus of full-length PLC-β3. A QuickChange® site-directed mutagenesis kit (Stratagene, La Jolla, CA) was used to

delete base pairs 'TG' of the stop codon sequence for PLC-β3 and provide the correct reading frame for fusion with the yellow fluorescent protein (YFP) sequence in the pEYFP-N2 plasmid. The vector pPLC-β3-N2-EYFP expresses YFP fused to the carboxy terminus of full-length PLC-β3.

Fragments of PLC-β3 were amplified by PCR to incorporate 5′ *Eco*R I and 3′ *Xho* I restriction sites using the following sets of primers: amino-terminal PH and EF hand domains (NT-β3; aa 2-315) amplified with 5′-ATATATGAATTCTGGCGGGCGCCCAG-3′ and 5′-ATATTCTCGAGTCACAGATCCAGGGCTTC-3′; catalytic X and Y domains and intervening sequence (XY-β3; aa 310-730) amplified with 5′-ATATATGAATTCTGCTGGAAGCCCTGGAT-3′ and 5′-TATATTCTCGAGTCAGACCCGCAA GGCATT-3′; C-tail domain (CT-β3, aa 861-1234) amplified with 5′-ATCGAATTCGGAACCCCATTAAGCAC GTCAG-3′ and 5′-TTCTCGAGTCAGAGCTG CGTGTTCTCC-3′; and C2/C-tail-deleted mutants (ΔC-β3; aa 2-730) amplified with 5′-TATATGAATTCTGGCGGGCGCCCAG-3′ and 5′-TATATTCTCGAGTCAGACCCGCAAGGCATT-3′. PCR-amplified cDNA sequences for NT-β3 and ΔC-β3 were ligated into *Eco*R I and *Xho* I restriction sites in pDNA3.1 (+)-FLAG and pCMV-Myc plasmids. XY-β3 and CT-β3 sequences were ligated into *Eco*R I and *Xho* I restriction sites in pCMV-Myc and pECFP-C2 plasmids. Protein structural domain boundaries for the protein fragments were defined by sequence alignment and analysis using CLUSTALW (1.82).

Full-length human PLC-β1a cDNA sequence was amplified by PCR to incorporate 5′ *Sal* I and 3′ *Kpn* I restriction sites and then subcloned into pCMV-Myc and pECFP-C2, creating the plasmids pCMV-Myc-PLC-β1 and pECFP-C2-PLC-β1. All constructs were confirmed by sequencing.

Cell culture and transfection. Human embryonic kidney cells, HEK 293, were cultured in 90% MEM, 10% fetal bovine serum, 100 units/ml penicillin, and 0.1 mg/ml streptomycin at 37°C under 5% CO_2 in humidified air. The day before transfection, HEK 293 cells were plated at a density of 8×10^5 cells/10 cm dish. Qiagen midiprep-purified DNA plasmids (5 μg total) were transiently transfected into HEK 293 cells by a calcium phosphate precipitation method as described previously *(Avram et al., 1999)*. Human astrocytoma 1321N1 cells were cultured in 90% DMEM, 10% fetal bovine serum, 100 units/ml penicillin, and 0.1 mg/ml streptomycin at 37°C under 5% CO_2 in humidified air as previously described *(Filtz et al., 1994)*. Native PLC-β1, PLC-β2, and hexahistidine-tagged (His_6) PLC-β3 were expressed in High-Five cells in suspension culture following baculovirus infection at a multiplicity of infection of 1 to 3. The cells were grown in Express Five SFM media at 27 °C and harvested 48 h post infection as described previously *(Paterson et al., 1995; Snyder et al., 2003)*.

Whole cell inositol phospholipid hydrolysis assays. HEK-293 cells were assayed for basal inositol phosphate accumulation essentially as described previously (Filtz and Niibori, 2004) with the following modifications. HEK-293 cells were seeded into 24 well plates at a density of 3×10^4 cells/well and allowed to attach overnight. Cells were transfected as described above with 0.2 μg plasmid DNA/well. Forty-eight hours

post-transfection, HEK-293 cells were labeled for 18 h overnight with 1 μCi/well ^{3}H-inositol in inositol-free DMEM. Medium was changed to 10 mM Hepes-buffered DMEM pH 7.4 and cells moved to a 37°C waterbath in room air. 10 mM LiCl (inositol phosphatase inhibitor) was added to all wells at time zero and the assays stopped after 30 minutes by addition of 5% trichloroacetic acid (TCA). ^{3}H-inositol phosphates accumulated in the presence of LiCl were collected by anion exchange chromatography and quantitated as previously described (Filtz and Niibori, 2004).

Co-immunoprecipitation. HEK 293 cells were washed thrice with ice-cold PBS 48 h after transfection, collected by scraping, and pelleted at 500 × g for 5 min. Cold lysis buffer (0.6 ml; 10 mM Tris pH 7.4, 5 mM $MgCl_2$, 2 mM EDTA, 0.1 mM PMSF, 1 μM pepstatin A, 10 μM leupeptin) was added to each sample and incubated on ice for 10 min. Cells were lysed with 15 strokes of a Dounce homogenizer and the lysate centrifuged at 500 × g, 4°C for 5 min to pellet nuclei and intact cells. Two different extraction protocols were utilized to prepare samples containing soluble PLC-β. For detergent extraction, the low speed supernatant was diluted in 1 volume of triton extraction buffer (100 mM Hepes pH 7.4, 5 mM EDTA, 300 mM NaCl, 1% Triton X-100, 2 mM DTT, 0.1 mM PMSF, 1 μM pepstatin A, 10 μM leupeptin) and incubated at 4°C for 1 h with inversion followed by centrifugation at 16,000 × g for 30 min at 4°C to pellet insolubles. For high pH extraction, 50 mM Na_2CO_3 was added to the low speed supernatant and incubated at 4°C for 1 h with inversion followed by centrifugation at 16,000 × g for 30 min at 4°C. The high pH extraction supernatant was neutralized to pH 7.3 with HCl.

Immunoprecipitation from cell extracts was accomplished as described previously *(McCullar et al., 2003)*. All antibodies were used at a concentration of 0.1 μg/ml, except anti-FLAG M5 at 2 μg/ml and secondary anti-IgG antibodies at 0.04 μg/ml. Immunoreactive bands were visualized using SuperSignal West Pico® chemiluminescent substrate followed by exposure to X-ray film for 20-30 s. X-ray film images of all immunoblots were quantitated by densitometry and analysis with NIH ImageJ v1.36b software.

Trichloroacetic acid precipitation. Cell lysates, prepared as above, were precipitated with 15% TCA on ice for 10 min, followed by centrifugation at 16,000 × g for 15 min at 4°C. The acid precipitated pellets were washed with 500 μl ice-cold acetone, re-centrifuged at 16,000 × g for 15 min at 4°C, and the pellets dried before separation by SDS-PAGE.

Purification of PLC-β subtypes from 1321N1 cells. Cells were hypotonically lysed and Dounce homogenized in 10 mM Hepes pH 7.4, 1 mM EDTA 2 mM $MgCl_2$, 1 mM DTT, and protease inhibitors (0.1 mM PMSF, 1 μM pepstatin A, 10 μM leupeptin, 2 mM benzamidine, and 10 μg/ml E-64). Cell debris and nuclei were pelleted at 1000 × g. The post-nuclear supernatant was extracted with 0.5% n-octyl-β-D-glucopyranoside. The clarified extract was adsorbed on to a Q-Sepharose FF column equilibrated with buffer A (25 mM Hepes, pH 7.4, 1 mM EDTA, 1 mM DTT, 0.1 mM PMSF) plus 100 mM NaCl. The column was eluted with buffer A plus 350 mM NaCl directly onto a heparin-Sepharose HP column. PLC-β3 was eluted by increasing NaCl to 700 mM. The heparin pool was buffer exchanged on G25-

Sephadex equilibrated with 100 mM potassium phosphate, pH 7.2, 1 mM DTT, 0.1 mM PMSF and adsorbed onto CHT-hydroxyapatite. The CHT column was washed with 370 mM potassium phosphate pH 7.2 and eluted with a ten column volume gradient to 1 M potassium phosphate, pH 7.2. Peak fractions were analyzed by western blots to identify PLC-β3 and confirm the lack of contamination with PLC-β1 subtype. To concentrate the sample, the CHT column pool was buffer exchanged on G25-Sephadex equilibrated with Buffer A, adsorbed onto Q-Sepharose HP and eluted with a six column volume gradient from 100 mM to 350 mM NaCl in buffer A. PLC-β3 eluted as a shouldered peak centered at 260 mM NaCl.

Purification of recombinant PLC-β from High-Five cells. PLC-β1 and PLC-β2 isoenzymes were expressed in and purified from baculovirus-infected insect High-Five cells as previously described *(Paterson et al., 1997)*. Amino-terminally hexahistidine-tagged recombinant PLC-β3 (His_6-PLC-β3) was purified from baculovirus-infected insect High-Five cell lysate. High-Five lysate was Dounce homogenized in 10 mM Hepes pH 7.4, 0.5 mM EDTA, 1 mM TCEP, and protease inhibitors. Whole cell homogenate was layered on a 15%/45% sucrose step gradient in 25 mM Hepes, pH 7.4, 1 mM TCEP, and protease inhibitors, then centrifuged at 126,000 × g for 1.5 h. The 15% layer and the 15%/60% sucrose interface were collected and extracted by addition of NaCl to 500 mM and Na_2CO_3 to pH 10, followed by centrifugation at 504,000 × g for 1 h. The soluble extract was neutralized, imidazole added to 20 mM, and adsorbed to a Ni-Sepharose column. The column was washed with 20 mM Hepes, pH 7.4, 20 mM imidazole, 500 mM NaCl, 0.5 mM TCEP, 0.1 mM PMSF, 1 μM

pepstatin A, and 2 mM benzamidine; His_6PLC-β3 was eluted in the same buffer with 250 mM imidazole. The amino-terminal hexahistidine tag was removed with TEV protease *(Kapust et al., 2001)* at a ratio of 45:1 (PLCβ3:TEV) during dialysis overnight against buffer A plus 100 mM NaCl. Subsequent chromatographic purification steps were as above for the purification from 1321N1 cells.

Size-exclusion chromatography. PLC-β proteins were analyzed on a Superdex 200 (1.0 × 30 cm) column equilibrated with 20 mM Hepes, pH 7.4, 140 mM NaCl, 0.5 mM EDTA, 1 mM DTT and operated at 0.5 ml/min at 4˚C. Protein elution from 100 μl injections was monitored by absorbance at 280 nm using a 0.5 cm in-line flow cell. For experiments at protein concentrations too low to be observed by absorbance, the eluate was fractionated. The fractions were precipitated in the presence of 50 μg BSA and 80% ice-cold acetone and detected by immunoblot analysis. Molecular mass was estimated from regression analysis *(Siegel and Monty, 1966)* of standard globular proteins. The protein standards (molecular mass and Stokes' radius as reported by the supplier) were thyroglobulin (669 kDa, 8.50 nm), ferritin (440 kDa, 6.10 nm), catalase (232 kDa, 5.22 nm), aldolase (158 kDa, 4.81 nm), BSA (67 kDa, 3.55 nm), and ovalbumin (43 kDa, 3.05 nm).

Microscopic FRET Protocol. HEK 293 cells grown on glass cover slips were transiently transfected by the calcium phosphate precipitation method with 0.1 μg of plasmid DNA unless otherwise indicated. Cells were washed twice with PBS after 48 h transfection, fixed in 3% formaldehyde for 20 minutes, and mounted on slides with a ProLong® antifade kit (Molecular Probes, Eugene, OR).

Microscopic fluorescence intensity measurements for FRET analysis were obtained by the method of Karpova *et al*. *(Karpova et al., 2003)*, which quantitates an increase in donor fluorescence following acceptor photobleaching. LP 530 and BP 470-500 filters were used for detection of YFP (acceptor) and CFP (donor) emission, respectively, on a Zeiss LSM510 confocal microscope (Carl Zeiss, Thornwood, NY) operating with a 30 mW argon laser tuned to 514 nm for YFP excitation and 458 nm for CFP excitation. Cells were examined with a 63× Zeiss oil immersion objective. For each cell, a region of interest was selected and photobleached at 514 nm (75% laser intensity) for 150 iterations. Before and after acceptor photobleaching, CFP and YFP images were collected to assess changes in donor and acceptor fluorescence. FRET efficiency in the region of interest was calculated as $E_F = (I_2-I_1)*100/I_2$, where I_1 is the CFP intensity immediately prior to photobleaching and I_2 is the CFP intensity immediately following photobleaching. For every cell, a non-photobleached region was monitored and its FRET efficiency (E_C) over the same time frame quantitated as a background control. The average FRET efficiency is stated as (E_F-E_C) ± SEM in the results section.

For calculation of distance between fluorescent pairs in the dimer construct (r_0), we used the equation $E = R_0^6/(R_0^6+r_0^6)$ where E is the average FRET efficiency as calculated above and R_0 is a Förster distance for CFP/YFP pairs of 4.9 nm as calculated previously *(Karpova et al., 2003; Patterson et al., 2000)*.

Results

Identification of PLC-β3 homodimers by co-immunoprecipitation. To investigate PLC-β3 dimerization, a co-immunoprecipitation assay was performed with extracts of cells that had been transfected with vectors containing full-length PLC-β3 tagged at its amino terminus with either FLAG or Myc epitopes (FLAG-β3 or Myc-β3). HEK 293 cells were hypotonically lysed 48 h post-transfection, extracted, and immunoprecipitated with anti-Myc- (Fig. 1, *IP: Myc*), anti-FLAG-(Fig. 1, *IP: FLAG*), or anti-PLC-β3 carboxy-terminal- (Fig. 1, *IP: β3*) selective antibodies. Immunoprecipitated samples were separated by SDS-PAGE, blotted onto nitrocellulose and probed with antibodies to detect anti-Myc, anti-FLAG or anti-PLC-β3 immunoreactive species. The co-expression of Myc-β3 and FLAG-β3 in transfected HEK 293 cells following co-transfection of both Myc- and FLAG-tagged full-length PLC-β3-containing plasmids was confirmed by TCA precipitation of cell lysates (Fig. 1, *lane 1)* or immunoprecipitation of extracts with anti-PLC-β3 selective antibodies (Fig. 1, *lane 2*).

Neither FLAG, Myc, nor PLC-β3 immunoreactivity was detected in non-transfected HEK 293 cells (Fig. 1, *lane 9*). To demonstrate that epitope-tagged full-length PLC-β3 constructs were appropriately detected by selective anti-epitope tag antibodies, but not cross-reactive to other antibodies on immunoblot, HEK 293 cells were singly transfected with either pCDNA3.1(+)-FLAG-PLC-β3 or pCMV-Myc-PLC-β3. In cells transfected with a single construct, FLAG-β3 immunoprecipitated with anti-FLAG antibody was detectable on anti-FLAG or anti-PLC-β3 immunoblots, but not on anti-Myc immunoblots, at the expected molecular weight of approximately

150,000 (Fig. 1, *lane 6*). Conversely, Myc-β3 immunoprecipitated with anti-Myc antibody was detectable on anti-Myc or anti-PLC-β3 immunoblots, but not on anti-FLAG immunoblots, at the expected molecular weight (Fig. 1, *lane 8*). In singly transfected cells, upon immunoprecipitation of FLAG-β3 transfected cell extracts with anti-Myc antibodies or of Myc-β3 transfected cell extracts with anti-FLAG antibodies, no immunoreactive bands were detected on any immunoblots (Fig. 1, *lanes 5* and *7*).

However, following co-transfection of both pCDNA3.1(+)-FLAG-PLC-β3 and pCMV-Myc-PLC-β3 into HEK 293 cells, either anti-Myc antibody (Fig. 1, *lane 4*) or anti-FLAG antibody (Fig. 1, *lane 3*) could immunoprecipitate protein bands of the expected molecular weight that were immunoreactive on blots developed with anti-Myc, anti-FLAG or anti-PLC-β3 antibodies (Fig. 1, *lanes 3* and *4*). These results demonstrate that co-expressed FLAG- and Myc-tagged PLC-β3s co-precipitate, likely due to formation of a PLC-β3 homodimer. Similar results were obtained when cells were extracted with a high pH, detergent-free protocol rather than a detergent extraction protocol (data not shown), suggesting that detergent was not inducing oligomerization. Immunoprecipitation with anti-PLC-β3 antibodies of lysates from Myc-β3 and FLAG-β3 doubly-transfected cells, followed by Western blot analysis of immunoprecipitates and densitometry, revealed that equivalent levels of each tagged construct were expressed in doubly transfected cells (Fig. 1, *lane 2*). Densitometric analysis of lanes 3 and 4 on the Myc and FLAG blots revealed that immunoprecipitation and immunodetection by opposite antibodies (e.g., IP:myc, FLAG blot) gave a signal 40-50% less than immunoprecipitation and

immunodetection by the same antibody. This reduction is expected in studies of homodimers where three species are expected to form in any co-transfected cell, for example, myc-β3/myc-β3, myc-β3/FLAG-β3, and FLAG-β3/FLAG-β3, in a ratio of 1:2:1.

Identification of PLC-β1 homodimers. To further investigate PLC-β isoenzyme dimerization, co-immunoprecipitation assays were performed with extracts of cells that had been transfected with vectors containing full-length PLC-β1 tagged at its amino terminus with either CFP or Myc epitopes (CFP-β1 or Myc-β1). The CFP-tagged PLC-β1 fragment was approximately 20 kDa larger than wild-type PLC-β1 by Western blot as expected (Fig. 2, *Lane 1*). We found that differentially-tagged full-length PLC-β1 constructs co-immunoprecipitated by either anti-GFP/CFP- or anti-Myc-selective antibodies are detectable on all immunoblots developed with anti-GFP/CFP-, anti-Myc-, or anti-PLC-β1-selective antibodies (Fig. 2, *lanes 3* and *4*), consistent with homodimer formation.

Attempts to isolate PLC-β1 and PLC-β3 heterodimers. To determine whether PLC-β1 and PLC-β3 are capable of forming heterodimers, immunoprecipitation assays were performed with extracts of endogenously expressing 1321N1 cells (Fig. 3A) and over-expressing HEK 293 cells transfected with pCDNA3.1(+)-FLAG-β3 and pCMV-Myc-β1 (Fig. 3B). PLC-β1 and PLC-β3 heterodimers were not detectable in either system. Following 1321N1 cell lysis and extraction, immunoprecipitation with anti-PLC-β1 antibodies only produced immunoreactive bands on immunoblots performed with anti-PLC-β1 and not anti-PLC-β3 antibodies. The converse

immunoprecipitation experiments performed with anti-PLC-β3 antibodies yielded similar results (Fig. 3A). Similar results were observed following immunoprecipitation of extracts from HEK 293 cells co-transfected to express FLAG-β3 and Myc-β1. Immunoprecipitation with anti-Myc antibodies only produced immunoreactive bands on immunoblots performed with anti-PLC-β1 and not anti-PLC-β3 antibodies (Fig. 3B, *lanes 2* and *6*). Similarly, immunoprecipitation with anti-FLAG antibodies only produced immunoreactive bands on immunoblots performed with anti-PLC-β3 and not anti-PLC-β1 antibodies (Fig. 3B, *lanes 1* and *4*).

Additionally, High-Five insect cells were co-infected with baculovirus constructs for the high-level co-expression of PLC-β1 and His_6PLC-β3. Ni-Sepharose chromatography of the cell lysate and immunoblot analysis of the column eluate showed that only His_6PLC-β3 adsorbed to the column (Fig. 3C, *lanes 1-5*). PLC-β1 was only found in the column flow-through (Fig. 3C, *lanes 6-7*), uncontaminated by full-length His_6PLC-β3. All data suggest that PLC-β1 and PLC-β3 do not form heterodimers, even when co-expressed in over-expressing cells.

PLC-β monomer/homodimer equilibria assessed by size-exclusion chromatography. To further establish the oligomerization states of PLC-β homodimers, we used SEC to assess the potential for monomer-homodimer equilibria. PLC-β1, PLC-β2, and PLC-β3 have predicted molecular masses of 138.3, 133.7, and 138.8 kDa respectively as monomers, or 276.6, 267.4, and 277.6 kDa respectively as homodimers. Preparations of catalytically active PLC-β3 from exogenously-expressing insect cells, loaded onto SEC at concentrations of 250 nM and greater, elute with an apparent

molecular size of 330 kDa assessed in comparison to globular protein standards (Fig. 4, *middle*). This data is consistent with the enzyme existing as a relatively asymmetric dimer with a Stokes' radius of 5.3 nm under the indicated conditions.

Compared to over-expressed recombinant PLC-β3 from insect cells, native PLC-β3 (purified to >90% from endogenously-expressing 1321N1 cells) eluted nearly identically at 305 kDa (data not shown). The purity of the preparation used in this experiment excludes the possibility that the high apparent molecular size results from a heterocomplex of PLC-β3 and some other protein.

PLC-β1 purified from baculovirus-infected insect cells also elutes as an apparent dimer of approximately 330 kDa (Fig. 4, *upper*). Overnight incubation at 4°C of PLC-β1 or PLC-β3 resulted in a slight shifting of the elution peaks, suggesting that some minor dissociation of homodimer may result (Fig. 4 *upper* and *middle*, *dashed* versus *dotted* smooth curves). At monomer loading concentrations ≤ 50 nM, Western blot-detected elution peaks of full-length PLC-β1 and PLC-β3 shift slightly and broaden a bit more toward the predicted elution volume of 13.1 ml for a monomer (Fig. 4 *upper* and *middle*, *squared traces*). Reducing agents (DTT) did not affect the migration of PLC-β3 on the SEC column, suggesting that dimer formation is not dependent on disulfide bonds (data not shown).

PLC-β2 eluted as an apparent dimer at a loading concentration of 2.8 μM, corresponding to a molecular size of 330 kDa, compared to the predicted monomeric molecular mass of 133.7 kDa (Fig. 4 *lower*, *solid smooth curve*). However, in contrast to PLC-β1 or PLC-β3, the elution profile of PLC-β2 at 200 nM became increasingly

biphasic with incubation time (Fig. 4 *lower*, *dashed* versus *dotted smooth curves*). Peak concentrations following 4°C overnight incubation of PLC-β2 at 200 nM corresponded to apparent molecular sizes of 240 kDa and 120 kDa, suggesting that PLC-β2 homodimer dissociates at <200 nM due to a lower homodimeric affinity than PLC-β1 or PLC-β3. SDS-PAGE analysis of the fractionated elute confirmed that the biphasic elution profile of PLC-β2 was not the result of degradation (data not shown).

Mapping of the domains involved in PLC-β3 dimerization. To further delineate the domains involved in dimerization of PLC-β3, and to identify the location of the dimerization domains, four different truncated fragments of PLC-β3, tagged with either FLAG, Myc or CFP epitopes, were constructed (Fig. 5A). These fragments included the amino-terminal PH/EF hand domains (NT-β3), the C-tail domain (CT-β3), the catalytic X and Y domains (XY-β3) and C2/C-tail-deleted PLC-β3 (ΔC-β3). In whole cell assays of transfected HEK-293 cells, the catalytic Myc-XY-β3 fragment increased inositol phospholipid hydrolysis two-fold, similar to the basal (non G-protein-stimulated) activity of transfected full-length PLC-β3. Following co-transfection into HEK 293 cells, FLAG and Myc epitope-tagged ΔC-β3 (Fig. 5B), CFP and Myc epitope-tagged XY-β3 (Fig. 5C), and CFP and Myc epitope-tagged CT-β3 (Fig. 5D) can be immunoprecipitated from cell extracts by an anti-epitope antibody and detected on immunoblot with either the same or the opposite anti-epitope antibody. For example, immunoprecipitation of FLAG- and Myc-tagged ΔC-β3 with anti-FLAG antibodies results in immunoreactivity on blots incubated with either anti-FLAG or

anti-Myc antibodies at the predicted MW (Fig. 5B, *lanes 4* and *5*). As expected, CFP-tagged fragments were detectable on immunoblot migrating approximately 20 kDa larger than Myc- or FLAG-tagged constructs (Fig. 5C and 5D). These results suggested that fragments containing the C-tail and/or catalytic X and Y domains form dimers independent of full-length protein. However, the differentially-tagged fragments containing C-tail or catalytic domains were not equally detectable to full-length protein on immunoblots following co-immunoprecipitation with the opposite antibody, suggesting that the subdomains may have lower affinities as homodimers than full-length PLC-β3. For example, densitometric analysis of Western blots demonstrated that immunoprecipitation of FLAG-ΔC-β3/Myc-ΔC-β3 with anti-FLAG antibodies reproducibly results in less than 20% of the signal on anti-Myc blots as compared to anti-FLAG blots (Fig. 5B, *lanes 4* and *5*). The same principle is observed with XY-β3 and CT-β3 (Fig. 5C, *lanes 3* versus *4*; Fig. 5D, *lanes 2* versus *3*).

Fragments of PLC-β3 devoid of catalytic and carboxy-terminal domains, FLAG-NT-β3 and Myc-NT-β3, did not appear to dimerize. FLAG-NT-β3 and Myc-NT-β3, containing the PH and EF hand domains of PLC-β3, only produced immunoreactive bands when immunoprecipitated from transfected HEK cell extracts and detected by immunoblot with the same anti-epitope antibody. FLAG-NT-β3 is not immunoprecipitated by anti-Myc epitope antibody nor is Myc-NT-β3 immunoprecipitated by anti-FLAG epitope antibody (Fig. 5E). Thus, the PH and EF hand domains fragment of PLC-β3 appeared to exist as a monomer when independent of full-length protein.

FRET analysis of PLC-β homodimer and heterodimer status in whole cells. The oligomerization status of PLC-β3 was assessed in whole cells by microscopic FRET. HEK 293 cells were transfected with pECFP-C2-PLC-β3 (CFP-PLC-β3), pEYFP-N2-PLC-β3 (PLC-β3- YFP) or pCDNA3.1(+)-YFP-PLC-β3 (YFP-PLC-β3). All three PLC-β3 plasmids expressed at similar levels in HEK 293 cells as assessed by Western blot (data not shown).

Transfected HEK 293 cells were examined for YFP and CFP emission at >530 nm and 470-500 nm, respectively, using a confocal fluorescent microcope. Overlap between the channels was undetectable as assessed by expressing YFP- and CFP-tagged constructs independently *(Karpova et al., 2003)*. Shown is a representative image of a CFP-PLC-β3/PLC-β3-YFP doubly transfected cell in the YFP emission channel (Fig. 6, *right panel*) and CFP emission channel (Fig. 6, *left panel*). A selected cell region was photobleached in the YFP channel and both pre-bleach images (Fig. 6, *upper panels*) and post-bleach images (Fig. 6, *bottom panels*) were collected. The post-bleach images display an almost complete loss of YFP intensity due to YFP photobleaching and a concurrent gain in CFP intensity in the bleached regions, indicative of fluorophore coupling.

FRET efficiencies based on donor intensity increases following acceptor photobleaching were calculated as described in Methods. The average FRET efficiency for cells transfected with both CFP-PLC-β3 and PLC-β3-YFP, which express CFP and YFP at opposite termini of PLC-β3, was 5.7 ± 0.4% (n = 52), statistically different compared to cells co-transfected with CFP- and YFP-containing

control plasmids, or with CFP-PLC-β3 alone (Table 1). In contrast, FRET experiments using a different PLC-β3 FRET pair, CFP-PLC-β3 and YFP-PLC-β3, both of which express CFP and YFP at the amino terminus of PLC-β3, gave an average FRET efficiency of 3.0 ± 0.6%, that was not different from controls, but different from the PLC-β3 FRET pair tagged at opposite ends (Table 1).

We did not obtain evidence of PLC-β1/PLC-β3 heterodimers in co-tranfected cells by FRET analysis. FRET efficiency for co-transfected CFP-PLC-β1 and PLC-β3-YFP (fluorescent tags at opposite ends) cells or for co-transfected CFP-PLC-β1 and YFP-PLC-β3 (fluorescent tags at amino termini) was no different from control CFP/YFP co-transfected cells (Table 1).

The FRET efficiency for coupling between CFP-PLC-β3 and PLC-β3-YFP in doubly transfected cells was not dependent on expression levels of the proteins. To control for protein expression effects on FRET efficiency, differing total amounts of CFP-PLC-β3 and PLC-β3-YFP plasmids were co-transfected into HEK-293 cells at a constant plasmid ratio of one to one. As expected, FRET analysis of cells transfected with CFP-PLC-β3 and PLC-β3-YFP at three different total DNA concentrations (0.05 μg, 0.1 ug, and 0.9 ug) revealed that FRET efficiencies did not vary significantly (6.2 ± 0.5 %, 6.3 ± 0.4 % and 5.4 ± 0.8 %, respectively; n=20-23) with varying DNA concentrations. However, overall fluorescence intensity did increase as expected for increased protein expression with increasing DNA transfected.

Using the average FRET efficiency value of 5.7% from the CFP-PLC-β3 and PLC-β3-YFP doubly transfected cells and a Förster distance for CFP/YFP pairs of 4.9

nm as calculated previously *(Karpova et al., 2003; Patterson et al., 2000)*, we calculated the distance between the two fluorophores linked to opposite ends of full-length PLC-β3 to be 7.8 nm.

Discussion

Using co-immunoprecipitation, SEC, and microscopic FRET analyses, we have demonstrated for the first time that full-length PLC-β isoenzymes can form homodimers in whole cells and crude cell extracts, suggesting that previous detection of PLC-β homodimers was not an artifact of purification or concentration *(Singer et al., 2002)*.

Based on our data with various fragments of PLC-β3, we conclude that at least two subdomains of PLC-β3 are involved in dimer formation: one in the catalytic X and Y domains, and the other in the carboxy-terminal C-tail domain. The extensive contacts between the C-tail dimers of turkey PLC-β in the crystal structure of Singer *et al*. suggest that the C-tail domain should be sufficient to maintain dimerization of the full-length protein *(Singer et al., 2002)*. While this is not disputed, additional sequence in the catalytic domain of PLC-β3 will dimerize independent of the C-tail. PLC-δ1, which lacks the C-tail motif of PLC-β isoenzymes, also purifies as a dimer *(Ellis et al., 1993)*, reinforcing the idea that the catalytic domains may participate in the dimer association. Based on our co-precipitation studies, the C-tail and catalytic domain fragments of PLC-β3 appear to self-associate with somewhat less affinity than

the full-length protein, suggesting that both domains play a role in high affinity homodimerization.

Using whole cell fluorescence microsopy, we observed fluorophore coupling between CFP and YFP when placed at opposite ends of full-length PLC-β3 for co-expression. The FRET efficiency between CFP-PLC-β3 and YFP-PLC-β3, in which CFP and YFP were placed at the same amino terminal end of full-length PLC-β3, was significantly lower than the oppositely placed fluorophore PLC-β3 FRET efficiency ($p < 0.001$). The FRET data obtained with oppositely and similarly oriented CFP and YFP constructs suggest that opposite termini in PLC-β3 may be in closer proximity than the same termini in the dimer structure. This result is consistent with the anti-parallel orientation of the homodimerized turkey PLC-β carboxy-terminal fragments upon crystallization. The crystallized turkey PLC-β C tail formed a structure of three long α helices, labeled A, B and C, of which part of αA and most of αB were involved in extensiver dimeric contacts along the long length of the dimer. Singer *et al*. noted that the most highly conserved amino acids among the C tails of PLC-β isoenzymes were not in the dimer contact regions but in the Gαq regulated regions *(Singer et al., 2002)*, suggesting that amino acids in the αB helix may play a role in the homodimeric specificity of PLC-β1 and PLC-β3.

The average FRET efficiency that we observed for oppositely oriented CFP- and YFP-tagged PLC-β3, 5.7%, is small but not without precedent in the literature for homodimers. Homodimerization of unstimulated leptin b receptors yields FRET efficiences of 4.9% by the acceptor photobleaching method, the same method used in

this study *(Biener et al., 2005)*. Homodimers are expected to yield FRET signals that are one-half of the intensity of heterodimers, resulting from the unavoidable formation of YFP-β3 /YFP-β3 dimer and CFP-β3 /CFP-β3 dimers that do not yield FRET signals upon acceptor photobleaching. In addition, our data demonstrating that acceptor photobleaching FRET efficiency between CFP-β3 and β3-YFP does not vary with varying DNA concentrations provides evidence that the FRET signal is not an artifact based on increasing fluorescence intensity with increasing expression levels.

FRET efficiency was used to calculate a distance of approximately 8 nm between CFP and YFP tags linked to opposite ends of PLC-β3. SEC data estimates an intramolecular diameter of 11 nm for PLC-β3. At a distance of 8 nm, the CFP and YFP tags are calculated to be within the hydrodynamic diameter of a dimeric PLC-β3. However, the calculation of distance between fluorescence resonance pairs, based on the Förster distance of isolated CFP and YFP, is complicated by many factors including the flexibility of linkers and the mobility of the CFP and YFP tags.

PLC-β1 and PLC-β3 are often co-expressed, and since they exist separately as homodimers, the possible formation of heterodimers was tested by attempting to co-immunoprecipitate both isoenzymes from natively-expressing 1321N1 cells; from co-transfected, over-expressing HEK 293 cells; by attempting co-purification from over-expressing baculovirus-infected insect cells; or by microscopic FRET analysis of PLC-β3-YFP and CFP-PLC-β1 co-transfected cells. We found that PLC-β3 does not form a heterodimer with PLC-β1 within detection limits under conditions in which homodimers are easily detected.

Full-length PLC-β3 appears to form a high-affinity, catalytically active homodimer that is not dependent on disulfide bonds and is resistant to detergent dissociation with 0.5 % octyl-β-D-glucopyranoside, 500 mM NaCl, or pH 10 extraction. Analytical SEC data suggest that PLC-β1 and PLC-β3 are predominantly homodimeric at monomer concentrations in excess of 0.2 μM. Broadening and slight rightward shifting toward lower molecular size of SEC peaks below 0.2 μM for PLC-β1 and PLC-β3 suggest that a small amount of monomer/homodimer interconversion occurs at physiological concentrations (estimated as approximately 10 nM or less in 1321N1 cell cytosol). For comparative purposes, we obtained experimental data on PLC-β2 oligomeric status. Guo *et al*. reported that purified PLC-β2 migrated as a monomer *(Guo et al., 2005)*. Under our purification conditions, PLC-β2, like PLC-β1 and PLC-β3, appears to form homodimers. Although protein detection limits restrict quantitation of the homodimer dissociation constants, the dimeric dissociation constant for PLC-β2 is clearly greater than the same constant for PLC-β1 or PLC-β3. Thus, the physiologic monomer/homodimer distribution of PLC-β2 is likely dependent on intracellular concentrations, while PLC-β3 is predicted to exist nearly exclusively as a homodimer. The lower affinity of PLC-β2 homodimers may allow for alternative heterodimer formations with PLC-δ partners, as suggested previously *(Guo et al., 2005)*. Considering that PLC-δ lacks a C tail domain, perhaps PLC-β2/PLCδ association occurs through the catalytic domains, consistent with our data demonstrating association of PLC-β3 catalytic fragments.

Cooperative protein dimers commonly decrease the range of activator concentrations over which an enzyme converts from fully inactive to fully active. PLC-β isoenzymes display steep concentration dependence curves for G protein activation, supporting a cooperative homodimer model *(Boyer et al., 1992b; Paterson et al., 1995; Paulssen et al., 1996)*. Additionally, by studying PLC-β1 C tail fragments or deletion mutants, Paulsen *et al*. and Ilkaeva *et al*. suggested that the GAP activity and Gαq activation of PLC-β1 may depend on the dimerization of the C tail domain *(Ilkaeva et al., 2002; Paulssen et al., 1996)*.

The existence of homo- and heterodimers of G protein-coupled receptors (GPCRs) has gained widespread acceptance *(Milligan, 2004)*. Heteroligomeric GPCR signaling complexes might easily incorporate PLC-β effector pairs. Indeed, the crystal structure of PLC-βT C tail dimer was modeled to accommodate docking of two molecules of Gαq *(Singer et al., 2002)*. A full understanding of the physiologic role of PLC-β dimerization will require accurate modeling of these enzymes' native microenvironments, including the subplasmalemmal surface and interactions with a wide array of potential binding partners.

Chapter 2 Figure 1

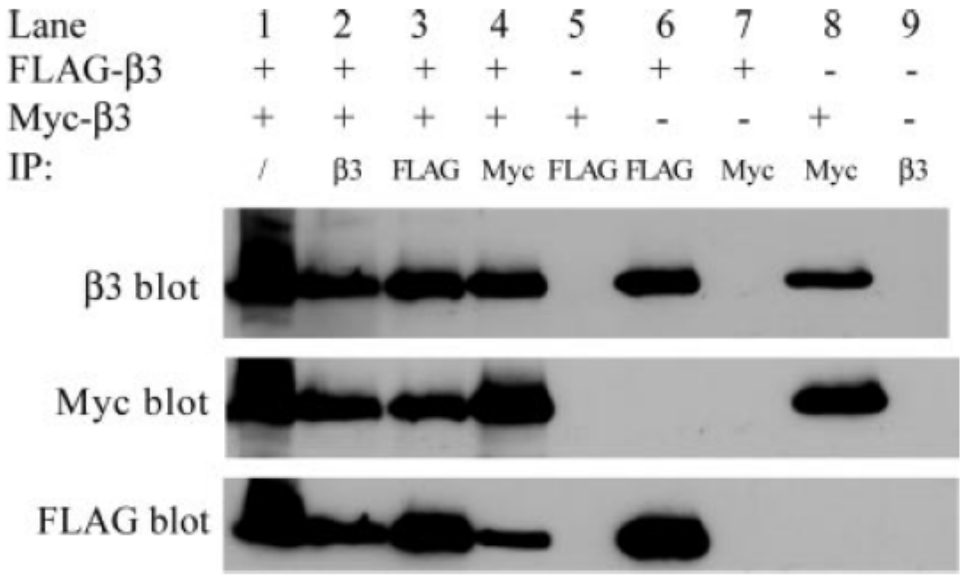

Fig. 2.1 Co-immunoprecipitation of differentially-tagged full-length PLC-β3 constructs.

Vectors encoding full-length human PLC-β3 fused to either amino-terminal FLAG tag (*FLAG-β3; lanes 1-4, 6 and 7*) or amino-terminal Myc tag (*Myc-β3; lanes 1-5 and 8*) were transfected into HEK 293 cells, either separately or together. Cells were harvested 48 h post-transfection and detergent cell extracts were immunoprecipitated with epitope-selective anti-FLAG antibody (*lanes 3, 5 and 6*), anti-Myc antibody (*lanes 4, 7 and 8*) or anti-PLC-β3 antibody (*lane 2 and 9*). Immunoprecipitated sample from non-transfected HEK 293 detergent cell extract is shown in *lane 9*. Detergent cell extracts from Myc-β3 and FLAG-β3 co-transfected HEK 293 lysates precipitated by TCA are shown in *lane 1*. Precipitated samples were size separated by SDS-PAGE and immunoreactive proteins detected by immunoblot with anti-PLC-β3 antibody (*upper blot*), anti-Myc antibody (*middle blot*), or anti-FLAG antibody (*lower blot*). Shown are immunoreactive bands migrating at approximately 150 kDa by SDS-PAGE, representative of two independent experiments.

Chapter 2 Figure 2

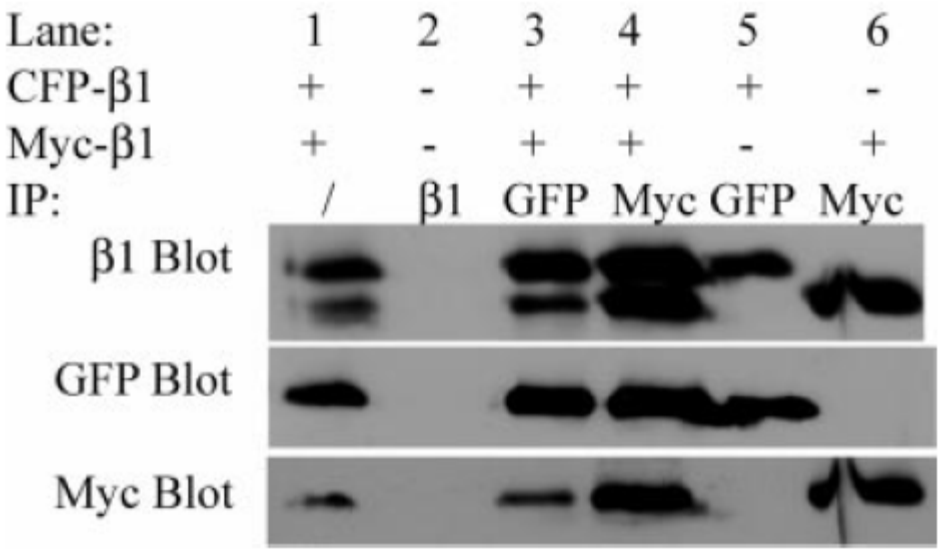

Fig. 2.2 Co-immunoprecipitation of differentially-tagged full-length PLC-β1.

Vectors with sequence encoding full-length PLC-β1 fused to either amino-terminal CFP tag (*CFP-β1; lanes 1, 3, 4 and 5*) or amino-terminal Myc tag (*Myc-β1; lanes 1, 3, 4 and 6*) were transfected into HEK 293 cells either separately or together. Cells were harvested 48 h post-transfection and detergent extracts were immunoprecipitated with anti-GFP/CFP antibody (*lanes 3 and 5*) or anti-Myc antibody (*lanes 4 and 6*). Detergent extracts from cell lysates of non-transfected HEK 293 were immunoprecipitated with anti-PLC-β1 antibodies (*lane 2*). Detergent extract from CFP-β1 and Myc-β1 co-transfected HEK 293 cell lysate was acid precipitated with TCA prior to immunoblotting (*lane 1*). Precipitated samples were size-separated by SDS-PAGE and immunodetected with anti-PLC-β1 antibody (*upper blot*), anti-GFP/CFP antibody (*middle blot*) or anti-Myc antibody (*lower blot*). Shown are immunoreactive bands migrating at approximately 150 kDa (*β1* and *Myc Blots*) and approximately 170 kDa (*β1* and *GFP blots*) by SDS-PAGE, representative of two independent experiments.

Chapter 2 Figure 3

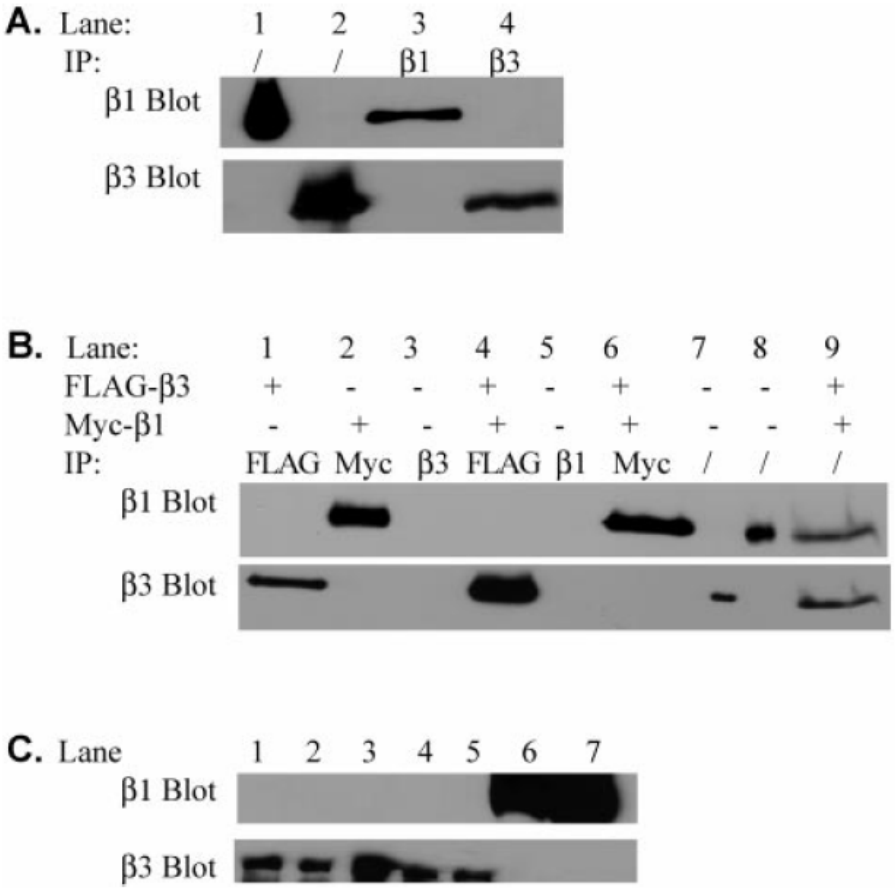

Fig. 2.3 No detection of heterodimer between PLC-β1 and PLC- β3.

(Continued)

(**A)** 1321N1 cells were lysed and detergent extracts were immunoprecipitated with anti-PLC-β1 antibody (*lane 3*) or anti-PLC-β3 antibody (*lane 4*) and were analyzed by immunoblot with anti-PLC-β1 antibody (*upper*) or anti-PLC-β3 antibody (*lower*). Purified PLC-β1 (0.5 μg**;** *lane 1*) and PLC-β3 (0.5 μg**;** *lane 3*) were included as controls. (**B**) Vectors containing sequence encoding either the full-length PLC-β3 fused to amino-terminal FLAG tag (*FLAG-β3; lanes 1, 4, 6 and 9*) or full-length PLC-β1 fused to amino-terminal Myc tag (*Myc-β1; lanes 2, 4, 6 and 9*) were transfected into HEK 293 cells either separately or together. Cells were harvested 48 h post-transfection, and detergent extracts were immunoprecipitated with anti-FLAG antibody (*lanes 1 and 4*), anti-Myc antibody (*lanes 2 and 6*), anti-PLC-β3 antibody (*lane 3*) or anti-PLC-β1 antibody (*lane 5*). Detergent extract from FLAG-β3 and Myc-β1 co-transfected HEK 293 lysate was acid precipitated with TCA (*lane 9*). Purified PLC-β1 (0.5 μg**;** *lane 8*) and PLC-β3 (0.5 μg**;** *lane 7*) were included as controls. Samples were size separated by SDS-PAGE and immunodetected by antibodies to PLC-β1 (*upper*) or PLC-β3 (*lower*). (**C**) Following purification using nickel affinity resin of lysates from High-Five insect cells co-infected to over-express both His_6-tagged PLC-β3 and PLC-β1, column fractions (*1-7*) were analyzed by immunoblot with anti-PLC-β1 antibody (*upper*) or anti-PLC-β3 antibody (*lower*). anes *1-5* represent fractions eluted with 250 mM imidazole while lanes *6* and *7* represent the column flow-through.

Chapter 2 Figure 4

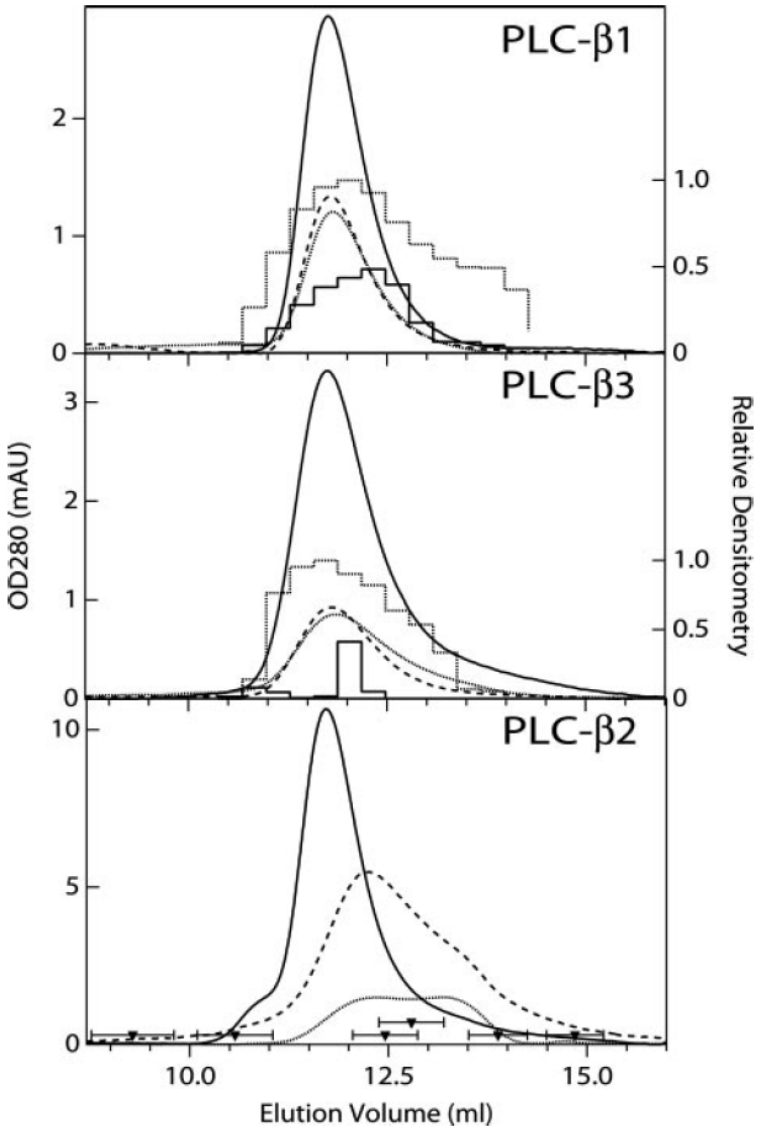

Fig. 2.4 Analytical size-exclusion chromatography of PLC-β1, PLC-β2 and PLC-β3 isolated from High-Five cells.

(Continued)

A Superdex 200 column (Vo = 8.04 ml, Vi = 20.46 ml) was operated as described in Experimental Procedures and calibrated with thyrogloblin (669 kDa), ferritin (440 kDa), catalase (232 kDa), adolase (158 kDa), bovine serum albumin (67 kDa), and ovalbumin (43 kDa). Calibration standard peak positions (Ve) are indicated at the bottom of the figure (▼); associated error bars indicate trace widths at half-height of standards. Elution profiles for experimental samples loaded at concentrations of 250 nM and greater were recorded as absorbance at 280 nm (smooth curves). Elution profiles of 50 nM and less concentrated samples, collected in 0.3 ml aliquots, were analyzed by Western blot and quantitated by Densitometry (squared line histogram traces). Varying concentrations of size-exclusion purified samples of PLC-β were maintained on ice for the indicated times in parentheses. PLC-β1 (*upper panel*): 482 nM (31 h, *solid curve*) eluted at 11.76 ml; 250 nM (3 h, *dashed curve*) eluted at 11.79 ml; 250 nM (24 h, *dotted curve*) eluted at 11.84 ml; 50 nM (22 h) elution peak was centered at 12.0 ml (*dotted squared line*); and 10 nM (5 h) was centered at 12.3 ml (*solid squared line*). PLC-β3 (*middle panel*): 717 nM (29 h, *solid curve*) eluted at 11.75 ml; 250 nM (1.5 h, *dashed curve*) at 11.81 ml; 250 nM (27 h, *dotted curve*) at 11.87 ml; 50 nM (20 h) elution peak was centered at 11.7 ml (*dotted squared line*); and 10 nM (8 h) was centered at 12.0 ml (*solid squared line*). PLC-β2 (*lower panel*): 2.8 μM (0 h, *solid curve*) eluted as single peak at 11.71 ml; 200 nM (2 h, *dashed curve*) eluted at 12.22 ml with a shoulder at approximately 13.5 ml; 200 nM (18 h, *dotted curve*) resolved into two peaks centered at 12.28 and 13.23 ml.

Chapter 2 Figure 5

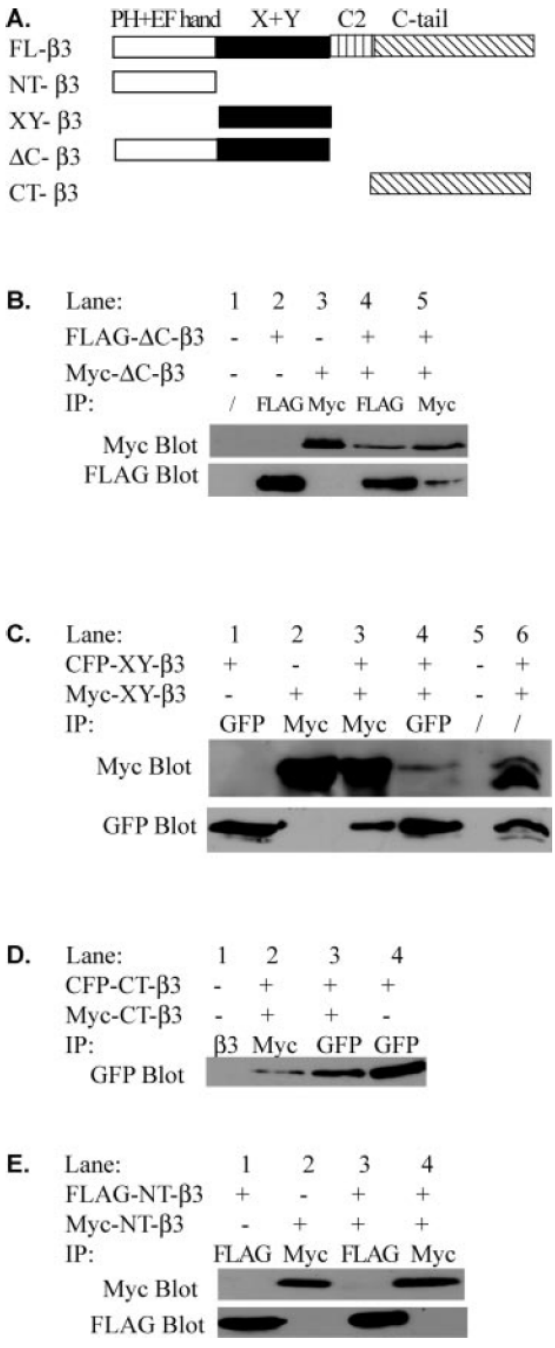

Fig. 2.5 Co-immunoprecipitation of differentially-tagged PLC-β3 subdomain fragments.

(Continured)

(**A**) Shown is a linear schematic of PLC-β3 fragments according to putative structural subdomains based on sequence similarity to known protein structural motifs. White bar indicates fragments spanning a putative PH domain and four EF hand domains (*PH + EF hand*). The black bar indicates a fragment spanning the catalytic X and Y domains and intervening domain (*X + Y*). The vertically hatched bar indicates a fragment with similarity to C2 domains (*C2*), and the diagonally hatched bar represents a fragment encompassing the structurally unique carboxy-terminal third of the protein (*C-tail*). (**B**) Vectors containing sequence for PLC-β3 C2/C-tail deletion mutants fused to either amino-terminal FLAG tag (*FLAG-ΔCβ3; lanes 2, 4 and 5*) or amino-terminal Myc tag (*Myc-ΔCβ3; lanes 3, 4 and 5*) were transfected into HEK 293 cells either separately or together. Cells were harvested 48 h post-transfection and detergent extracts were immunoprecipitated with epitope-selective anti-FLAG antibody (*lanes 2 and 4*) or anti-Myc antibody (*lanes 3 and 5*). Detergent extracts from non-transfected HEK 293 cells were also precipitated by TCA (*lane 1*). Precipitated samples were size separated by SDS-PAGE and immunoreactive proteins detected with anti-Myc antibody (*upper blot*) or anti-FLAG antibody (*lower blot*). Shown are immunoreactive bands migrating at approximately 80 kDa by SDS-PAGE. (**C**) Vectors containing sequence encoding the catalytic domain of PLC-β3 fused to either amino-terminal CFP tag (*CFP-XY-β3; lanes 1, 3, 4, 6*) or amino-terminal Myc tag (*Myc-XY-β3; lanes 2, 3, 4, 6*) were transfected into HEK 293 cells either separately or in combination. Detergent extracts of transfected cell were immunoprecipitated with anti-GFP/CFP antibody (*IP:GFP, lanes 1, 4*) or anti-Myc antibody (*IP:Myc, lanes 2, 3*). Detergent cell extracts from non-transfected HEK 293 cell lysate (*IP:/, lane 5*) or co-transfected HEK 293 cell lysate (*IP:/, lane 6*) were precipitated by TCA as controls. Precipitated samples were immunodetected with anti-Myc antibody (*upper blot*) or anti-GFP/CFP antibody (*lower blot*). Shown are immunoreactive bands migrating at approximately 50 kDa (*upper blot*) and approximately 70 kDa (*lower blot*). (**D**) Vectors containing sequence encoding the C-tail domain of PLC-β3 fused to either amino-terminal CFP tag (*CFP-CT-β3; lanes 2, 3 and 4*) or amino-terminal Myc tag (*Myc-CT-β3; lanes 2 and 3*) were transfected into HEK 293 cells either separately or together. Detergent cell extracts were immunoprecipitated with anti-β3 antibody (*lane 1*), anti-GFP antibody (*lanes 3 and 4*) or anti-Myc antibody (*lane 2*), and immunodetected with anti-GFP/CFP antibody. Shown are immunoreactive bands migrating at approximately 80 kDa. (**E**) Vectors containing sequence encoding the amino-terminal PH and EF hand domains of PLC-β3 fused to either amino-terminal FLAG tag (*FLAG-NT-β3; lanes 1, 3 and 4*) or amino-terminal Myc tag (*Myc-NT-β3; lanes 2, 3 and 4*) were transfected into HEK 293 cells either separately or together. Detergent cell extracts were immunoprecipitated with anti-FLAG antibody (*lanes 1 and 3*) or anti-Myc antibody (*lanes 2 and 4*) and immunoreactive proteins detected with anti-Myc antibody (*upper blot*) or anti-FLAG antibody (*lower blot*). Shown are immunoreactive bands migrating at approximately 40 kDa by SDS-PAGE, representative of two independent experiments.

Chapter 2 Figure 6

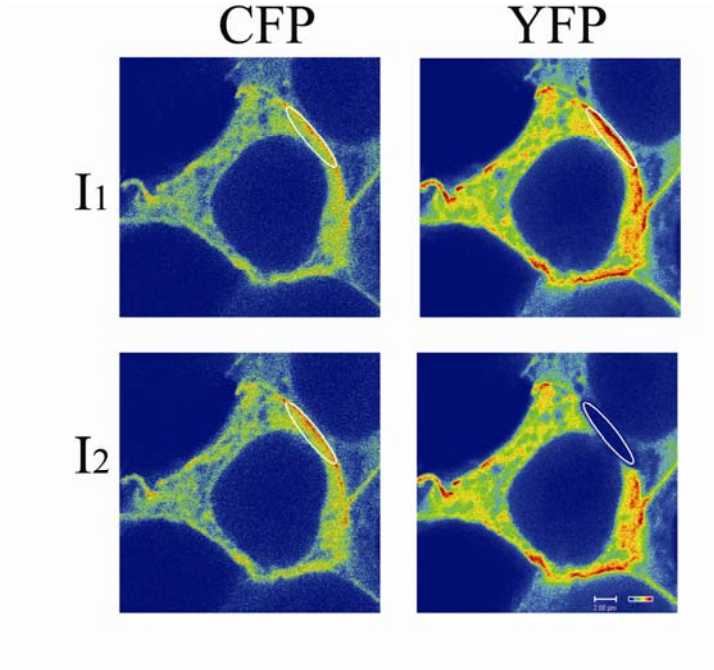

Fig. 2.6 FRET in HEK 293 cells co- transfected with CFP-β3 and β3-YFP plasmids.

HEK-293 cells were co-transfected with vectors constructed to express full-length PLC-β3 fused with CFP or YFP at the amino or carboxy terminus, respectively. Pseudocolored cell images obtained in the YFP emission channel using a LP540 nm filter (*YFP, upper panel*) and in the CFP emission channel using a 470-500 nm filter (*CFP, lower panel*) are shown immediately before (I_1) and after (I_2) photobleaching as described in Experimental Procedures. The region isolated for photobleaching is indicated by the outlined oval. Scale bar shown represents 2 μm. This image represents 52 similarly analyzed images.

Chapter 2 Table 1

Table 2.1 FRET Efficiency between various PLC-β3 and PLC-β1 fluorescently tagged pairs in transfected HEK 293 cells.

Transfection	FRET efficiency
CFP-PLC-β3 + PLC-β3-YFP	5.7 ± 0.4% (n = 52)
CFP-PLC-β3	-0.6 ± 0.7% (n = 32) ***
CFP + YFP	3.0 ± 0.4% (n=30) ***
CFP-PLC-β3 + YFP-PLC-β3	3.0 ± 0.6% (n = 29) ***
CFP-PLC-β1 + PLC-β3-YFP	2.1 ± 0.5% (n = 31) ***
CFP-PLC-β1 + YFP-PLC-β3	3.2 ± 0.7% (n = 21) **

FRET efficiency was assessed by the acceptor photobleaching protocol in HEK 293 cells transfected to express the indicated constructs. Data represent the mean ± the standard error for the number of cells indicated (n). A statistically significant FRET efficiency difference between CFP-PLC-β3 + PLC-β3-YFP transfected cells and all other controls are indicated by ** $p < 0.01$ or *** $p < 0.001$.

Chapter 3: PI(3,4,5)P_3 Potentiates Phospholipase C-β Activity

Yong Zhang, Sun Hyung Kwon, Walter K. Vogel, and Theresa M. Filtz

Molecular Pharmacology

c/o The American Society for Pharmacology and Experimental Therapeutics

9650 Rockville Pike

Bethesda, MD 20814-3995

In progress

Abstract

Phospholipase C-β (PLC-β) isozymes are key effectors in G protein-coupled signaling pathways. Previously, we had shown that PLC-β1 and PLC-β3 bound immobilized PIP_3. In this study, PIP_3 was found to potentiate Ca^{2+}-stimulated PLC-β activities using an *in vitro* reconstitution assay. LY294002, a specific PI 3-kinase inhibitor, significantly inhibited 10 minutes agonist-stimulated total IP accumulation. Both LY294002 and wortmannin inhibited 90 seconds agonist-stimulated IP_3 accumulation in intact cells. Moreover, transfected p110CAAX, a constitutively activated PI 3-Kinase catalytic subunit, increased 90 seconds oxytocin-stimulated IP_3 accumulation. Receptor-ligand binding assays indicated that LY294002 did not affect G protein-coupled receptors directly, suggesting a physiological role for PIP_3 in directly potentiating PLC-β activity. When co-expressed with p110CAAX, fluorescence-tagged PLC-β3 was increasingly localized to the plasma membrane. Conversely, a greater proportion of PLC-β3 associated with cytosolic fraction following H9c2 cells treatment with LY294002. Additional observations suggest that the C-tail domain of PLC-β1 and β3, not the PH or catalytic XY domain, is important for membrane association.

Introduction

Phosphoinositide-specific phospholipase C (PLC) isozymes are key effector enzymes in multiple cellular signaling pathways, hydrolyzing phosphatidylinositol 4,5-bisphosphate ($PI(4,5)P_2$) into inositol 1,4,5-triphosphate (IP_3) and diacylglycerol (DAG), second messengers which subsequently regulate Ca^{2+} release from intracellular stores and protein kinase C activation. To date, thirteen identified mammalian PLC isozymes have been classified by sequence homology into six families, PLC-β, -γ, -δ, -ε, -ζ, and -η, each having a unique mechanism of activation and regulation (Rhee, 2001). The activation of PLC-β isoenzymes is regulated by GTP-bound Gα subunit of $G\alpha_q$ family, Gβγ subunit and the small GTPase Rac (Harden and Sondek, 2006). G protein-coupled receptors (GPCR) that activate PLC-β include angiotensin receptors, histamine receptors, oxytocin receptors, muscarinic receptors, α_1-adrenergic receptors, lysophosphatidic acid receptors and endothelin receptors among many others, indicating the crucial roles of PLC-β in cell signaling cascades (Rhee, 2001).

The PLC-β family exists as four identified isoforms, β1 – β4. Among them, PLC-β1 and β3 are ubiquitously expressed in a variety of tissues, whereas β2 and β4 have limited tissue distribution. Identified by sequence homology, PLC-β isozymes contain at least five distinct structural domains, including a PH (pleckstrin homology), four EF-hand domains, catalytic X and Y domains, a C2 domain, and a unique C-tail (carboxy-terminal) domain (Rhee, 2001). The amino-terminal PH domain of PLC-β is known as a protein interaction domain that binds to Gβγ (Wang et al., 1999b) or Rac1

(Jezyk et al., 2006) in certain contexts. The central XY domain is highly conserved among PLC isozymes and structurally forms a catalytic TIM (Triosephosphate isomerase) barrel to create the catalytic pocket for PI(4,5)P_2 binding (Jezyk et al., 2006). PLC-β isozymes are distinguished by a structurally unique C-tail domain (approximately 400 amino acids) that is involved in regulation by $G\alpha_q$ subunits (Kim et al., 1996b; Rhee, 2001) and dimerization (Ilkaeva et al., 2002; Singer et al., 2002; Zhang et al., 2006).

There are at least eight mammalian phosphatidylinositol 3-kinases (PI 3-kinases) which are divided into three classes according to their structure and substrate specificity. Of particular interest are the class 1 PI 3-kinases, the only class that produces phosphatidylinositol 3,4,5-trisphosphate (PIP_3) and comprises a p110 catalytic subunit and a separate regulatory subunit. Class 1 PI 3-kinases are further subdivided into class 1A (PI 3-kinase-α, -β, -δ), which are activated by receptor tyrosine kinases, and class 1B (PI 3-kinase-γ), which is uniquely activated by heterotrimeric G proteins (Foster et al., 2003). Stimulation of a range of receptors, such as growth factor receptors and G protein-coupled receptors, results in the activation of PI 3-kinases, which generate PIP_3 by phosphorylation of PI(4,5)P_2 at the 3-position of the inositol ring. PIP_3 has been proposed as a second messenger that affects numerous cellular responses, including exocytosis, cytoskeleton remodeling, chemotaxis, and regulation of ion channels (Blazer-Yost and Nofziger, 2005). PIP_3 mediates its effects by directly regulating functional activity and/or acting as a docking site for a number of proteins containing PH domains such as Akt/PKB

(protein kinase B), Btk (Bruton's tyrosine kinase) and GRP1 (general receptor for phosphoinositides-1), and recruiting them to the plasma membrane (Rameh and Cantley, 1999a).

Previously, we have reported that several phosphatidylinositides, including PIP_3, bound PLC-β1 and PLC-β3 *in vitro* using a phospholipid protein overlay assay (McCullar et al., 2007). To further understand the interaction between PIP_3 and PLC-β, we sought to determine the effect of PIP_3 on PLC-β activity *in vitro* and in intact cells. Since PIP_3 is a poor substrate of PLC-β (Serunian et al., 1989), our data suggest that PIP_3 could be an important allosteric regulator of PLC-β activity.

Materials and methods

Materials Carbamylcholine chloride (carbachol) and oxytocin were obtained from Calbiochem (San Diego, California). LY294002 and phosphor-Akt (Ser473) antibody were from Cell Signaling Technology (Danvers, MA) and wortmannin was from LC Laboratories (Woburn, MA). $PI(4,5)P_2$, $PI(3,5)P_2$, PE (Phosphatidylethanolamine) and PIP_3 ($PI(3,4,5)P_3$) were purchased from Avanti Polar Lipids (Alabaster, AL). [^{3}H]oxytocin and [^{3}H]$PI(4,5)P_2$ were from PerkinElmer (Waltham, MA). [^{3}H]myo-inositol and [^{3}H]QNB were from American Radiolabeled Chemicals (St. Louis, MO). Atropine sulfate was from Acros Organics (Geel, Belgium) and OptiPrep solution was from Axis-Shield PoC (Oslo, Norway). PLC-β1 antibody (G12), PLC-β2 antibody, PLC-β3 antibody (H-84), cadherin (C-19) antibody and horseradish peroxidase-conjugated secondary antibody were from Santa Cruz

Biotechnology (Santa Cruz, CA); β-actin antibody was from Abcam (Cambridge, MA).

Plasmids pCDNA3-hOTR (human oxytocin receptor) was purchased from UMR cDNA Resource Center (Rolla, MO) and p110-CAAX was a gift from Dr. Andrew Henderson (Cook et al., 2002). GFP-Akt-PH and GFP-Akt-PH (R25C) were gifts from Dr. Craig Montell (Kwon et al., 2007). PH domain of PLC-β3 (PH-β3, residues 1-138) amplified by PCR (polymerase chain reaction**)** using the following sets of primers: 5'-ATGAATTCATGGCGGGCGCCCAGC-3' and 5'-CTCGAGTCACAGCTTGAATAGCTCCTCAGAC-3' and PH domain of PLC-β1 (PH-β1, residues 1-166) was amplified with 5'GATGTCGACCATGGCCGGGGCTCAAC-3' and 5'-GATGGTACCTCATTCTGGAGTGACTTGCAGCTT-3'. PCR-amplified PH-β3 was ligated into EcoRI and SalI sites of pEGFP-C2 vector (Clontech, Mountain View, CA) and PH-β1 was ligated into SalI and KpnI sites in pEGFP-C4 vector. Full length PLC-β3 was subcloned into EcoRI and XhoI sites of pEGFP-C4 vector. All constructs were confirmed by sequencing.

Cell culture and generation of HEK 293 Cells Stably Expressing OTR 1321N1, H9c2 and HEK 293 cells were cultured in 90% DMEM, 10% fetal bovine serum, 100 units/ml penicillin, and 0.1 mg/ml streptomycin at 37°C under 5% CO_2 in humidified air (Zhang et al., 2006). One day prior to transfection, HEK 293 cells were plated at a density of 5×10^5 cells/10 cm culture dish. pCDNA3-OTR plasmid (4 μg /10 cm plate), which includes a neomycin resistance gene, was transfected into cells using JetPEI kit

(Polyplus-transfection, New York, NY) according to the manufacturer's instructions. Forty-eight hours after transfection, cells were selected by treatment with 0.7 mg/ml G418 for at least 4 weeks following transfection. Drug-resistant clones were isolated, expanded and evaluated for OTR receptor expression by binding assay as described below.

Protein expression and purification PLC-β1, PLC-β2, PLC-β3, $G\alpha_{11}$ and $G\beta_1\gamma_2$ were expressed in Sf9 cells following baculovirus infection and purified as described previously (Kozasa, 2004; Zhang et al., 2006).

Reconstitution assay The catalytic activity of PLC-β was quantitated using $[^3H]PIP_2$ substrate as described previously (McCullar et al., 2007). Briefly, 35 ng of purified PLC-β3 was added in 20 μl Buffer 1 (50mM HEPES pH 7.2, 3 mM EGTA, 80 mM KCl, 1mM DTT). 15 μM $PI(4,5)P_2$, 135 μM PE, and 9000 DPM $[^3H]PI(4,5)P_2$ with or without 5 μM PIP_3 or 5 μM $PI(3,5)P_2$ were dried under nitrogen and resuspended in 20 μl Buffer 1 by 3 × 10 sec bursts of sonication. For assay of G-protein-stimulated activity of PLC-β, 10 μl of Buffer 2 (50 mM HEPES pH 7.2, 1mM EDTA, 3 mM EGTA, 5mM $MgCl_2$, 1 mM DTT, 100 mM NaCl, 1% cholate) containing 60 ng Gβγ or 50 ng Gα11 with or without prior activation by 0.15 μM GTPγS was added to each reaction. For assays of Ca^{2+}-stimulated (non-G protein activated) PLC-β activity, 12 ng PLC-β1, 40 ng PLC-β2 or 35 ng PLC-β3 was added in Buffer 2 without G-protein along with 10 μl Buffer 1 with 9 mM $CaCl_2$ to yield a final assay volume of 60 μl. Reactions were incubated at 30°C for 12 min and terminated by the addition of 375 μl of chloroform, methanol and hydrochloric acid in

a ratio of 80:40:1, followed by the addition of 125 µl chloroform and 125 µl 0.1 N HCl with vigorous mixing. Aqueous and organic phases were separated by centrifugation for 5 min at 3000 ×g. [^{3}H]IP_3 product was quantitated by scintillation counting of 320 µl of the upper phase. Triplicate samples were tested in two separate experiments.

Inositol phosphate assay Whole cell inositol phosphate (IP) assays were performed in 1321N1 cells or HEK 293 cells expressing OTR as previously described (McCullar et al., 2007). 1×10^5 1321N1 cells or HEK 293 cells were subcultured in 24-well plates overnight and then labeled overnight with 2 mCi/ml [^{3}H]myo-inositol in bicarbonate-buffered inositol-free DMEM without additives. For assay, cells were pre-treated with 0.1% DMSO or 50 µM LY294002 for 30 min in 10 mM LiCl, 20mM Hepes-buffered DMEM (pH 7.4) at 37°C in room air. 1321N1 cells were stimulated with 1 mM carbachol and HEK 293 were stimulated with 100 nM oxytocin for 10 min. Cells were lysed and total inositol phosphates (IP) were extracted and quantitated.

Inositol trisphosphate (IP_3) accumulation assay 1321N1 cells or HEK 293 cells stably expressing hOTR were seeded at 2×10^5 cells/well in 12-well plates, allowed to attach overnight, and labeled for 18 h with 2 mCi/ml [^{3}H]myo-inositol in inositol-free, bicarbonate-buffered DMEM. Following radiolabeling, cells were pre-treated with 0.1% DMSO or 50 µM LY294002 or 0.5 µM wortmanin for 30 min in 0.5 ml 10 mM LiCl, 20mM Hepes-buffered DMEM (pH 7.4) at 37°C in room air. 1321N1 cells were then stimulated with 1 mM carbachol and HEK 293 cells was stimulated with 100 nM oxytocin for 90 second. The reaction was stopped by adding 1 ml 15% trichloroacetic

acid solution directly to the wells. The cell lysates were extracted three times with ether and IP_3 was separated by anion exchange chromatography and quantitated as described previously (McCullar et al., 2007). Briefly, 2 ml H_2O was added to the extracted cell lysates which were applied to 0.5 ml of AG1-X8 anion-exchange resin (Formate form, 200–400 mesh, Bio-Rad) in chromatography columns. Columns were rinsed with 8 ml dH_2O, washed with 10 ml 25 mM sodium borate, 60 mM sodium formate, and eluted with 5 ml 0.1 M formic acid/0.2 M ammonium formate (IP containing fraction), 5 ml 0.1 M formic acid/0.4 M ammonium formate (IP_2 containing fraction), and 5 ml 0.1 M formic acid/1.0 M ammonium formate (IP_3 containing fraction).

Membrane preparation 1321N1 cells or HEK 293 cells were washed thrice with ice-cold PBS, collected by scraping, and pelleted at 500 ×g for 5 min. Ice-cold hypotonic lysis buffer (25 mM Hepes, pH 7.4, 2 mM EDTA, 0.1 mM PMSF, 1 μM pepstatin A, 10 μM leupeptin) was added to each sample and incubated on ice for 15 min. Cells were lysed with 15 strokes of a Dounce homogenizer and the lysate centrifuged at 500 ×g, 4°C for 5 min to pellet nuclei and intact cells. The resulting supernatants were centrifuged at 200,000 ×g, 4°C for 30 min. The resulting crude membrane pellets were suspended in binding buffer (25 mM Tris, pH 7.4, 10 mM $MgCl_2$, 0.1 mM PMSF, 1 μM pepstatin A, 10 μM leupeptin). Protein concentration was determined using Bradford reagent (Bio-Rad, Hercules, CA) with BSA as standard (Bishop and Stormshak, 2006).

Receptor binding assays Cell membranes were diluted to 0.5-1 μg/μl in binding buffer (25 mM Tris, pH 7.4, 10 mM $MgCl_2$, 0.2% BSA). Total binding assays (200 μl final volume) containing 50-100 μg cell membranes, varying concentrations of [^{3}H]OT (for transfected HEK 293 membranes) or [^{3}H]QNB (for 1321N1 cell membranes) and 50 μM LY294002 or 0.1% DMSO vehicle were incubated at 30°C for 30 min. Nonspecific binding was assessed by including 2 μM unlabeled OT for [^{3}H]OT binding or by including 0.1 mM atropine sulfate for [^{3}H]QNB binding. Following incubation, assays were filtered though No. 32 glass-fiber filters (Whatman, Sanford, ME) on a Brandel Cell Harvester (Gaithersburg, MD), washed three times with ice-cold binding buffer and radioactivity retained by filters quantitated using a Beckman LS 6500 Scintillation counter (Bishop and Stormshak, 2006).

Fluorescence microscopy HEK 293 cells grown on poly-lysine coated glass cover slips were transiently transfected by JetPEI kit with 100 ng of plasmid DNA. Cells were washed twice with PBS after 48 h transfection, fixed in 3% formaldehyde (Tousimis, Rockville, MD) for 20 minutes at room temperature, and mounted on slides with a ProLong antifade kit (Molecular Probes, Eugene, OR). Confocal images were obtained using a Zeiss LSM510 confocal microscope (Carl Zeiss, Thornwood, NY) with a 63× oil immersion objective as previously described (Zhang et al., 2006).

OptiPrep density gradient centrifugation and Western blot OptiPrep (60% iodixanol) density gradient to isolate post-nuclear membranes from cytosol was performed as described in the manufacturer's protocol (Axis-Shield application S28). Briefly, H9c2 cells were lysed in ice-cold hypotonic buffer (25 mM Hepes, pH 7.4, 2

mM EDTA, 0.1 mM PMSF, 1 uM pepstatin A, 10 uM leupeptin) and homogenized by 15 strokes using a Dounce homogenizer. After removal of nuclei and intact cells by low speed centrifugation (500 ×g for 5 min), the resulting supernatant (166 μl) was mixed with 50% OptiPrep solution to make a final 30% solution. On top of the 30% sample layer, 500 μl of 25% OptiPrep solution and 100 μl of 5% OptiPrep solutions were overlaid to achieve a discontinuous gradient. The OptiPrep gradient was centrifuged at 120,000 rpm (510,000 ×g) for 1h at 4°C in a Beckman TLX Optima ultracentrifuge, using the TLA 120.2 rotor. After collecting the 5%/25% interface (membranes) and the bottom 30% fraction (cytosol), proteins were precipitated with chloroform and methanol before separation by SDS-PAGE and visualization by western blot. For phosphor-Akt assay, cells were serum-starving overnight before pretreatment with vehicle or inhibitor in Kreg's solution (118 mM NaCl, 4.69 mM KCl, 1.18 mM $MgSO_4$, 1.29 mM $CaCl_2$, 1.18 mM KH_2PO_4, 11.67 mM glucose, and 25mM Hepes, pH 7.4) for 30 min and stimulation with agonists. All primary antibodies were used at a concentration of 0.1 μg/ml, and secondary antibodies at 0.04 μg/ml. Immunoreactive bands were detected using SuperSignal West Pico chemiluminescent substrates (Pierce, Rockford, IL).

Curve fitting and data analysis Curve fitting and data analysis were performed using GraphPad Prism 4 (GraphPad software, San Diego, CA). All saturation isotherm specific binding data were best fit to a one-site binding parabola. Data are presented as mean ± S.E.M with $p < 0.05$ considered significant as determined by Student's unpaired two-tailed *t*-test.

Results

PIP_3 increases Ca^{2+}-stimulated PLC-β activity *in vitro* Previously, we had shown that several phospholipids, including PIP_3, could bind PLC-β1 and PLC-β3 using a phopholipid blot (PipStrip®) protein overlay with antibody detection (McCullar et al., 2007). Because PIP_3 is critical in the signaling transduction, we sought to determine whether PIP_3 affected PLC-β activity *in vitro*, despite a lack of known PLC-β hydrolytic activity towards PIP_3. A reconstitution assay was performed using purified PLC-β protein, purified G protein subunits with or without activator (GTPγS) and purified lipids. As illustrated in Figure 1A, PIP_3 increased basal (in the presence of inactivated $G\alpha_{11}$) PLC-β3 activity by 38.7% while having no effect on PLC-β3 activity stimulated by GTPγS-activated $G\alpha_{11}$ ($G\alpha_{11}$ + GTPγS). PIP_3 also increased Ca^{2+}-stimulated PLC-β3 activity by 54.1% but not Gβγ-stimulated PLC-β3 activity (Fig. 1B). Importantly, $PI(3,5)P_2$, another negatively charged non-substrate phospholipid, did not change either Ca^{2+}-stimulated or Gβγ-stimulated PLC-β3 activity (Fig. 1C), suggesting a unique effect of PIP_3 compared to other phosphoinositol phospholipids. Moreover, PIP_3 potentiated the Ca^{2+}-stimulated activities of PLC-β3 as well as PLC-β1 and PLC-β2 by 60.7% and 30.4%, respectively (Fig. 1D), suggesting a general effect of PIP_3 on Ca^{2+}-stimulated PLC-β isozyme activities.

PI 3-Kinase inhibitor inhibits PLC activity in whole cells To ascertain the potential PIP_3 effect on PLCβ activity in a more physiological context, we treated

1321N1 cells with LY294002 (LY), a specific phosphoinositide 3-kinase (PI 3-Kinase) inhibitor**,** and assayed for inositol phosphates (IP) accumulation. 1321N1 cells express muscarinic receptors which are coupled to PLC-β, presumably PLC-β1 (Kim et al., 1997a). In the unstimulated basal state, LY294002 did not affect IP accumulation in 1321N1 cells. However, when 1321N1 cells were stimulated for 10 minutes with 1 mM carbachol, a muscarinic receptor agonist, LY294002 significantly inhibited carbachol-stimulated IP accumulation. LY294002 inhibition of carbachol-stimulated IP accumulation was dose dependent with 10 μM and 50 μM LY294002 significantly inhibiting IP hydrolysis by 20.6% and 43.6%, respectively (Fig. 2A).

To determine whether the inhibition of PLC activity by LY294002 was cell line specific or receptor specific, similar experiments were conducted in another cell model, transfected HEK 293 cells stably expressing human oxytocin receptor (hOTR). HEK 293 cells express PLC-β1 and PLC-β3 predominantly and hOTR receptors presumably couple to PLC-β3 (Zhong et al., 2003). In this system, 50 μM LY294002 had no significant effect on basal IP accumulation but markedly inhibited 100 nM oxytocin (OT)-stimulated IP accumulation by 45.0% (Fig. 2B). Similar data were obtained in HEK 293 cells expressing ovine OTR (data not shown).

To verify the activity of LY294002 in whole cells to reduce PIP_3 levels by inhibition of PI 3-kinase, we monitored Akt phosphorylation which is responsive to changing PIP_3 levels (Rameh and Cantley, 1999b). In unstimulated cells, weak Akt phosphorylation was detected in 1321N1 cells (Fig. 2C, lane 1) and 50 μM LY294002 was without effect as expected (Fig. 2C, lane 2) by monitoring with phospho-specific

anti-Akt antibodies. However, when 1321N1 cells were treated with 1 mM carbachol for 10 minutes to stimulate PLC-β activity, phospho-specific Akt bands were noticeably increased in intensity (Fig. 2C, lanes 3 and 4); carbachol-induced Akt phosphorylation was abolished by treatment with LY294002 (Fig. 2C, lanes 5 and 6). Similar LY294002 effect on oxytocin (OT)-induced Akt phosphorylation was observed in OTR-expressing HEK 293 cells (data not shown).

PI 3-Kinase activity is related to PLC-β activity in whole cells To rule out the involvement of other PLC isozymes besides PLC-β in IP accumulation stimulated by 10 minutes of agonist treatment (e.g. transactivation of PLC-δ or PLC-ε), we repeated the above experiments restricting agonist treatment to 90 seconds and selectively recovering IP_3 for quantitation. Previous experiments demonstrated that the majority of IP_3 production following G protein-coupled receptor activation was attributable to PLC-β activation when cells were stimulated by agonists up to 90 seconds (Kelley et al., 2006). 50 μM LY294002 had no effect on basal IP_3 accumulation but inhibited 90 seconds carbachol-stimulated IP_3 accumulation by 47 % in 1321N1 cells or oxytocin-stimulated IP_3 accumulation by 60 % in hOTR expressing HEK 293 cells (Fig. 3A and 3B). Furthermore, LY294002 inhibited IP_3 accumulation by 59 % in H9c2 cells, rat myoblast cells which exclusively express PLC-β3 but not other PLC-β isozymes (supplemental data, Fig. 10), when stimulated with carbachol for 90 seconds (data not shown).

To substantiate that LY294002 was blocking PI 3-kinase to inhibit agonist-stimulated IP3 accumulation, we reproduced the effects of LY294002 to inhibit 90

seconds OT-induced IP3 accumulation in hOTR expressing HEK 293 cells with a structurally unrelated PI 3-kinase inhibitor, wortmannin, as shown in Fig. 3C. Wortmannin (500 nM) inhibited oxytocin-stimulated IP_3 accumulation by 29 % while it had no effect on basal IP_3 accumulation. The difference in effectiveness of wortmannin versus LY294002 in this system (29 % versus 60%) is attributable to the sub-maximal dose of wortmannin chosen to avoid non-selective inhibition of myosin light chain kinase at 1 μM or greater (Nakanishi et al., 1992).

To attempt to address the effects of increased PIP_3 levels on PLC-β activity, we measured agonist-stimulated IP_3 accumulation in cells transfected with p110CAAX, a constitutively activated PI 3-Kinase catalytic subunit widely used to increase cellular PIP_3 concentration (Cook et al., 2002; Egawa et al., 1999). In hOTR expressing HEK 293 cells, p110CAAX transfection increased oxytocin-stimulated IP_3 accumulation by 25.9% compared to non-transfected cells (Fig. 4A). Phospho-Akt Western blot assays suggested that over-expression of p110CAAX induced Akt phosphorylation (Fig. 4B, lanes 3 and 4) as compared to mock transfected HEK 293 cells (Fig. 4B, lanes 1 and 2) in the absence of agonist stimulation. Thus, increasing PI 3-kinase activity does not affect basal IP_3 levels, but potentiates agonist-stimulated IP_3 accumulation.

PI 3-Kinase inhibitor does not affect G protein-coupled receptors To address whether LY294002 may reduce PLC-β-mediated signal transduction by directly inhibiting G protein-coupled receptors, receptor-ligand binding assays were conducted. As illustrated in Fig. 5A, 1321N1 cells exhibited saturable and specific muscarinic

receptor binding sites for [^{3}H]QNB. 50 μM LY294002 had no effect on [^{3}H]QNB specific binding in terms of total binding sites or affinity for [^{3}H]QNB. No significant differences in the apparent B_{max} values (41.0 ± 2.0 vs. 39.5 ± 1.74 fmol/mg protein for control and LY294002 treated groups, respectively) or the apparent K_d values (3.12 ± 0.37 vs. 3.02 ± 0.32 nM for control and LY294002 treated groups, respectively) were detected between DMSO vehicle treatment and LY294002 treatment.

In addition, [^{3}H]OT binding assay was performed in hOTR expressing HEK 293 cells (Fig. 5B). When membrane preparations from HEK 293 cells were treated with 0.1% DMSO or 50 μM LY294002, the specific [^{3}H]OT binding curves almost overlapped. As above, no significant differences in the apparent B_{max} values (601.0 ± 9.3 vs. 592.7 ± 7.3 fmol/mg protein for control and LY294002 treatment groups, respectively) or the apparent K_d values (4.38 ± 0.19 vs. 4.13 ± 0.14 nM for control and LY294002 treated groups, respectively) were detected. These data suggest LY294002 had no direct effect on agonist binding to G protein-coupled receptors to inhibit IP accumulation.

Membrane association of PLC-β3 is related to PIP_3 PIP_3 has been well documented to act as a docking site for a range of proteins containing pleckstrin homology (PH) domains, such as Akt/PKB, by recruitment to the plasma membrane (Rameh and Cantley, 1999a). To further dissect the mechanism by which PIP_3 potentiates PLC-β activity, we attempted to assess PLC-β3 localization under varying cellular PIP_3 concentrations. We sought to detect the intracellular localization of PLC-β3 under conditions of increased PIP_3 levels by co-transfecting constitutively activated

p110CAAX with GFP (green fluorescent protein)-tagged PLC-β constructs. As control experiments for visualizing membrane and cytoplasmic protein localization, GFP-tagged Akt-PH domain, a PIP_3 binding probe, or a non-PIP_3 binding mutant, GFP-Akt-PH (R25C) was transfected into HEK 293 cells (Kwon et al., 2007). As expected, GFP-Akt-PH was exclusively localized at membrane (Fig. 6A, left panel), whereas its non-PIP_3 binding mutant, GFP-Akt-PH (R25C), was expressed in the cytosol and nuclei (Fig. 6A, right panel). When GFP-PLC-β3 was co-transfected with vector (pSG5) into HEK 293 cells, PLC-β3 mainly localized to the cysotol (Fig. 6B, left panel). This majority cytosolic localization of transfected GFP-PLC-β3 is a pattern that we have observed previously (Zhang et al., 2006). Interestingly, GFP-PLC-β3 was increasingly localized to the plasma membrane when co-transfected with p110CAAX into HEK 293 cells (Fig. 6B, right panel), suggesting that increased PIP_3 levels in the p110CAAX-transfected cells may influence PLC-β3 subcellular localization.

To further investigate the relation between PLC-β3 localization and PIP_3 concentration, we employed H9c2 cells and separated cell membrane and cytosolic fractions by OptiPrep discontinuous gradients. Of interest, in control H9c2 cells (DMSO vehicle-treated), nearly all endogenous PLC-β3 is detected in the membrane fraction (Fig. 7, lanes 2 and 4 in top panel). However, after H9c2 cells were treated with 50 μM LY294002, increased PLC-β3 was detected in the cytosolic fraction as compared to controls (Fig. 7, lanes 3 and 4 in top panel). As a control for sample loading, β-actin expression detected by Western blot was similar in both cytosolic fractions regardless of treatment (Fig. 7, lanes 3 and 4 in middle panel). Cadherin, a

membrane selective marker, was not detectable in the cytosolic fractions, suggesting no detectable membrane contamination (Fig. 7, lanes 3 and 4 in bottom panel). These studies suggest that inhibition of PI 3-kinase by LY294002, and presumably a decrease in PIP_3 levels, cause PLC-β to have somewhat lowered affinity for the plasma membrane of H9c2 cells.

The C-tail, but not PH or XY, domain of PLC-β is important for membrane association of the full length protein To further delineate the domain of PLC-β involved in membrane localization and potential PIP_3 interaction, GFP tagged subdomain fragments of PLC-β1 or PLC-β3 were constructed and transfected into HEK 293 cells. First, the PH domain of PLC-β was examined because PH domains have been described in multiple protein contexts as phosphoinositide binding domains (Lemmon, 2007) and PLC-β has a putative PH domain homology sequence at its amino terminus (Jezyk et al., 2006). Both the GFP tagged PH domain of PLC-β1 (Fig. 8A, left panel) and PLC-β3 (Fig. 8A, right panel) were detected predominantly in the cytosol of transfected HEK 293 cells. Co-expression of either PH construct with p110CAAX did not affect the localization pattern (data not shown). Secondly, the subcellular localization of the catalytic XY domain was examined because XY domains bind PIP_2, the primary PLC-β substrate. Similarly to the PH domain, the GFP-tagged XY domains of PLC-β1 and PLC-β3 were found predominantly in the cytosol of transfected HEK 293 cells (Fig. 8B); no change was observed upon co-transfection with p110CAAX (data not shown). These data suggested other domains

of PLC-β besides the PH domain and catalytic XY domains, are important for PLC-β membrane association.

Previous studies indicated that polybasic amino acid clusters bind negatively charged PIP_2 and PIP_3 to target proteins to the plasma membrane (Heo et al., 2006). A sequence alignment analysis among human PLC-β family isozymes by Clustal W software identified two polybasic cluster motifs within the C-tail domain of PLC-β (Fig. 9A) (Kim et al., 1996b). Within these two clusters, positively charged amino acids (arginine and lysine) and hydrophobic amino acids (such as valaine and leucine) were discovered conserved among PLC-β family. Similarly to the Ak-PH domain, the GFP tagged C-tail domains of PLC-β1 (Fig. 9B, left panel) and PLC-β3 (Fig. 9B, right panel) including the two polybasic clusters were exclusively localized at the plasma membrane. Co-expression with p110CAAX had no further effect on the C-tail domain localization (data not shown).

Discussion

Previously, we observed that PLC-β bound PIP_3 along with several other anionic phospholipids on nitrocellulose membranes, implying that PIP_3 might have an effect on PLC-β (McCullar et al., 2007). In the present study, we quantitated PIP_3's effect on PLC-β activity *in vitro,* defined the effect of blocking PIP_3 increases with PI 3-kinase inhibitor on inositol phosphate accumulation in whole cells, and investigated the role of PIP_3 in PLC-β3 localization. Cumulatively, these data support a role for PIP_3 in potentiating Ca^{2+}-stimulated PLC-β activity.

Our *in vitro* phospholipase activity data suggest that PIP_3 potentiates Ca^{2+}-stimulated, but not G protein-stimulated, PLC-β activity (Fig. 1). Previous studies have determined that PIP_3 is a very poor substrate of PLC-β (Serunian et al., 1989), which excludes the possibility that the increased IP_3 accumulation was a result of hydrolysis of PIP_3 at the concentrations tested. In addition, $PI(3,5)P_2$, another negatively charged phosphatidylinositol phospholipid, did not affect PLC-β3 activity, which is consistent with other studies showing that $PI(3,4)P_2$ has no effect on PLC-β activity (Bae et al., 1998). These data illustrate that the effect of PIP_3 on PLC-β is specific and not due to non-specific binding of anionic phospholipids. Thus, PIP_3 ptoentially allosterically increases Ca^{2+}-stimulated PLC-β activity.

In our *in vitro* assay system, free Ca^{2+} concentration is 0.15 μM, which is in the range of normal physiological Ca^{2+} concentrations (0.05-0.5 μM). PLC-β catalytic activity is very sensitive to changes in Ca^{2+} in the physiological range (Jhon et al., 1993a; Young et al., 2003). Moreover, by pre-incubating whole cells with EGTA and

thapsigargin to block the increase of cytosolic Ca^{2+}, IP_3 production stimulated by carbachol in SH-SY5Y cells was reduced by 47 ± 4% (Wojcikiewicz et al., 1994). Thus 50% of the activation of PLC-β in whole cells following GPCR stimulation may be attributable to the feed forward rise in cytosolic Ca^{2+} to further stimulate PLC-β in a very short time frame. Therefore, although PIP_3 appears to mostly affect Ca^{2+} stimulated PLC-β activity *in vitro*, it may significantly affect GPCR-stimulated IP accumulation in whole cells.

To test this hypothesis, we used LY294002 and wortmannin, structurally unrelated and widely studied PI 3-kinase inhibitors. LY294002 (50 μM) completely and specifically abolishes PI 3-kinase activity, but not other protein kinases such as PKA, PKC, MAP kinase, Src or diacylglycerol kinase (Vlahos et al., 1994). Furthermore, multiple reports have demonstrated that LY294002 does not affect the cellular level of PIP_2, a substrate of PLC-β (Cheatham et al., 1994; Tolloczko et al., 2004; Vlahos et al., 1995; Vlahos et al., 1994). Here, we observed that LY294002 inhibited carbachol and OT-stimulated IP accumulation in 1321N1 cells and HEK 293 cells expressing OTR, respectively (Fig. 2). LY294002 inhibition of OT effects was reproduced with wortmannin. However, wortmannin has a lower selectivity for PI 3-kinase than LY294002, so we limited dose to 0.5 μM resulting in consistent but reduced effectiveness compared to LY294002.

Our findings of PI 3-kinase inhibition leading to reduced agonist-induced IP_3 accumulation are reminiscent of previous reports. LY294002 diminished serotonin - induced inositol phosphate formation in primary cultures of rat smooth muscle cells

(Tolloczko et al., 2004). Wortmannin (0.1 μM) inhibited lysophosphatidic acid-induced IP_3 formation by 50% in Cos-7 cells (Razzini et al., 2000). However, a mechanism for these observations was not previously determined.

Although carbachol and oxytocin are agonists for $G\alpha_q$-coupled receptors and can activate PLC-β, other PLC isoforms, such as PLC-γ, PLC-δ or PLC-ε, might be trans-activated when cells are stimulated for 10 minutes. A recent study demonstrates that PLC-β3 is predominantly involved in acute IP accumulation (up to 90 seconds) while PLC-ε is involved in sustained IP accumulation when Rat-1 fibroblast cells are stimulated by different agonists for G protein-coupled receptors (Kelley et al., 2006). To rule out the involvement of PLC isozymes besides PLC-β in LY294002 inhibition of IP accumulation, 1321N1 cells, HEK 293 cells expressing OTR, and H9c2 cells were stimulated with agonists for only 90 seconds and assayed for IP_3 accumulation. LY294002 inhibits IP_3 accumulation at the early time point (Fig. 3 and data not shown).

LY294002 does not affect agonist binding to G protein-coupled receptors in our system. From our [^{3}H]QNB binding data in 1321N1 cells and [^{3}H]OT binding data in HEK 293 cells expressing OTR, no change of apparent B_{max} or K_d were observed when cell membrane fractions were treated with LY294002 (Fig. 4). Nevertheless, LY294002 may affect G protein-coupled activation of phosphatidylinositol phospholipid hydrolysis through targets in the signaling cascade between agonist activation of the receptor and stimulation of PLC-β. RGS (Regulator of G Protein Signaling) proteins are important signaling factors involved in regulation of IP_3

accumulation. Previous reports suggest that PIP_3 binds to RGS4 and inhibits its GTPase-accelerating activity (Ishii et al., 2002; Popov et al., 2000b). Suppression of RGS inhibition activity may play a role in potentiation of PLC-β activity by PIP_3 in whole cell assays. While we do not rule out an effect of PIP_3 to stimulate PLC-β by attenuation of RGS inhibition, our *in vitro* assay data demonstrate that PIP_3 can directly affect PLC-β activity. Defining the relative overall contribution of RGS suppression and direct potentiation of PLC-β activity by PIP_3 to increase agonist-induced inositol phosphate accumulation awaits further study.

To define a possible mechanism by which PIP_3 potentiates PLC-β activity in whole cells, we investigated the effect of increased PIP_3 levels on the localization of PLC-β3 by co-transfecting p110CAAX, a constitutively active PI 3-kinase (Cook et al., 2002; Egawa et al., 1999). Interestingly, more PLC-β3 localized at the membrane in cells co-transfected with p110CAAX (Fig. 6).

PIP_3 recruits several PH domain-containing proteins to the plasma membrane (Rameh and Cantley, 1999a). Although the PH domain of PLC-δ1 binds $PI(4,5)P_2$ with high affinity and specificity (Garcia et al., 1995), the PH domain of PLC-β was found predominantly in the cytosol of transfected HEK 293 cells (Fig. 8), suggesting other domains of PLC-β are important for membrane association. Previous work on the structure of PLC-β2 (Jezyk et al., 2006), as well as homology models of PLC-β isozymes (Singh and Murray, 2003), indicate that the PLC-β PH domains lack electrostatic potentials to bind phosphoinositide phospholipids with any significant affinity.

To identify a potential PIP_3 binding domain in PLC-β3, we scanned the amino acid sequence for polybasic clusters that may bind negatively charged lipids for membrane targeting (Heo et al., 2006). Two polybasic amino acid clusters were identified within the C-tail of PLC-β3 (Fig. 9); these clusters were previously identified in PLC-β1 as involved in $G\alpha_q$-dependent activation (Kim et al., 1996b). Additionally, the crystal structure of the C-tail of turkey PLC-β is highly electrostatically polarized with a large basic surface (Singer et al., 2002), suggesting a role the C-tail domain in membrane and anionic phospholipid binding.

Lipids are known to be important in PLC regulation. PLC-γ can be activated by PIP_3. The PH domain and Src homology 2 (SH2) domains of PLC-γ have been proposed to be important for PIP_3 binding (Bae et al., 1998; Falasca et al., 1998). PI 3-kinase inhibitor (LY294002) blocks the stimulation of PLC-γ activity by calcium in human keratinocytes (Xie et al., 2005), which is similar to our *in vitro* data on LY294002 inhibition of Ca^{2+}-stimulated PLC-β activity. Phosphatidic acid (PA) has been demonstrated to bind PLC-β1 and increases Ca^{2+}-stimulated activity *in vitro* (Litosch, 2000) through a region that includes the αA helix and flexible loop of the $G\alpha_q$-binding domain of the C tail (Ross et al., 2006). Moreover, one group has reported that the PLC-β1 PH domain translocates rapidly but transiently to the plasma membrane upon stimulation of cells with serum or lysophosphatidic acid, and the PLC-β1 PH domain appears to bind PI-3P *in vitro* (Razzini et al., 2000).

Interestingly, modulation of PI 3-kinase has been reported to affect agonist-stimulated smooth muscle contraction (Northcott et al., 2005; Su et al., 2004), a

physiological effect of PLC-β activation (Murthy and Makhlouf, 1995a; Murthy and Makhlouf, 1995b). In aortic strips from normal Wistar-Kyoto rats, LY294002 inhibits noradrenaline-induced contraction mediated by α1-adrenergic receptors coupled to $G\alpha_q$ (Northcott et al., 2005). Similarly, using intact medial strips of the swine carotid artery, histamine-stimulated contraction was significantly decreased in the presence of LY294002 (Su et al., 2004). A PI3Kγ knockout study indicated that PI3Kγ makes a small but significant contribution to thrombin-stimulated calcium response in platelets (Lian et al., 2005), suggesting that PI3Kγ, which is uniquely activated by heterotrimeric G proteins (Foster et al., 2003), plays a role in the PLC-β-mediated release of calcium. However, LY294002, an inhibitor affecting all known PI 3-kinases, impairs the thrombin-induced calcium rise by a larger extent (Lian et al., 2005), implicating that more than one PI 3-kinase isoforms, rather than PI3Kγ alone, are involved in PLC-β activation, presumably through elevation of PIP_3. These data support our findings for a physiological relevance of PIP_3 effects on PLC-β at the organ level. Although these phenomena are intriguing, the related molecular mechanisms for LY294002 inhibition of PLC-β-dependent processes were not clearly defined. Based on our data, we propose a model whereby agonists of GPCR induce PIP_3 production, presumably via PI 3-kinase coupled to Gβγ, and potentiate PLC-β activity, possibly by membrane recruitment, repression of RGS activity or both.

Chapter 3 Figure 1

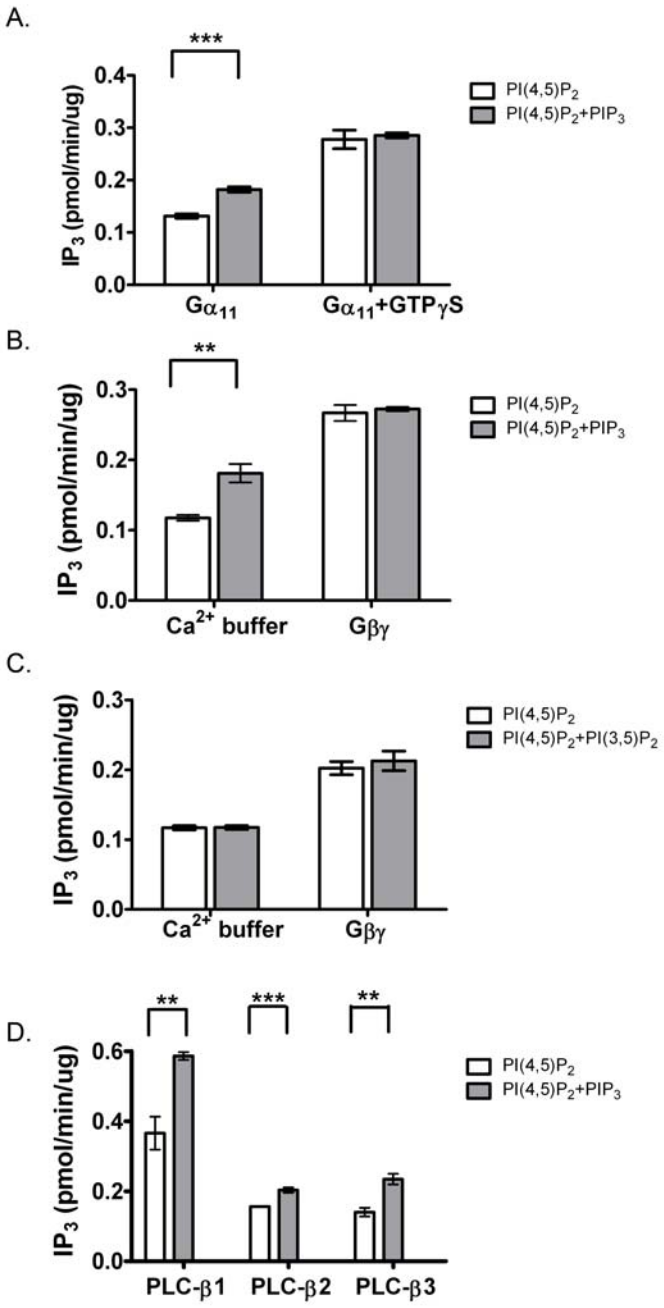

Fig. 3.1 PIP_3 increases Ca^{2+} stimulated, but not $G\alpha_{11}$ or $G\beta\gamma$ stimulated, PLC-β activity *in vitro*

(Continued)

Reconstitution PIP_2 hydrolysis assay was performed as described in materials and methods. **A,** Stimulation of PLC-β3 (35 ng) activity by 50 ng $G\alpha_{11}$ or GTPγS-activated $G\alpha_{11}$ ($G\alpha_{11}$ + GTPγS) was quantitated in the presence of 15 μM $PI(4,5)P_2$ (white bar) or 15 μM $PI(4,5)P_2$ plus 5 μM PIP_3 (gray bar). **B,** Stimulation of PLC-β3 (35 ng) activity by 0.15 μM free Ca^{2+} (Ca^{2+} buffer) or 60 ng $G\beta_1\gamma_2$ (Gβγ) was quantitated in the presence of 15 μM $PI(4,5)P_2$ (white bar) or 15 μM $PI(4,5)P_2$ plus 5 μM PIP_3 (gray bar). **C,** Stimulation of PLC-β3 (35 ng) activity by 0.15 μM free Ca^{2+} (Ca^{2+} buffer) or 60 ng $G\beta_1\gamma_2$ (Gβγ) was quantitated in the presence of 15 μM $PI(4,5)P_2$ (white bar) or 15 μM $PI(4,5)P_2$ plus 5 μM $PI(3,5)P_2$ (gray bar). **D**, Ca^{2+} stimulated PLC-β1 (12 ng), PLC-β2 (40 ng) or PLC-β3 (35 ng) activity was quantitated in the presence of 15 μM $PI(4,5)P_2$ (white bar) or 15 μM $PI(4,5)P_2$ plus 5 μM PIP_3 (gray bar). Results are mean ± S.D for triplicate determination and are representative of two experiments. ** indicates $p < 0.01$ and *** indicates $p < 0.001$ compared with controls.

Chapter 3 Figure 2

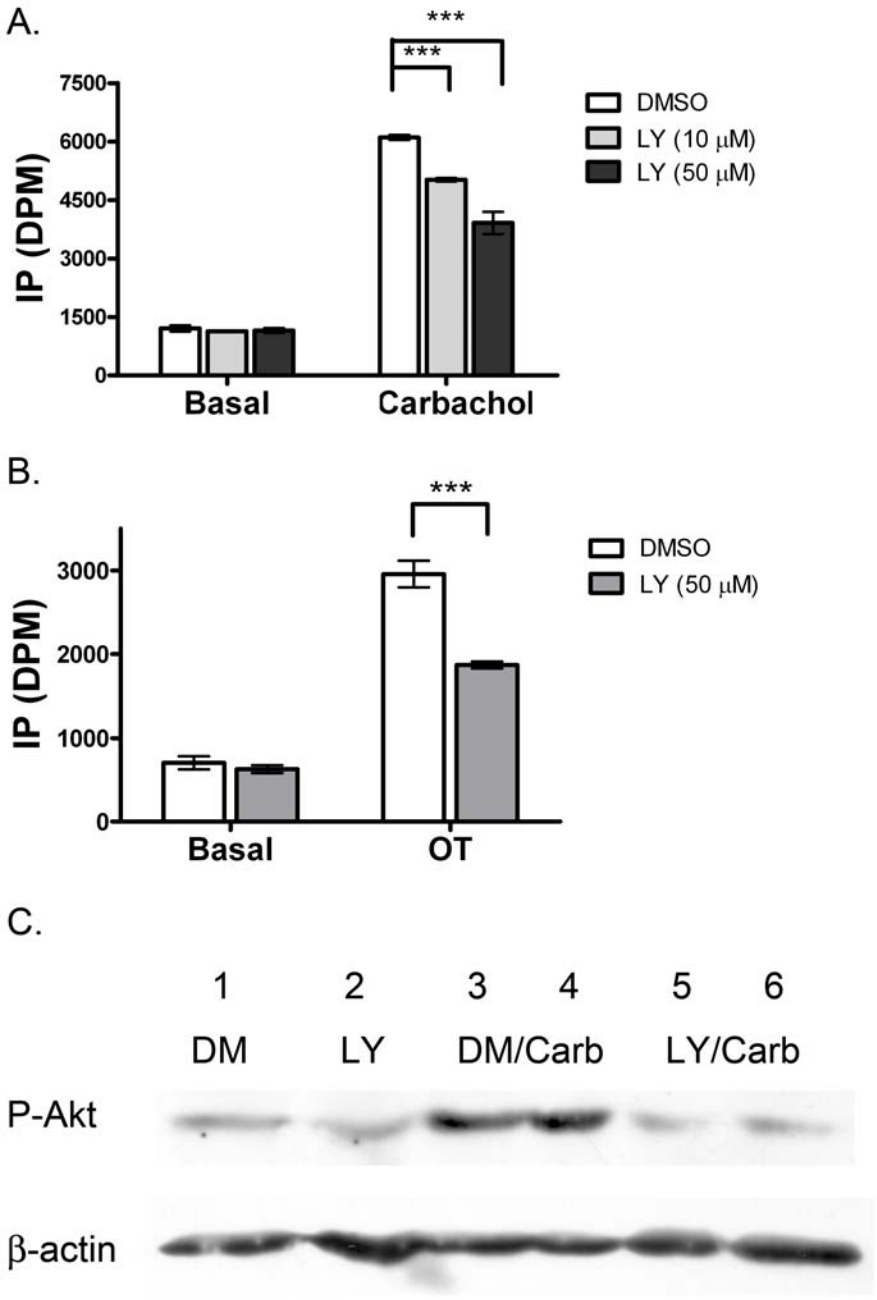

Fig. 3.2 LY294002 inhibits agonist-stimulated IP accumulation in whole cells

(Continued)

A, 1321N1 cells were pre-treated with 0.1% DMSO vehicle (white bars) or two concentrations of LY294002, 10 μM (grey bars) or 50 μM (black bars), for 30 minutes followed by stimulation with 1 mM Carbachol (Carbachol) or DMEM vehicle (Basal) for 10 minutes. Cells were lysed and total inositol phosphates (IP) were extracted and quantitated as described in materials and methods. **B,** Transfected HEK 293 cells stably expressing human oxytocin receptor were pre-treated with 0.1% DMSO vehicle (white bars) or 50 μM LY294002 (grey bars) for 30 minutes followed by stimulation with 100 nM oxcytocin (OT) or DMEM vehicle (Basal) for 10 minutes. Cells were lysed and total inositol phosphates (IP) were quantitated. Results are mean ± S.D for triplicate determination and *** indicates $p < 0.001$ compared with DMSO controls. **C**, 1321N1 cells were serum-starving overnight before pretreatment with 0.1% DMSO (DM, lanes 1, 3 and 4) or 50 μM LY294002 (LY, lanes 2, 5 and 6) in Kreg's solution for 30 min and stimulation with 1mM carbachol for 10 minutes (Carb, lanes 3-6). Cell lysates were separated by SDS-PAGE, and Phosphor-Akt (top panel) or β-actin (bottom panel) was detected by Western blot with selective antibodies. Shown are representative of two experiments.

Chapter 3 Figure 3

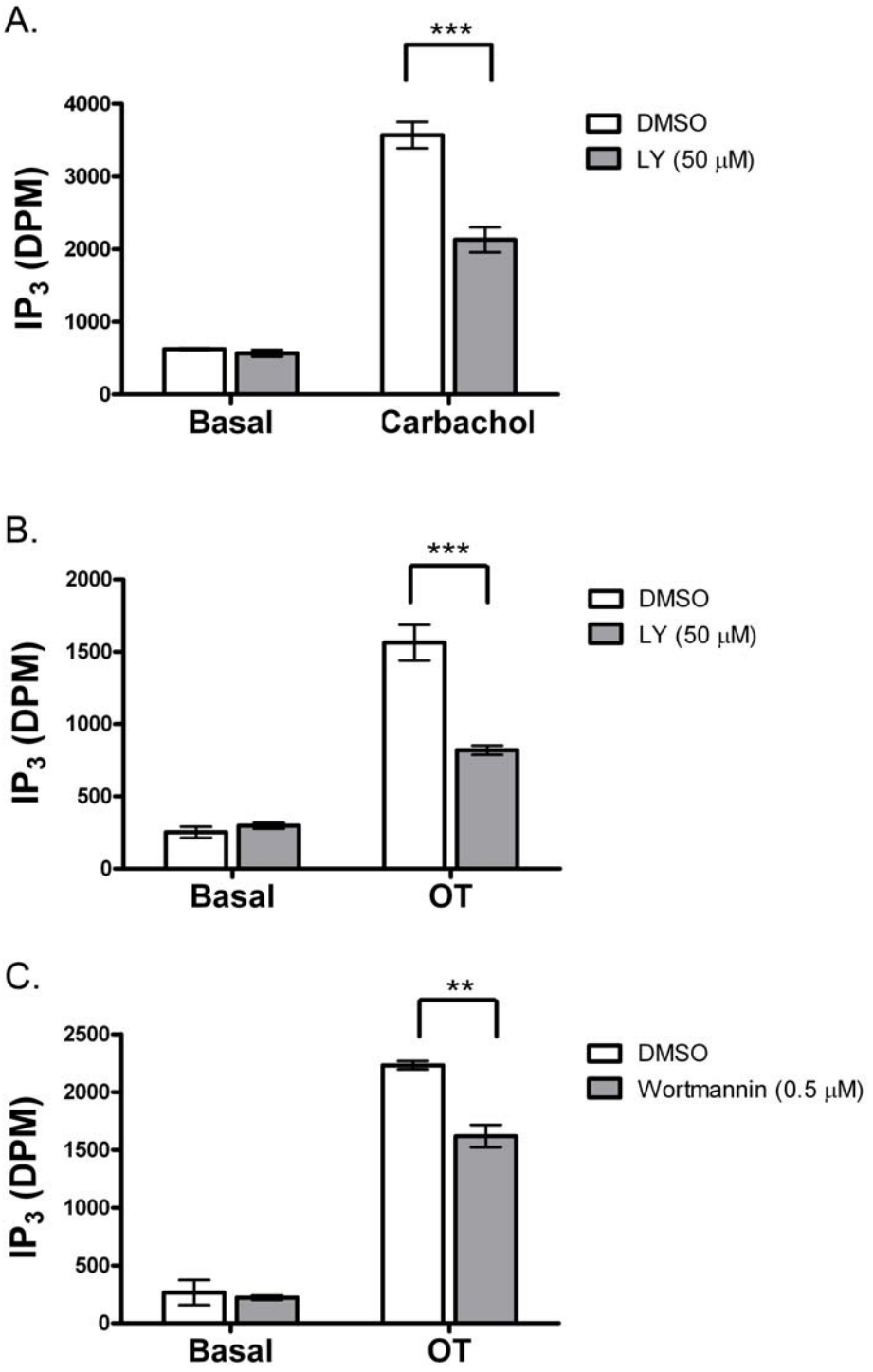

Fig. 3.3 PI 3-kinase inhibitors inhibit agonist-stimulated IP_3 accumulation in whole cells

(Continued)

A, 1321N1 cells were pre-treated with 0.1% DMSO vehicle (white bars) or 50 μM LY294002 (grey bars) for 30 minutes followed by stimulation with 1 mM Carbachol or DMEM vehicle (Basal) for 90 seconds. Cells were lysed and total inositoltrisphosphate (IP_3) was extracted and quantitated as described materials and methods. **B,** Transfected HEK 293 cells stably expressing human oxytocin receptor were pre-treated with 0.1% DMSO vehicle (white bars) or 50 μM LY294002 (grey bars) for 30 minutes followed by stimulation with 100 nM oxcytocin (OT) or DMEM vehicle (Basal) for 90 seconds. Cells were lysed and total inositol trisphosphate (IP_3) was quantitated. **C**, Transfected HEK 293 cells stably expressing human oxytocin receptor were pre-treated with 0.05% DMSO vehicle (white bars) or 0.5 μM wortmannin (grey bars) for 30 minutes followed by stimulation with 100 nM oxcytocin (OT) or DMEM vehicle (Basal) for 90 seconds. Cells were lysed and total inositol trisphosphate (IP_3) was quantitated. Results are mean ± S.D for triplicate determination and are representative of two experiments. *** indicates $p < 0.001$ and ** indicates $p < 0.01$ compared with DMSO controls.

Chapter 3 Figure 4

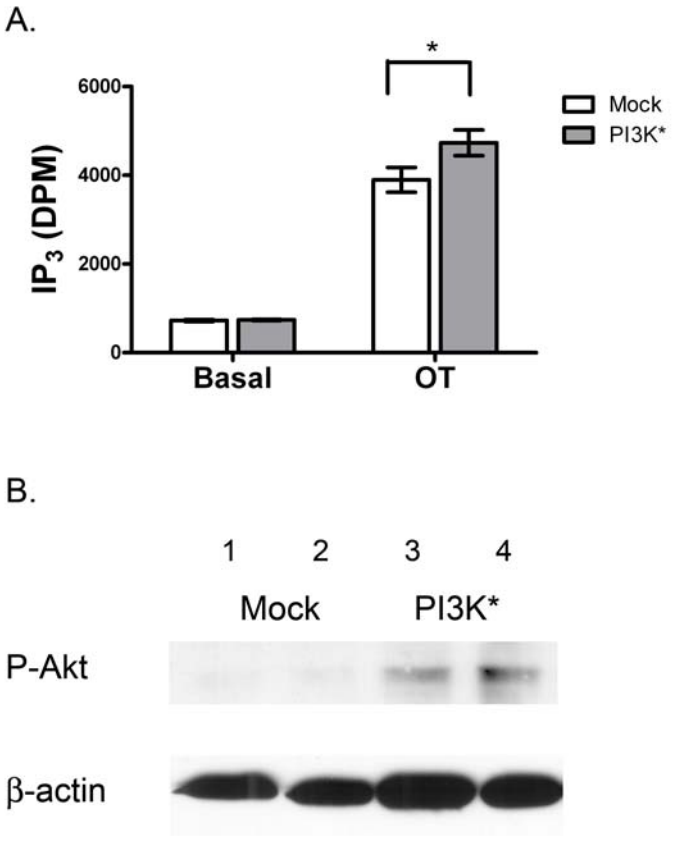

Fig. 3.4 p110CAAX, constitutively activated PI 3-kinase, potentiates agonist-stimulated IP_3 accumulation in whole cells.

A, HEK 293 cells stably expressing human oxytocin receptor were transfected with vehicle control (Mock) or p110CAAX (PI3K*) for 48 hours followed by stimulation with 100 nM oxcytocin (OT) or DMEM vehicle (Basal) for 90 seconds. Cells were lysed and total inositol trisphosphate (IP_3) was quantitated. Results are mean ± S.D for triplicate determination and * indicates $p < 0.05$ compared with DMSO controls. **B**, HEK 293 cells were transfected with vehicle control (Mock, lanes 1 and 2) or p110CAAX (PI3K*, lanes 3 and 4) for 48 hours and cell lysates were separated by SDS-PAGE. Phosphor-Akt (top panel) or β-actin (bottom panel) was detected by Western blot with selective antibodies. Shown are representative of two experiments.

Chapter 3 Figure 5

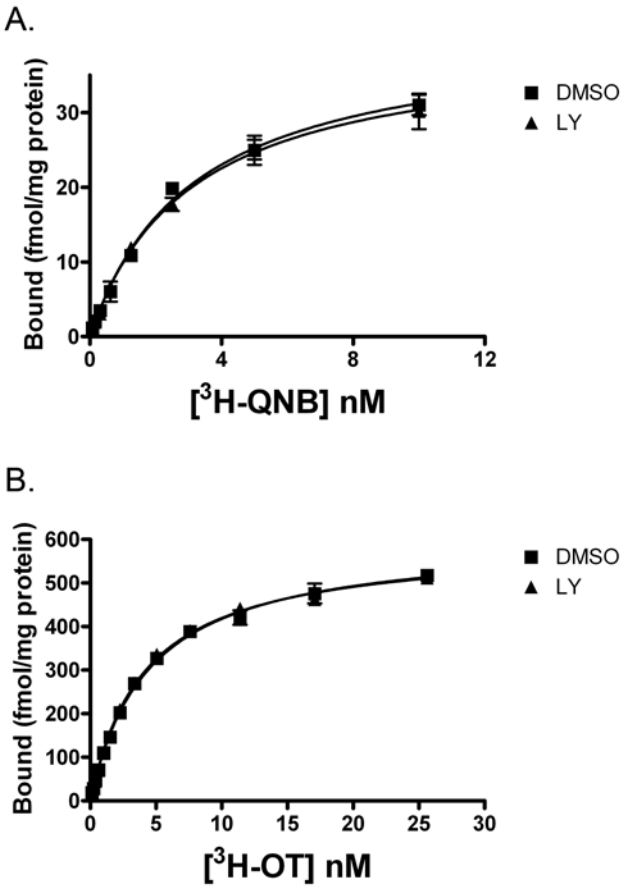

Fig.3.5 LY294002 does not affect muscarinic or oxytocin receptor binding.

A, Membranes from 1321N1 cells which express muscarinic receptors were prepared and incubated with indicated concentrations of [^{3}H]QNB (total binding) in the presence of 50 μM LY294002 (triangles) or 0.1% DMSO vehicle (squares) at 30°C for 30 min. Nonspecific binding was assessed in the presence of 0.1 mM atropine. Derived specific [^{3}H]QNB binding was fit to one site curve by GraphPad Prism 4. **B,** Membrane proteins from transfected HEK 293 cells stably expressing human oxytocin receptors were prepared and incubated with indicated concentrations of [^{3}H]OT (total binding) in the presence of 50 μM LY294002 (triangles) or 0.1% DMSO vehicle (squares) at 30°C for 30 min. Nonspecific binding was assessed in the presence of 2 μM unlabeled OT. Derived specific [^{3}H]OT binding was fit to a one site curve using GraphPad Prism 4. Results are representative of two independent experiments.

Chapter 3 Figure 6

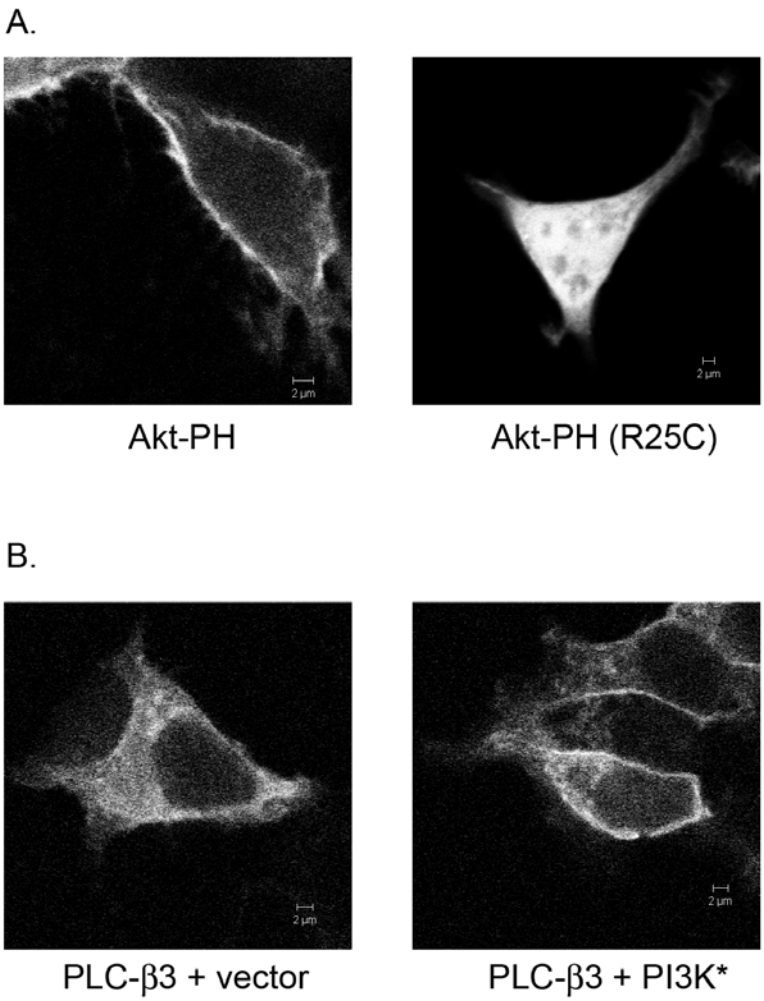

Fig. 3.6 p110CAAX, constitutively activated PI 3-kinase, increases PLC-β3 membrane association.

A, HEK 293 cells were transiently transfected with GFP tagged Akt-PH domain (Akt-PH) or GFP tagged Akt-PH R25C mutant (Akt-PH (R25C)). **B,** HEK 293 cells were co-transfected with GFP tagged PLC-β3 plus mock vector (PLC-β3+vector) or GFP tagged PLC-β3 plus p110CAAX (PLC-β3+PI3K*). After transfected 48 hours, cells were fixed and GFP fluorescence was detected at 488 nm by confocal microscopy. Scale bar is 2 μm. Shown are representative figures from two independent experiments.

Chapter 3 Figure 7

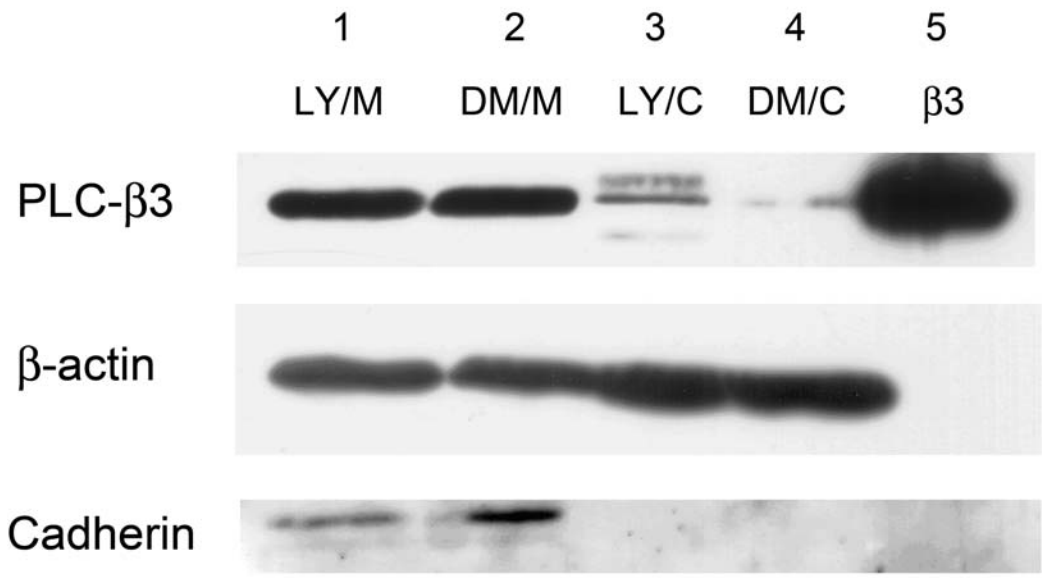

Fig. 3.7 LY294002 decreases PLC-β3 membrane association in H9c2 cells

H9c2 cells were pre-treated by 50 μM LY294002 (LY, lanes 1 and 3) or 0.1% DMSO (DM, lanes 2 and 4) for 1 hour, lysed and cell fractions separated by discontinuous OptiPrep gradient centrifugation. Membrane fractions (M, lanes 1 and 2) and cytosol fractions (C, lanes 3 and 4) were loaded onto SDS-PAGE for protein separation. PLC-β3 (top panel), β-actin (middle panel) or cadherin (bottom panel) were visualized by Western blot with selective antibodies. 100 ng purified PLC-β3 (lane 5) was included as a positive control for the anti-PLC-β3 Western blot. Shown are representative blots from two independent experiments.

Chapter 3 Figure 8

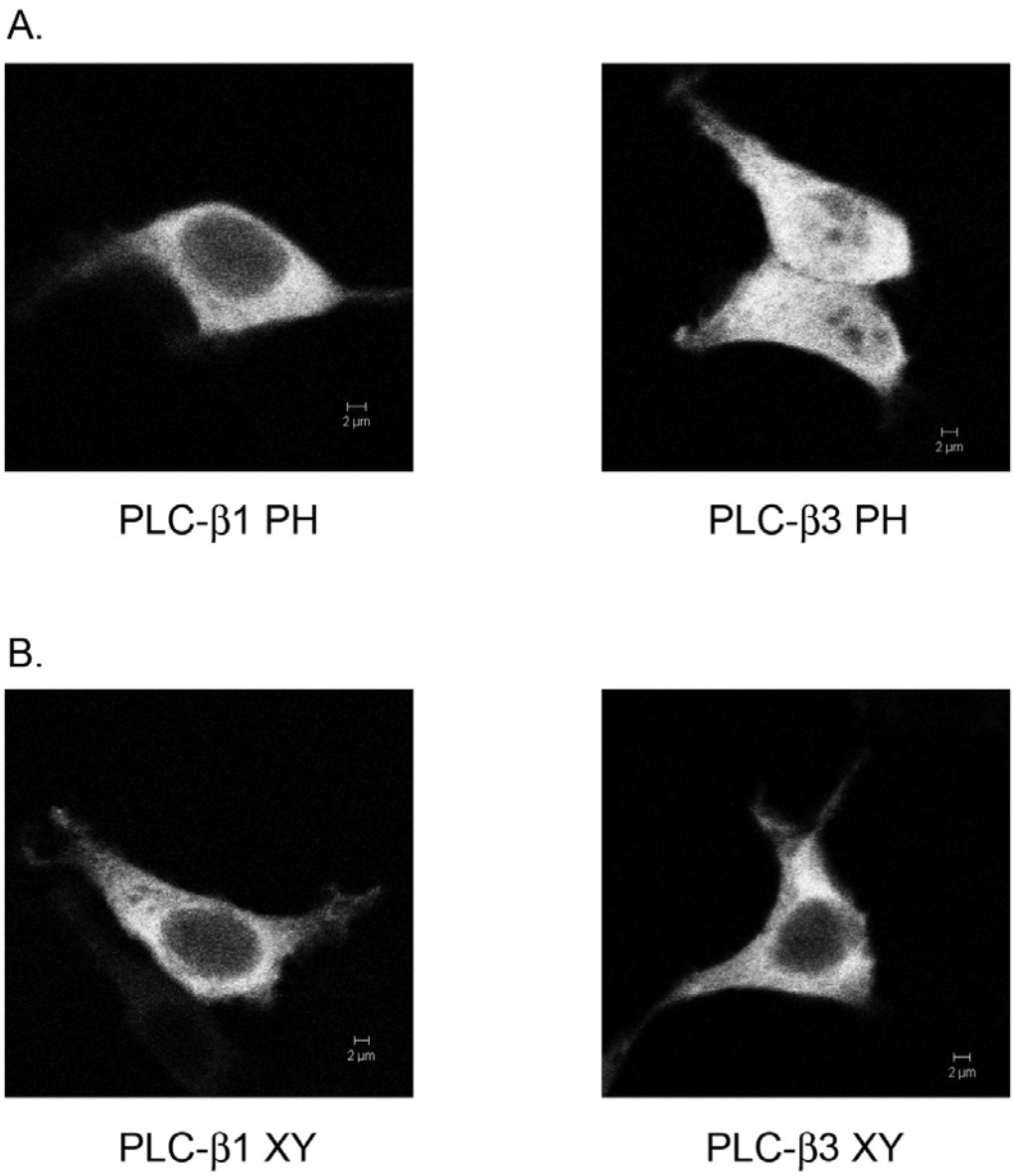

Fig. 3.8 PH domain and catalytic XY domain of PLC-β are not important for membrane targeting.

A, HEK 293 cells were transiently transfected with GFP tagged PLC-β1 PH domain (PLC-β1 PH) or GFP tagged PLC-β3 PH domain (PLC-β3 PH). **B,** HEK 293 cells were transiently transfected with GFP tagged PLC-β1 XY domain (PLC-β1 XY) or GFP tagged PLC-β3 XY domain (PLC-β3 XY). After transfected 48 hours, cells were fixed and GFP fluorescence was detected at 488 nm by confocal microscopy. Scale bar is 2 μm. Shown are representative figures from two independent experiments.

Chapter 3 Figure 9

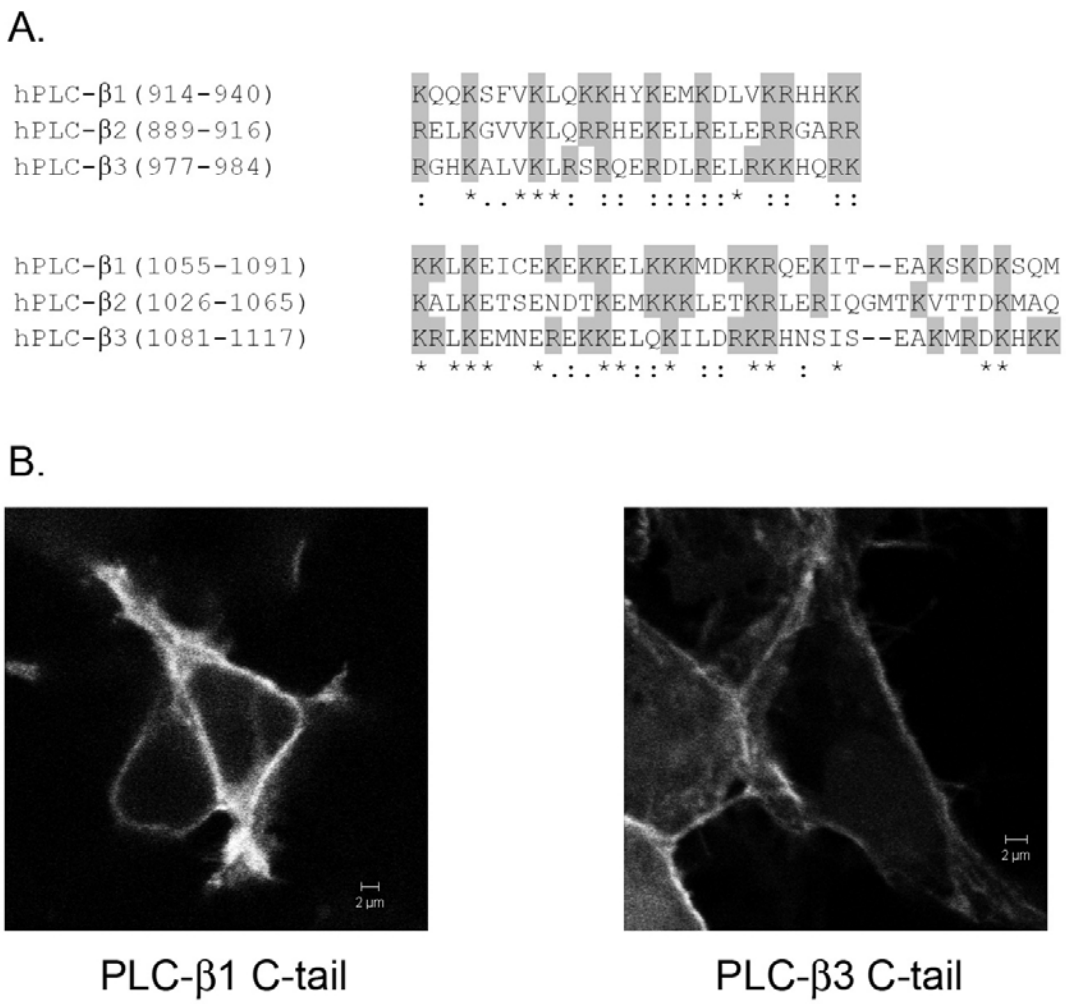

Fig. 3.9 C-tail domain of PLC-β is important in the membrane association.

A, Two polybasic clusters were identified in human PLC-β C-tail domains by sequence alignment. Shaded residuals are conserved positively charged amino acids (arginine and lysine). **B**, HEK 293 cells were transiently transfected with GFP tagged PLC-β1 C-tail domain (PLC-β1 C-tail) or GFP tagged PLC-β3 C-tail domain (PLC-β3 C-tail). After transfected 48 hours, cells were fixed and GFP fluorescence was detected at 488 nm by confocal microscopy. Scale bar is 2 μm. Shown are representative figures from two independent experiments.

Chapter 3 Figure 10 (Supplementary Figure)

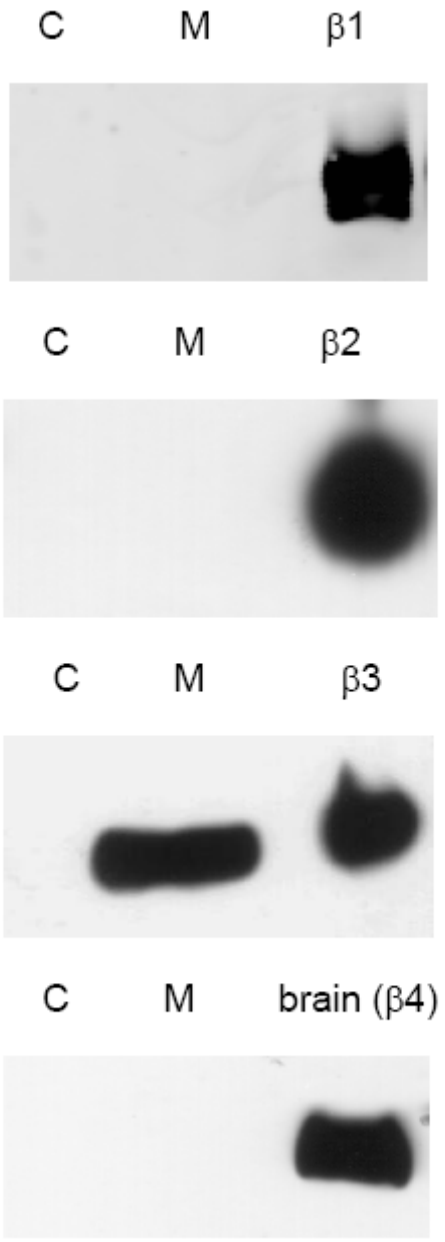

Fig. 3.10 Identification of PLC-β isozymes expressed in H9c2 cells.

(Continued)

H9c2 cells were lysed and cellular fractions were separated by discontinuous OptiPrep gradient centrifugation. Membrane co-fractioning proteins (M) and the cytosol co-fractioning proteins (C) were separated by SDS-PAGE for protein separation. PLC-β1 (top panel), PLC-β2 (second panel), PLC-β3 (third panel) or PLC-β4 (bottom panel) were visualized by Western blot with selective antibodies. Purified PLC-β1, PLC-β2, PLC-β3 and mouse brain lysate (β4) were included as positive controls.

Chapter 4: General Conclusion

Phospholipase C-βs (PLC-β) are one of the key effectors in G protein-coupled signaling pathway, which are controlled by multiple regulators. Our data suggest that phospholipase C-β can form dimers through interaction of the catalytic domains and the C-tail domains. Structural studies have demonstrated that the C-tail domain of turkey PLC-β2 forms an antiparallel dimer (Singer et al., 2002). Because the C-tail domain of PLC-β is crucial for $G\alpha_q$-stimulated activation and also acts as a GTPase accelerating protein (GAP), dimerization of PLC-β may be important for $G\alpha_q$ interaction. The existence of homo- and heterodimers of G protein-coupled receptors has gained widespread acceptance. It is intriguing to speculate that $G\alpha_q$-coupled receptors might assemble large signaling complexes containing homerdimeric PLC-βs and pairs of $G\alpha_q$ subunits, as proposed by Harden and Sondek. Indeed, this model is supported by the structural study which suggested that dimerized C-tail of PLC-β permits the symmetrical docking of two $G\alpha_q$ subunits (Singer et al., 2002). Our data suggest PLC-β3 and PLC-β1 form higher affinity homodimers than PLC-β2, which is the PLC-β isozyme least responsive to $G\alpha_q$ stimulation. The lower affinity homodimerzation of PLC-β2 may reduce its coupling to $G\alpha_q$.

Interestingly, the isolated catalytic domains of PLC-β3 also form a dimer in our co-immunoprecipitation studies, suggesting that the dimeric structure may influence PLC-β catalytic activity. Moreover, several former studies also suggested that PLC-β dimer may be active (Banno et al., 1994; Moriyama et al., 1990). Future studies may address whether functional dimers of PLC-β3 can be detected by site directed

mutagenesis and whether these mutants have reduced sensitivity to G proteins or reduced catalytic activity.

We found that PIP_3 potentiates Ca^{2+}-stimulated PLC-β activities. Former studies suggested that phosphatidic acid (PA), another acidic phospholipid, increases Ca^{2+}-stimulated PLC-β1 activity *in vitro* and the C-tail of PLC-β1 has been shown important for PA stimulation (Litosch, 2000). In addition, PLC-γ can be activated by PIP_3 *in vitro*, and the PI 3-kinase inhibitor (LY294002) blocks calcium-stimulated PLC-γ activity in human keratinocytes (Xie et al., 2005), which is similar to our *in vitro* data on Ca^{2+}-stimulated PLC-β activity. Furthermore, our data suggest that LY294002 inhibits G protein-coupled receptor-stimulated IP_3 accumulation in 1321N1 cells, HEK cells expressing oxytocin receptors, and H9c2 cells, implying a significance of PI 3-kinase activity and increased PIP_3 levels on regulation of PLC-β in intact cells.

One hypothesis to explain our data is that agonists of G protein-coupled receptors activate PI3Kγ via Gβγ, and increase PIP_3 concentration in cells, thus augmenting PLC-β activity, Indeed, a PI3Kγ knockout study indicated that PI3Kγ makes a small but significant contribution to thrombin-stimulated calcium response in platelets (Lian et al., 2005), suggesting that PI3Kγ plays a role in PLC-β-mediated calcium response. However, LY294002, an inhibitor affecting all known PI 3-kinases, impairs the thrombin-induced calcium rise by a larger extent (Lian et al., 2005), implicating that more than one PI 3-kinases isoforms, rather than PI3Kγ alone, are involved in potentiating PLC-β activation, presumably through PIP_3.

Our data suggest that PIP_3 increases Ca^{2+}-stimulated PLC-β activity. It may be worth examining the effect of PIP_3 on the interaction of calmodulin with PLC-β. Ca^{2+}/calmodulin may compete with PIP_3 to bind RGS4 (Popov et al., 2000a), and PIP_3 binding disrupts the association of calmodulin and TRPC6 channel (Kwon et al., 2007). Our group has shown that calmodulin potentiates Gβγ-stimulated PLC-β activity *in vitro* (McCullar et al., 2007), and PIP_3 could modulate that interaction.

By changing cellular PIP_3 concentration via overexpression of a constitutively active PI 3-kinase and use of a PI 3-kinase inhibitor, we showed that PIP_3 affects PLC-β3 localization. Further experiments suggest that the C-tail domain of PLC-β, but not the PH domain and XY catalytic domain, is important for membrane association in the basal state. Since transfected full-length PLC-β3 primarily localizes at the cytosol of HEK-293 cells in the unstimulated state, the amino terminal domains of full-length PLC-β may modify the strong membrane affinity of the C-tail domain to regulate access to substrates.

An unanswered question is why do most PLC-βs, including PLC-β1 or PLC-β3 in 1321N1 cells, HEK-293 cells, mouse brain and heart, localize primarily to the cytoplasm. One hypothesis is that PLC-β membrane localization is inhibited by some unknown regulator(s), possibly by protein(s), in certain cells or tissues. To answer this question, we need to identify more PLC-β interacting proteins and characterize their effect on PLC-β's localization.

Taken together, our work in this thesis suggests that PLC-βs are regulated by multiple mechanisms including formation of dimers and potentiation by non-substrate

lipid such as PIP_3. Obviously, more studies will be required to elucidate the details of the signaling pathways which fine tune regulation of PLC-β isozymes. This study contributes to our understanding of PLC-β in an incredible diversity of signaling systems and provides new insight for the future research.

Bibliography

Alessi DR and Cohen P (1998) Mechanism of activation and function of protein kinase B. *Curr Opin Genet Dev* **8**(1):55-62.

Ali H, Fisher I, Haribabu B, Richardson RM and Snyderman R (1997) Role of phospholipase Cbeta3 phosphorylation in the desensitization of cellular responses to platelet-activating factor. *J Biol Chem* **272**(18):11706-11709.

Ali H, Sozzani S, Fisher I, Barr AJ, Richardson RM, Haribabu B and Snyderman R (1998) Differential regulation of formyl peptide and platelet-activating factor receptors. *JBiolChem* **273**(18):11012-11016.

Ananthanarayanan B, Das S, Rhee SG, Murray D and Cho W (2002) Membrane targeting of C2 domains of phospholipase C-delta isoforms. *J Biol Chem* **277**(5):3568-3575.

Anderson KE, Lipp P, Bootman M, Ridley SH, Coadwell J, Ronnstrand L, Lennartsson J, Holmes AB, Painter GF, Thuring J, Lim Z, Erdjument-Bromage H, Grewal A, Tempst P, Stephens LR and Hawkins PT (2000) DAPP1 undergoes a PI 3-kinase-dependent cycle of plasma-membrane recruitment and endocytosis upon cell stimulation. *Curr Biol* **10**(22):1403-1412.

Aoki K, Nakamura T, Fujikawa K and Matsuda M (2005) Local phosphatidylinositol 3,4,5-trisphosphate accumulation recruits Vav2 and Vav3 to activate Rac1/Cdc42 and initiate neurite outgrowth in nerve growth factor-stimulated PC12 cells. *Mol Biol Cell* **16**(5):2207-2217.

Arthur JF, Matkovich SJ, Mitchell CJ, Biden TJ and Woodcock EA (2001) Evidence for Selective Coupling of alpha 1-Adrenergic Receptors to Phospholipase C-beta 1 in Rat Neonatal Cardiomyocytes. *J Biol Chem* **276**(40):37341-37346.

Avram D, Ishmael JE, Nevrivy DJ, Peterson VJ, Lee SH, Dowell P and Leid M (1999) Heterodimeric interactions between chicken ovalbumin upstream promoter-transcription factor family members ARP1 and ear2. *J Biol Chem* **274**(20):14331-14336.

Bach TL, Chen QM, Kerr WT, Wang Y, Lian L, Choi JK, Wu D, Kazanietz MG, Koretzky GA, Zigmond S and Abrams CS (2007) Phospholipase cbeta is critical for T cell chemotaxis. *J Immunol* **179**(4):2223-2227.

Bae YS, Cantley LG, Chen CS, Kim SR, Kwon KS and Rhee SG (1998) Activation of phospholipase C-γ by phosphatidylinositol 3,4,5-trisphosphate. *J Biol Chem* **273**(8):4465-4469.

Bahk YY, Lee YH, Lee TG, Seo J, Ryu SH and Suh PG (1994) Two forms of phospholipase C-beta 1 generated by alternative splicing. *J Biol Chem* **269**(11):8240-8245.

Bahk YY, Song H, Baek SH, Park BY, Kim H, Ryu SH and Suh PG (1998) Localization of two forms of phospholipase C-beta1, a and b, in C6Bu-1 cells. *Biochim Biophys Acta* **1389**(1):76-80.

Banno Y, Asano T and Nozawa Y (1994) Proteolytic modification of membrane-associated phospholipase C-beta by mu-calpain enhances its activation by G-protein beta gamma subunits in human platelets. *FEBS Lett* **340**(3):185-188.

Banno Y, Nakashima S, Hachiya T and Nozawa Y (1995) Endogenous cleavage of phospholipase C-beta 3 by agonist-induced activation of calpain in human platelets. *J Biol Chem* **270**(9):4318-4324.

Barr AJ, Ali H, Haribabu B, Snyderman R and Smrcka AV (2000) Identification of a region at the N-terminus of phospholipase C-β3 that interacts with G protein βγ subunits. *Biochem* **39**:1800-1806.

Beekman A, Helfrich B, Bunn PA, Jr. and Heasley LE (1998) Expression of catalytically inactive phospholipase Cbeta disrupts phospholipase Cbeta and mitogen-activated protein kinase signaling and inhibits small cell lung cancer growth. *Cancer Res* **58**(5):910-913.

Benes CH, Wu N, Elia AE, Dharia T, Cantley LC and Soltoff SP (2005) The C2 domain of PKCdelta is a phosphotyrosine binding domain. *Cell* **121**(2):271-280.

Berridge MJ (1993) Inositol trisphosphate and calcium signalling. *Nature* **361**:315-325.

Berstein G, Blank JL, Jhon D-Y, Exton JH, Rhee SG and Ross EM (1992) Phospholipase C-β1 is a GTPase-activating protein for $G_{q/11}$, its physiologic regulator. *Cell* **70**:411-418.

Bertagnolo V, Benedusi M, Querzoli P, Pedriali M, Magri E, Brugnoli F and Capitani S (2006) PLC-beta2 is highly expressed in breast cancer and is

associated with a poor outcome: a study on tissue microarrays. *Int J Oncol* **28**(4):863-872.

Bertagnolo V, Marchisio M, Pierpaoli S, Colamussi ML, Brugnoli F, Visani G, Zauli G and Capitani S (2002) Selective up-regulation of phospholipase C-beta2 during granulocytic differentiation of normal and leukemic hematopoietic progenitors. *J Leukoc Biol* **71**(6):957-965.

Biener E, Charlier M, Ramanujan KV, Daniel N, Eisenberg A, Bjorbaek C, Herman B, Gertler A and Djiane J (2005) Quantitative FRET imaging of leptin receptor oligomerization kinetics in single cells. *Biol Cell* **97**(12):905-919.

Bishop CV and Stormshak F (2006) Nongenomic action of progesterone inhibits oxytocin-induced phosphoinositide hydrolysis and prostaglandin F2alpha secretion in the ovine endometrium. *Endocrinology* **147**(2):937-942.

Blazer-Yost BL and Nofziger C (2005) Phosphoinositide lipid second messengers: new paradigms for transepithelial signal transduction. *Pflugers Arch* **450**(2):75-82.

Bloomquist BT, Shortridge RD, Schneuwly S, Perdew M, Montell C, Steller H, Rubin G and Pak WL (1988) Isolation of a putative phospholipase C gene of Drosophila, norpA, and its role in phototransduction. *Cell* **54**(5):723-733.

Bolland S, Pearse RN, Kurosaki T and Ravetch JV (1998) SHIP modulates immune receptor responses by regulating membrane association of Btk. *Immunity* **8**(4):509-516.

Boyer JL, Waldo GL and Harden TK (1992a) Beta gamma-subunit activation of G-protein-regulated phospholipase C. *J Biol Chem* **267**(35):25451-25456.

Boyer JL, Waldo GL and Harden TK (1992b) βγ-Subunit activation of G-protein-regulated phospholipase C. *JBiolChem* **267**:25451-25456.

Bunce MW, Bergendahl K and Anderson RA (2006) Nuclear PI(4,5)P(2): a new place for an old signal. *Biochim Biophys Acta* **1761**(5-6):560-569.

Cai Y, Stafford LJ, Bryan BA, Mitchell D and Liu M (2005) G-protein-activated phospholipase C-beta, new partners for cell polarity proteins Par3 and Par6. *Oncogene* **24**(26):4293-4300.

Chakrabarti S, Liu NJ and Gintzler AR (2003) Reciprocal modulation of phospholipase Cbeta isoforms: adaptation to chronic morphine. *Proc Natl Acad Sci U S A* **100**(23):13686-13691.

Chang JS, Kim SK, Kwon TK, Bae SS, Min DS, Lee YH, Kim SO, Seo JK, Choi JH and Suh PG (2005) Pleckstrin homology domains of phospholipase C-gamma1 directly interact with beta-tubulin for activation of phospholipase C-gamma1 and reciprocal modulation of beta-tubulin function in microtubule assembly. *J Biol Chem* **280**(8):6897-6905.

Charest PG and Firtel RA (2006) Feedback signaling controls leading-edge formation during chemotaxis. *Curr Opin Genet Dev* **16**(4):339-347.

Cheatham B, Vlahos CJ, Cheatham L, Wang L, Blenis J and Kahn CR (1994) Phosphatidylinositol 3-kinase activation is required for insulin stimulation of pp70 S6 kinase, DNA synthesis, and glucose transporter translocation. *Mol Cell Biol* **14**(7):4902-4911.

Chidiac P and Ross EM (1999) Phospholipase C-beta 1 Directly Accelerates GTP Hydrolysis by Galpha q and Acceleration Is Inhibited by Gbeta gamma Subunits. *J Biol Chem* **274**(28):19639-23699.

Chin D and Means AR (2000) Calmodulin: a prototypical calcium sensor. *Trends Cell Biol* **10**(8):322-328.

Cho W and Stahelin RV (2006) Membrane binding and subcellular targeting of C2 domains. *Biochim Biophys Acta* **1761**(8):838-849.

Choi S, Kim HJ, Ko YS, Jeong SW, Kim YI, Simonds WF, Oh JW and Nah SY (2001) G alpha(q/11) coupled to mammalian phospholipase C beta 3-like enzyme mediates the ginsenoside effect on Ca(2+)-activated Cl(-) current in the Xenopus oocyte. *J Biol Chem* **276**(52):48797-48802.

Chubet RG and Brizzard BL (1996) Vectors for expression and secretion of FLAG epitope-tagged proteins in mammalian cells. *Biotechniques* **20**(1):136-141.

Cook B, Bar-Yaacov M, Cohen Ben-Ami H, Goldstein RE, Paroush Z, Selinger Z and Minke B (2000) Phospholipase C and termination of G-protein-mediated signalling in vivo. *Nat Cell Biol* **2**(5):296-301.

Cook JA, August A and Henderson AJ (2002) Recruitment of phosphatidylinositol 3-kinase to CD28 inhibits HIV transcription by a Tat-dependent mechanism. *J Immunol* **169**(1):254-260.

Cote JF, Motoyama AB, Bush JA and Vuori K (2005) A novel and evolutionarily conserved PtdIns(3,4,5)P3-binding domain is necessary for DOCK180 signalling. *Nat Cell Biol* **7**(8):797-807.

Crljen V, Visnjic D and Banfic H (2004) Presence of different phospholipase C isoforms in the nucleus and their activation during compensatory liver growth. *FEBS Lett* **571**(1-3):35-42.

Cunningham ML, Filtz TM and Harden TK (1999) Protein kinase C-promoted inhibition of Galpha(11)-stimulated phospholipase C-beta activity. *Mol Pharmacol* **56**(2):265-271.

Czech MP (2000) PIP2 and PIP3: complex roles at the cell surface. *Cell* **100**(6):603-606.

Deems RA and Dennis EA (1975) Characterization and physical properties of the major form of phospholipase A2 from cobra venom (Naja naja naja) that has a molecular weight of 11,000. *J Biol Chem* **250**(23):9008-9012.

Dowler S, Currie RA, Downes CP and Alessi DR (1999) DAPP1: a dual adaptor for phosphotyrosine and 3-phosphoinositides. *Biochem J* **342 (Pt 1)**:7-12.

Drayer AL, Meima ME, Derks MW, Tuik R and van Haastert PJ (1995) Mutation of an EF-hand Ca(2+)-binding motif in phospholipase C of Dictyostelium discoideum: inhibition of activity but no effect on Ca(2+)-dependence. *Biochem J* **311 (Pt 2)**:505-510.

Egawa K, Sharma PM, Nakashima N, Huang Y, Huver E, Boss GR and Olefsky JM (1999) Membrane-targeted phosphatidylinositol 3-kinase mimics insulin actions and induces a state of cellular insulin resistance. *J Biol Chem* **274**(20):14306-14314.

Ellis MV, Carne A and Katan M (1993) Structural requirements of phosphatidylinositol-specific phospholipase C delta 1 for enzyme activity. *Eur J Biochem* **213**(1):339-347.

Ellis MV, James SR, Perisic O, Downes CP, Williams RL and Katan M (1998) Catalytic domain of phosphoinositide-specific phospholipase C (PLC).

Mutational analysis of residues within the active site and hydrophobic ridge of plcdelta1. *J Biol Chem* **273**(19):11650-11659.

Essen LO, Perisic O, Cheung R, Katan M and Williams RL (1996) Crystal structure of a mammalian phosphoinositide-specific phospholipase C δ. *Nature* **380**(6575):595-602.

Essen LO, Perisic O, Lynch DE, Katan M and Williams RL (1997) A ternary metal binding site in the C2 domain of phosphoinositide-specific phospholipase C-delta1. *Biochemistry* **36**(10):2753-2762.

Faenza I, Bavelloni A, Fiume R, Lattanzi G, Maraldi NM, Gilmour RS, Martelli AM, Suh PG, Billi AM and Cocco L (2003) Up-regulation of nuclear PLCbeta1 in myogenic differentiation. *J Cell Physiol* **195**(3):446-452.

Faenza I, Bavelloni A, Fiume R, Santi P, Martelli AM, Maria Billi A, Lo Vasco VR, Manzoli L and Cocco L (2004) Expression of phospholipase C beta family isoenzymes in C2C12 myoblasts during terminal differentiation. *J Cell Physiol* **200**(2):291-296.

Faenza I, Matteucci A, Manzoli L, Billi AM, Aluigi M, Peruzzi D, Vitale M, Castorina S, Suh P-G and Cocco L (2000) A role for nuclear phospholipase Cβ1 in cell cycle control. *JBiol Chem* **275**:30520-30524.

Faenza I, Ramazzotti G, Bavelloni A, Fiume R, Gaboardi GC, Follo MY, Gilmour RS, Martelli AM, Ravid K and Cocco L (2007) Inositide-dependent phospholipase C signaling mimics insulin in skeletal muscle differentiation by affecting specific regions of the cyclin d3 promoter. *Endocrinology* **148**(3):1108-1117.

Falasca M, Logan SK, Lehto VP, Baccante G, Lemmon MA and Schlessinger J (1998) Activation of phospholipase Cγ by PI 3-kinase-induced PH domain-mediated membrane targeting. *Embo J* **17**(2):414-422.

Ferguson KM, Lemmon MA, Schlessinger J and Sigler PB (1995) Structure of the high affinity complex of inositol trisphosphate with a phospholipase C pleckstrin homology domain. *Cell* **83**(6):1037-1046.

Filtz TM, Cunningham ML, Stanig KJ, Paterson A and Harden TK (1999) Phosphorylation by protein kinase C reduces catalytic activity of avian phospholipase C-β. *BiochemJ* **338**:257-264.

Filtz TM, Li Q, Boyer JL, Nicholas RA and Harden TK (1994) Expression of a cloned P_{2Y}-purinergic receptor that couples to phospholipase C. *MolPharmacol* **46**:8-14.

Filtz TM and Niibori Y (2004) Desensitization of angiotensin-stimulated inositol phosphate accumulation in human vascular smooth muscle cells. *Eur J Pharmacol* **502**(1-2):11-19.

Fiume R, Faenza I, Matteucci A, Astolfi A, Vitale M, Martelli AM and Cocco L (2005) Nuclear phospholipase C beta1 (PLCbeta1) affects CD24 expression in murine erythroleukemia cells. *J Biol Chem* **280**(25):24221-24226.

Flick JS and Thorner J (1993) Genetic and biochemical characterization of a phosphatidylinositol-specific phospholipase C in Saccharomyces cerevisiae. *Mol Cell Biol* **13**(9):5861-5876.

Foster FM, Traer CJ, Abraham SM and Fry MJ (2003) The phosphoinositide (PI) 3-kinase family. *J Cell Sci* **116**(Pt 15):3037-3040.

Frech M, Andjelkovic M, Ingley E, Reddy KK, Falck JR and Hemmings BA (1997) High affinity binding of inositol phosphates and phosphoinositides to the pleckstrin homology domain of RAC/protein kinase B and their influence on kinase activity. *J Biol Chem* **272**(13):8474-8481.

Fukami K (2002) Structure, regulation, and function of phospholipase C isozymes. *J Biochem (Tokyo)* **131**(3):293-299.

Garcia P, Gupta R, Shah S, Morris AJ, Rudge SA, Scarlata S, Petrova V, McLaughlin S and Rebecchi MJ (1995) The Pleckstrin homology domain of Phospholipase C-δ1 binds with high affinity to phosphatidyl 4,5-bisphosphate in bilayer membranes. *Biochemistry* **34**:16228-16234.

Gifford JL, Walsh MP and Vogel HJ (2007) Structures and metal-ion-binding properties of the Ca2+-binding helix-loop-helix EF-hand motifs. *Biochem J* **405**(2):199-221.

Grobler JA, Essen LO, Williams RL and Hurley JH (1996) C2 domain conformational changes in phospholipase C-delta 1. *Nat Struct Biol* **3**(9):788-795.

Guo Y, Rebecchi M and Scarlata S (2005) Phospholipase Cbeta2 binds to and inhibits phospholipase Cdelta1. *J Biol Chem* **280**(2):1438-1447.

Han J, Luby-Phelps K, Das B, Shu X, Xia Y, Mosteller RD, Krishna UM, Falck JR, White MA and Broek D (1998) Role of substrates and products of PI 3-kinase in regulating activation of Rac-related guanosine triphosphatases by Vav. *Science* **279**(5350):558-560.

Han SK, Mancino V and Simon MI (2006) Phospholipase Cbeta 3 mediates the scratching response activated by the histamine H1 receptor on C-fiber nociceptive neurons. *Neuron* **52**(4):691-703.

Hannan AJ, Blakemore C, Katsnelson A, Vitalis T, Huber KM, Bear M, Roder J, Kim D, Shin HS and Kind PC (2001) PLC-beta1, activated via mGluRs, mediates activity-dependent differentiation in cerebral cortex. *Nat Neurosci* **4**(3):282-288.

Hansen CA, Schroering AG and Robishaw JD (1995) Subunit expression of signal transducing G proteins in cardiac tissue: implications for phospholipase C-beta regulation. *J Mol Cell Cardiol* **27**(1):471-484.

Harden TK and Sondek J (2006) Regulation of phospholipase C isozymes by ras superfamily GTPases. *Annu Rev Pharmacol Toxicol* **46**:355-379.

Haslam RJ, Koide HB and Hemmings BA (1993) Pleckstrin domain homology. *Nature* **363**(6427):309-310.

Heinz DW, Essen LO and Williams RL (1998) Structural and mechanistic comparison of prokaryotic and eukaryotic phosphoinositide-specific phospholipases C. *J Mol Biol* **275**(4):635-650.

Heo WD, Inoue T, Park WS, Kim ML, Park BO, Wandless TJ and Meyer T (2006) PI(3,4,5)P_3 and PI(4,5)P_2 lipids target proteins with polybasic clusters to the plasma membrane. *Science* **314**(5804):1458-1461.

Hepler JR, Kozasa T, Smrcka AV, Simon MI, Rhee SG, Sternweis PC and Gilman AG (1993) Purification from Sf9 cells and characterization of recombinant Gq alpha and G11 alpha. Activation of purified phospholipase C isozymes by G alpha subunits. *J Biol Chem* **268**(19):14367-14375.

Heyworth PG, Bohl BP, Bokoch GM and Curnutte JT (1994) Rac translocates independently of the neutrophil NADPH oxidase components p47phox and p67phox. Evidence for its interaction with flavocytochrome b558. *J Biol Chem* **269**(49):30749-30752.

Hilpela P, Vartiainen MK and Lappalainen P (2004) Regulation of the actin cytoskeleton by PI(4,5)P2 and PI(3,4,5)P3. *Curr Top Microbiol Immunol* **282**:117-163.

Hinchliffe KA (2001) Cellular signalling: stressing the importance of PIP3. *Curr Biol* **11**(9):R371-372.

Homma Y, Takenawa T, Emori Y, Sorimachi H and Suzuki K (1989) Tissue- and cell type-specific expression of mRNAs for four types of inositol phospholipid-specific phospholipase C. *BiochemBiophysResCommun* **164**:406-412.

Hubbard KB and Hepler JR (2006) Cell signalling diversity of the Gqalpha family of heterotrimeric G proteins. *Cell Signal* **18**(2):135-150.

Hwang J-I, Heo K, Shin K-J, Kim E, Yun C-HC, Ryu SH, Shin H-S and Suh P-G (2000) Regulation of Phospholipase C-beta 3 Activity by Na+/H+ Exchanger Regulatory Factor 2. *J Biol Chem* **275**(22):16632-16637.

Hwang JI, Kim HS, Lee JR, Kim E, Ryu SH and Suh PG (2005) The interaction of phospholipase C-beta3 with Shank2 regulates mGluR-mediated calcium signal. *J Biol Chem* **280**(13):12467-12473.

Ilkaeva O, Kinch LN, Paulssen RH and Ross EM (2002) Mutations in the carboxyl-terminal domain of phospholipase C-β1 delineate the dimer interface and a potential Galphaq interaction site. *J Biol Chem* **277**(6):4294-4300.

Illenberger D, Schwald F and Gierschik P (1997) Characterization and purification from bovine neutrophils of a soluble guanine-nucleotide-binding protein that mediates isozyme-specific stimulation of phospholipase C beta2. *Eur J Biochem* **246**(1):71-77.

Illenberger D, Schwald F, Pimmer D, Binder W, Maier G, Dietrich A and Gierschik P (1998) Stimulation of phospholipase C-beta2 by the Rho GTPases Cdc42Hs and Rac1. *Embo J* **17**(21):6241-6249.

Illenberger D, Walliser C, Nurnberg B, Diaz Lorente M and Gierschik P (2003a) Specificity and structural requirements of phospholipase C-beta stimulation by Rho GTPases versus G protein beta gamma dimers. *J Biol Chem* **278**(5):3006-3014.

Illenberger D, Walliser C, Strobel J, Gutman O, Niv H, Gaidzik V, Kloog Y, Gierschik P and Henis YI (2003b) Rac2 regulation of phospholipase C-beta 2 activity and mode of membrane interactions in intact cells. *J Biol Chem* **278**(10):8645-8652.

Ishii M, Inanobe A and Kurachi Y (2002) PIP_3 inhibition of RGS protein and its reversal by Ca^{2+}/calmodulin mediate voltage-dependent control of the G protein cycle in a cardiac K+ channel. *Proc Natl Acad Sci U S A* **99**(7):4325-4330.

Ishiki M and Klip A (2005) Minireview: recent developments in the regulation of glucose transporter-4 traffic: new signals, locations, and partners. *Endocrinology* **146**(12):5071-5078.

Jaffe AB and Hall A (2005) Rho GTPases: biochemistry and biology. *Annu Rev Cell Dev Biol* **21**:247-269.

James SR, Paterson A, Harden TK and Downes CP (1995) Kinetic analysis of phospholipase Cβ isoforms using phospholipid-detergent mixed micelles. *JBiolChem* **270**:11872-11881.

Janetopoulos C and Devreotes P (2006) Phosphoinositide signaling plays a key role in cytokinesis. *J Cell Biol* **174**(4):485-490.

Jenco JM, Becker KP and Morris AJ (1997) Membrane-binding properties of phospholipase C-beta1 and phospholipaseC-beta2: role of the C-terminus and effects of polyphosphoinositides, G-proteins and Ca2+. *Biochem J* **327 (Pt 2)**:431-437.

Jezyk MR, Snyder JT, Gershberg S, Worthylake DK, Harden TK and Sondek J (2006) Crystal structure of Rac1 bound to its effector phospholipase C-β2. *Nat Struct Mol Biol* **13**(12):1135-1140.

Jhon D, Lee H, Park D, Lee C, Lee K, Yoo O and Rhee S (1993a) Cloning, sequencing, purification, and Gq-dependent activation of phospholipase C-β3. *J Biol Chem* **268**(9):6654-6661.

Jhon DY, Lee HH, Park D, Lee CW, Lee KH, Yoo OJ and Rhee SG (1993b) Cloning, sequencing, purification, and Gq-dependent activation of phospholipase C-beta 3. *J Biol Chem* **268**(9):6654-6661.

Jiang H, Kuang Y, Wu Y, Smrcka A, Simon MI and Wu D (1996a) Pertussis toxin-sensitive activation of phospholipase C by the C5a and fMet-leu-phe receptors. *JBiolChem* **271**:13430-13434.

Jiang H, Kuang Y, Wu Y, Xie W, Simon MI and Wu D (1997) Roles of phospholipase C beta 2 in chemoattractant-elicited responses. *PNAS* **94**(15):7971-7975.

Jiang H, Lyubarsky A, Dodd R, Vardi N, Pugh E, Baylor D, Simon MI and Wu D (1996b) Phospholipase C beta 4 is involved in modulating the visual response in mice. *ProcNatlAcadSciUSA* **93**(25):14598-14601.

Jiang H, Wu D and Simon MI (1994) Activation of phospholipase C beta 4 by heterotrimeric GTP-binding proteins. *J Biol Chem* **269**(10):7593-7596.

Jones GA and Carpenter G (1993) The regulation of phospholipase C-y1 by phosphatidic acid. *JBiochem* **268**(October 5):20845-20850.

Kam Y and Exton JH (2002) Dimerization of phospholipase d isozymes. *Biochem Biophys Res Commun* **290**(1):375-380.

Kapust RB, Tözser J, Fox JD, Anderson DE, Cherry S, Copeland TD and Waugh DS (2001) Tobacco etch virus protease: mechanism of autolysis and rational design of stable mutants with wild-type catalytic proficiency. *Protein Eng* **14**(12):993-1000.

Karpova TS, Baumann CT, He L, Wu X, Grammer A, Lipsky P, Hager GL and McNally JG (2003) Fluorescence resonance energy transfer from cyan to yellow fluorescent protein detected by acceptor photobleaching using confocal microscopy and a single laser. *J Microsc* **209**(Pt 1):56-70.

Kashiwada M, Lu P and Rothman PB (2007) PIP3 pathway in regulatory T cells and autoimmunity. *Immunol Res* **39**(1-3):194-224.

Kelley GG, Kaproth-Joslin KA, Reks SE, Smrcka AV and Wojcikiewicz RJ (2006) G-protein-coupled receptor agonists activate endogenous phospholipase Cε and phospholipase Cβ3 in a temporally distinct manner. *J Biol Chem* **281**(5):2639-2648.

Kim CG, Park D and Rhee SG (1996a) The role of carboxyl-terminal basic amino acids in Gqalpha-dependent activation, particulate association, and nuclear localization of phospholipase C-beta1. *J Biol Chem* **271**(35):21187-21192.

Kim CG, Park D and Rhee SG (1996b) The role of the carboxyl terminal basic amino acids in Gqα-dependent activation, particulate association, and nuclear localization of phospholipase C-β1. *JBiolChem* **271**:21187-21192.

Kim D, Jun KS, Lee SB, kang N-G, Min DS, Kim Y-H, Ryu SH, Suh P-G and Shin H-S (1997a) Phospholipase C isozymes selectively couple to specific neurotransmitter receptors. *Nature* **389**:290293.

Kim D, Jun KS, Lee SB, Kang NG, Min DS, Kim YH, Ryu SH, Suh PG and Shin HS (1997b) Phospholipase C isozymes selectively couple to specific neurotransmitter receptors. *Nature* **389**(6648):290-293.

Kim MJ, Min DS, Ryu SH and Suh PG (1998) A cytosolic, galphaq- and betagamma-insensitive splice variant of phospholipase C-beta4. *J Biol Chem* **273**(6):3618-3624.

Kim YH, Song M, Oh YS, Heo K, Choi JW, Park JM, Kim SH, Lim S, Kwon HM, Ryu SH and Suh PG (2006) Inhibition of phospholipase C-beta1-mediated signaling by O-GlcNAc modification. *J Cell Physiol* **207**(3):689-696.

Klarlund JK, Guilherme A, Holik JJ, Virbasius JV, Chawla A and Czech MP (1997) Signaling by phosphoinositide-3,4,5-trisphosphate through proteins containing pleckstrin and Sec7 homology domains. *Science* **275**(5308):1927-1930.

Klarlund JK, Rameh LE, Cantley LC, Buxton JM, Holik JJ, Sakelis C, Patki V, Corvera S and Czech MP (1998) Regulation of GRP1-catalyzed ADP ribosylation factor guanine nucleotide exchange by phosphatidylinositol 3,4,5-trisphosphate. *J Biol Chem* **273**(4):1859-1862.

Klarlund JK, Tsiaras W, Holik JJ, Chawla A and Czech MP (2000) Distinct polyphosphoinositide binding selectivities for pleckstrin homology domains of GRP1-like proteins based on diglycine versus triglycine motifs. *J Biol Chem* **275**(42):32816-32821.

Kouchi Z, Shikano T, Nakamura Y, Shirakawa H, Fukami K and Miyazaki S (2005) The Role of EF-hand Domains and C2 Domain in Regulation of Enzymatic Activity of Phospholipase C{zeta}. *J Biol Chem* **280**(22):21015-21021.

Kozasa T (2004) Purification of G protein subunits from Sf9 insect cells using hexahistidine-tagged α and βγ subunits. *Methods Mol Biol* **237**:21-38.

Kozasa T, Hepler JR, Smrcka AV, Simon MI, Rhee SG, Sternweis PC and Gilman AG (1993) Purification and characterization of recombinant G16 alpha from Sf9 cells: activation of purified phospholipase C isozymes by G-protein alpha subunits. *Proc Natl Acad Sci U S A* **90**(19):9176-9180.

Ku CY, Qian A, Wen Y, Anwer K and Sanborn BM (1995) Oxytocin stimulates myometrial guanosine triphosphatase and phospholipase-C activities via coupling to G alpha q/11. *Endocrinology* **136**(4):1509-1515.

Kuang Y, Wu Y, Smrcka A, Jiang H and Wu D (1996) Identification of a phospholipase C-β2 region that interacts with Gβγ. *ProcNatlAcadSciUSA* **93**:2964-2968.

Kwon Y, Hofmann T and Montell C (2007) Integration of phosphoinositide- and calmodulin-mediated regulation of TRPC6. *Mol Cell* **25**(4):491-503.

Lanzafame AA, Turnbull L, Amiramahdi F, Arthur JF, Huynh H and Woodcock EA (2006) Inositol phospholipids localized to caveolae in rat heart are regulated by alpha1-adrenergic receptors and by ischemia-reperfusion. *Am J Physiol Heart Circ Physiol* **290**(5):H2059-2065.

Lee CH, Park D, Wu D, Rhee SG and Simon MI (1992) Members of the Gq alpha subunit gene family activate phospholipase C beta isozymes. *J Biol Chem* **267**(23):16044-16047.

Lee CW, Lee KH, Lee SB, Park D and Rhee SG (1994) Regulation of phospholipase C-beta 4 by ribonucleotides and the alpha subunit of Gq. *J Biol Chem* **269**(41):25335-25338.

Lee CW, Park DJ, Lee KH, Kim CG and Rhee SG (1993) Purification, molecular cloning, and sequencing of phospholipase C-beta 4. *JBiolChem* **268**(28):21318-21327.

Lee SB, Rao AK, Lee KH, Yang X, Bae YS and Rhee SG (1996) Decreased expression of phospholipase C-beta 2 isozyme in human platelets with impaired function. *Blood* **88**(5):1684-1691.

Lemmon MA (2007) Pleckstrin homology (PH) domains and phosphoinositides. *Biochem Soc Symp*(74):81-93.

Lemmon MA, Ferguson KM and Abrams CS (2002) Pleckstrin homology domains and the cytoskeleton. *FEBS Lett* **513**(1):71-76.

Letunic I, Copley RR, Pils B, Pinkert S, Schultz J and Bork P (2006) SMART 5: domains in the context of genomes and networks. *Nucleic Acids Res* **34**(Database issue):D257-260.

Li Z, Jiang H, Xie W, Zhang Z, Smrcka AV and Wu D (2000) Roles of PLC-beta2 and -beta3 and PI3Kgamma in chemoattractant-mediated signal transduction. *Science* **287**(5455):1046-1049.

Lian L, Wang Y, Draznin J, Eslin D, Bennett JS, Poncz M, Wu D and Abrams CS (2005) The relative role of PLC{beta} and PI3K{gamma} in platelet activation. *Blood* **106**(1):110-117.

Litosch I (2000) Regulation of phospholipase C-beta(1) activity by phosphatidic acid. *Biochemistry* **39**(26):7736-7743.

Litosch I (2002) Phosphatidic acid modulates G protein regulation of phospholipase C-beta1 activity in membranes. *Cell Signal* **14**(3):259-263.

Litosch I (2003) Regulation of phospholipase C-beta activity by phosphatidic acid: isoform dependence, role of protein kinase C, and G protein subunits. *Biochemistry* **42**(6):1618-1623.

Liu M and Simon MI (1996) Regulation by cAMP-dependent protein kinase of a G-protein-mediated phospholipase C. *Nature* **382**:83-87.

Liu NJ, Chakrabarti S and Gintzler AR (2004) Chronic morphine-induced loss of the facilitative interaction between vasoactive intestinal polypeptide and delta-opioid: involvement of protein kinase C and phospholipase Cbetas. *Brain Res* **1010**(1-2):1-9.

Lomasney JW, Cheng H-F, Roffler SR and King K (1999) Activation of Phospholipase C δ1 through C2 domain by a Ca^{2+}-enzyme-phosphatidylserine ternary complex. *JBiolChem* **274**:21995-22001.

Lukinovic-Skudar V, Donlagic L, Banfic H and Visnjic D (2005) Nuclear phospholipase C-beta1b activation during G2/M and late G1 phase in nocodazole-synchronized HL-60 cells. *Biochim Biophys Acta* **1733**(2-3):148-156.

Ma HW, Blitzer RD, Healy EC, Premont RT, Landau EM and Iyengar R (1993) Receptor-evoked Cl- current in Xenopus oocytes is mediated through a beta-

type phospholipase C. Cloning of a new form of the enzyme. *J Biol Chem* **268**(27):19915-19918.

Macia E, Paris S and Chabre M (2000) Binding of the PH and polybasic C-terminal domains of ARNO to phosphoinositides and to acidic lipids. *Biochemistry* **39**(19):5893-5901.

Mahon MJ, Donowitz M, Yun CC and Segre GV (2002) Na(+)/H(+) exchanger regulatory factor 2 directs parathyroid hormone 1 receptor signalling. *Nature* **417**(6891):858-861.

Mahon MJ and Segre GV (2004) Stimulation by Parathyroid Hormone of a NHERF-1-assembled Complex Consisting of the Parathyroid Hormone I Receptor, Phospholipase C{beta}, and Actin Increases Intracellular Calcium in Opossum Kidney Cells. *J Biol Chem* **279**(22):23550-23558.

Martelli AM, Billi AM, Manzoli L, Faenza I, Aluigi M, Falconi M, De Pol A, Gilmour RS and Cocco L (2000) Insulin selectively stimulates nuclear phosphoinositide-specific phospholipase C (PI-PLC) beta1 activity through a mitogen-activated protein (MAP) kinase-dependent serine phosphorylation. *FEBS Lett* **486**(3):230-236.

Martelli AM, Gilmour RS, Bertagnolo V, Neri LM, Manzoli L and Cocco L (1992) Nuclear localization and signalling activity of phosphoinositidase C beta in Swiss 3T3 cells. *Nature* **358**(6383):242-245.

McCullar JS, Larsen SA, Millimaki RA and Filtz TM (2003) Calmodulin Is a Phospholipase C-β Interacting Protein. *J Biol Chem* **278**(36):33708-33713.

McCullar JS, Malencik DA, Vogel WK, Crofoot KM, Anderson SR and Filtz TM (2007) Calmodulin potentiates Gβγ activation of phospholipase C-β3. *Biochem Pharmacol* **73**(2):270-278.

Milligan G (2004) G protein-coupled receptor dimerization: function and ligand pharmacology. *Mol Pharmacol* **66**(1):1-7.

Moriyama T, Narita H, Oki M, Matsuura T and Kito M (1990) Purification of polymeric phospholipase Cs from human platelets. *J Biochem (Tokyo)* **108**(3):414-419.

Morris AJ, Waldo GL, Downes CP and Harden TK (1990a) A receptor and G-protein-regulated polyphosphoinositide-specific phospholipase C from turkey erythrocytes. I. Purification and properties. *J Biol Chem* **265**(23):13501-13507.

Morris AJ, Waldo GL, Downes CP and Harden TK (1990b) A receptor and G-protein-regulated polyphosphoinositide-specific phospholipase C from turkey erythrocytes. II. P2Y-purinergic receptor and G-protein-mediated regulation of the purified enzyme reconstituted with turkey erythrocyte ghosts. *J Biol Chem* **265**(23):13508-13514.

Murthy KS, Coy DH and Makhlouf GM (1996) Somatostatin receptor-mediated signaling in smooth muscle. Activation of phospholipase C-beta3 by Gbetagamma and inhibition of adenylyl cyclase by Galphai1 and Galphao. *J Biol Chem* **271**(38):23458-23463.

Murthy KS and Makhlouf GM (1995a) Adenosine A1 receptor-mediated activation of phospholipase C-β3 in intestinal muscle: dual requirement for alpha and beta gamma subunits of Gi3. *Mol Pharmacol* **47**(6):1172-1179.

Murthy KS and Makhlouf GM (1995b) Functional characterization of phosphoinositide-specific phospholipase C-β1 and -β3 in intestinal smooth muscle. *Am J Physiol* **269**(4 Pt 1):C969-978.

Murthy KS and Makhlouf GM (1995c) Functional characterization of phosphoinositide-specific phospholipase C-β1 and -β3 in intestinal smooth muscle. *Am J Physiol* **269**(4 Pt 1):C969-978.

Murthy KS and Makhlouf GM (1996) Opioid mu, delta, and kappa receptor-induced activation of phospholipase C-beta 3 and inhibition of adenylyl cyclase is mediated by Gi2 and G(o) in smooth muscle. *Mol Pharmacol* **50**(4):870-877.

Naito Y, Okada M and Yagisawa H (2006) Phospholipase C Isoforms Are Localized at the Cleavage Furrow during Cytokinesis. *J Biochem (Tokyo)* **140**(6):785-791.

Nakamura M, Sato K, Fukaya M, Araishi K, Aiba A, Kano M and Watanabe M (2004) Signaling complex formation of phospholipase Cbeta4 with metabotropic glutamate receptor type 1alpha and 1,4,5-trisphosphate receptor at the perisynapse and endoplasmic reticulum in the mouse brain. *Eur J Neurosci* **20**(11):2929-2944.

Nakanishi S, Kakita S, Takahashi I, Kawahara K, Tsukuda E, Sano T, Yamada K, Yoshida M, Kase H, Matsuda Y and et al. (1992) Wortmannin, a microbial product inhibitor of myosin light chain kinase. *J Biol Chem* **267**(4):2157-2163.

Nakashima S, Banno Y, Watanabe T, Nakamura Y, Mizutani T, Sakai H, Zhao Y, Sugimoto Y and Nozawa Y (1995) Deletion and site-directed mutagenesis of EF-hand domain of phospholipase C-delta 1: effects on its activity. *Biochem Biophys Res Commun* **211**(2):365-369.

Nalefski EA and Falke JJ (1996) The C2 domain calcium-binding motif: structural and functional diversity. *ProtScience* **5**:2375-2390.

Nomikos M, Blayney LM, Larman MG, Campbell K, Rossbach A, Saunders CM, Swann K and Lai FA (2005) Role of phospholipase C-zeta domains in Ca2+-dependent phosphatidylinositol 4,5-bisphosphate hydrolysis and cytoplasmic Ca2+ oscillations. *J Biol Chem* **280**(35):31011-31018.

Northcott CA, Hayflick J and Watts SW (2005) Upregulated function of phosphatidylinositol-3-kinase in genetically hypertensive rats: a moderator of arterial hypercontractility. *Clin Exp Pharmacol Physiol* **32**(10):851-858.

Oh YS, Jo NW, Choi JW, Kim HS, Seo SW, Kang KO, Hwang JI, Heo K, Kim SH, Kim YH, Kim IH, Kim JH, Banno Y, Ryu SH and Suh PG (2004) NHERF2 specifically interacts with LPA2 receptor and defines the specificity and efficiency of receptor-mediated phospholipase C-beta3 activation. *Mol Cell Biol* **24**(11):5069-5079.

Oikawa T, Yamaguchi H, Itoh T, Kato M, Ijuin T, Yamazaki D, Suetsugu S and Takenawa T (2004) PtdIns(3,4,5)P3 binding is necessary for WAVE2-induced formation of lamellipodia. *Nat Cell Biol* **6**(5):420-426.

Pandey GN, Dwivedi Y, Pandey SC, Teas SS, Conley RR, Roberts RC and Tamminga CA (1999) Low phosphoinositide-specific phospholipase C activity and expression of phospholipase C beta1 protein in the prefrontal cortex of teenage suicide subjects. *Am J Psychiatry* **156**(12):1895-1901.

Park D, Jhon D-Y, Kriz R, Knopf J and Rhee SG (1992a) Cloning, sequencing, expression, and G_q-independent activation of phospholipase C-β2. *JBiolChem* **267**:16048-16055.

Park D, Jhon D-Y, Lee C-W, Lee K-H and Rhee SG (1993a) Activation of phospholipase C isozymes by G protein βγ subunits. *JBiolChem* **268**:4573-4576.

Park D, Jhon DY, Kriz R, Knopf J and Rhee SG (1992b) Cloning, sequencing, expression, and Gq-independent activation of phospholipase C-beta 2. *J Biol Chem* **267**(23):16048-16055.

Park D, Jhon DY, Lee CW, Ryu SH and Rhee SG (1993b) Removal of the carboxyl-terminal region of phospholipase C-beta 1 by calpain abolishes activation by G alpha q. *J Biol Chem* **268**(5):3710-3714.

Park SU, Shin CY, Ryu JS, La HO, Park SY, Song HJ, Min YS, Kim DS and Sohn UD (2006) Signal transduction of bombesin-induced circular smooth muscle cell contraction in cat esophagus. *World J Gastroenterol* **12**(14):2259-2263.

Paterson A, Boyer JL, Watts VJ, Morris AJ, Price EM and Harden TK (1995) Concentration of enzyme-dependent activation of PLC-β1 and PLC-β2 by $G\alpha_{11}$ and βg subunits. *CellSignaling* **7**:709-720.

Paterson A, Filtz TM and Harden TK (1997) Baculovirus-promoted expression, purification and functional assay of G-protein regulated PLC-β isoenzymes, in *Signaling by Inositol Lipids and Inositol Phosphates* (Shears S ed) pp 85-98, Oxford University Press.

Patterson GH, Piston DW and Barisas BG (2000) Forster distances between green fluorescent protein pairs. *Anal Biochem* **284**(2):438-440.

Paulssen RH, Woodson J, Liu Z and Ross EM (1996) Carboxyl-terminal fragments of phospholipase C-beta1 with intrinsic Gq GTPase-activating protein (GAP) activity. *J Biol Chem* **271**(43):26622-26629.

Peruzzi D, Aluigi M, Manzoli L, Billi AM, Di Giorgio FP, Morleo M, Martelli AM and Cocco L (2002) Molecular characterization of the human PLC beta1 gene. *Biochim Biophys Acta* **1584**(1):46-54.

Pochynyuk O, Tong Q, Staruschenko A and Stockand JD (2007) Binding and direct activation of the epithelial Na+ channel (ENaC) by phosphatidylinositides. *J Physiol* **580**(Pt. 2):365-372.

Popov SG, Krishna UM, Falck JR and Wilkie TM (2000a) Ca2+/Calmodulin reverses phosphatidylinositol 3,4, 5-trisphosphate-dependent inhibition of

regulators of G protein-signaling GTPase-activating protein activity. *J Biol Chem* **275**(25):18962-18968.

Popov SG, Krishna UM, Falck JR and Wilkie TR (2000b) Ca^{2+}/Calmodulin reverses phosphatidylinositol 3,4,5-triphosphate-dependent inhibition of regulators of G protein-signaling GTPase-activating protein activity. *JBiolChem* **275**(25):18962-18968.

Popova JS, Garrison JC, Rhee SG and Rasenick MM (1997) Tubulin, Gq, and phosphatidylinositol 4,5-bisphosphate interact to regulate phospholipase Cbeta1 signaling. *JBiolChem* **272**(10):6760-6765.

Popova JS, Greene AK, Wang J and Rasenick MM (2002) Phosphatidylinositol 4,5-bisphosphate modifies tubulin participation in phospholipase Cbeta1 signaling. *J Neurosci* **22**(5):1668-1678.

Popova JS and Rasenick MM (2000) Muscarinic Receptor Activation Promotes the Membrane Association of Tubulin for the Regulation of Gq-Mediated Phospholipase Cbeta 1 Signaling. *J Neurosci* **20**(8):2774-2782.

Popova JS and Rasenick MM (2003) G beta gamma mediates the interplay between tubulin dimers and microtubules in the modulation of Gq signaling. *J Biol Chem* **278**(36):34299-34308.

Rameh LE and Cantley LC (1999a) The role of phosphoinositide 3-kinase lipid products in cell function. *J Biol Chem* **274**(13):8347-8350.

Rameh LE and Cantley LC (1999b) The role of phosphoinositide 3-kinase lipid products in cell function. *Biological Chemistry* **274**:8347-8350.

Razzini G, Brancaccio A, Lemmon MA, Guarnieri S and Falasca M (2000) The role of the pleckstrin homology domain in membrane targeting and activation of phospholipase Cbeta(1). *J Biol Chem* **275**(20):14873-14881.

Rhee S-G (2001) Regulation of phosphoinositide-specific phospholipase C. *AnnuRevBiochem* **70**:281-312.

Roberts MF, Deems RA and Dennis EA (1977) Dual role of interfacial phospholipid in phospholipase A2 catalysis. *Proc Natl Acad Sci U S A* **74**(5):1950-1954.

Ross EM, Mateu D, Gomes AV, Arana C, Tran T and Litosch I (2006) Structural determinants for phosphatidic acid regulation of phospholipase C-beta1. *J Biol Chem* **281**(44):33087-33094.

Rossler P, Kroner C, Freitag J, Noe J and Breer H (1998) Identification of a phospholipase C beta subtype in rat taste cells. *Eur J Cell Biol* **77**(3):253-261.

Runnels LW, Jenco J, Morris A and Scarlata S (1996) Membrane binding of phospholipases C-beta 1 and C-beta 2 is independent of phosphatidylinositol 4,5-bisphosphate and the alpha and beta gamma subunits of G proteins. *Biochemistry* **35**(51):16824-16832.

Runnels LW and Scarlata SF (1999) Determination of the affinities between heterotrimeric G protein subunits and their phospholipase C-beta effectors. *JBiochem* **38**:1488-1496.

Ryu SH, Cho KS, Lee KY, Suh PG and Rhee SG (1986) Two forms of phosphatidylinositol-specific phospholipase C from bovine brain. *Biochem Biophys Res Commun* **141**(1):137-144.

Ryu SH, Suh PG, Cho KS, Lee KY and Rhee SG (1987) Bovine brain cytosol contains three immunologically distinct forms of inositolphospholipid-specific phospholipase C. *Proc Natl Acad Sci U S A* **84**(19):6649-6653.

Saito K, Scharenberg AM and Kinet JP (2001) Interaction between the Btk PH domain and phosphatidylinositol-3,4,5-trisphosphate directly regulates Btk. *J Biol Chem* **276**(19):16201-16206.

Salim K, Bottomley MJ, Querfurth E, Zvelebil MJ, Gout I, Scaife R, Margolis RL, Gigg R, Smith CI, Driscoll PC, Waterfield MD and Panayotou G (1996) Distinct specificity in the recognition of phosphoinositides by the pleckstrin homology domains of dynamin and Bruton's tyrosine kinase. *Embo J* **15**(22):6241-6250.

Sankaran B, Osterhout J, Wu D and Smrcka AV (1998) Identification of a structural element in phospholipase C-β2 that interacts with G protein βγ subunits. *JBiolChem* **273**:7148-7154.

Saunders CM, Larman MG, Parrington J, Cox LJ, Royse J, Blayney LM, Swann K and Lai FA (2002) PLC zeta: a sperm-specific trigger of Ca(2+) oscillations in eggs and embryo development. *Development* **129**(15):3533-3544.

Schelling JR, Nkemere N, Konieczkowski M, Martin KA and Dubyak GR (1997) Angiotensin II activates the beta 1 isoform of phospholipase C in vascular smooth muscle cells. *Am J Physiol* **272**(5 Pt 1):C1558-1566.

Schnabel P and Camps M (1998) Activation of a phospholipase Cbeta2 deletion mutant by limited proteolysis. *Biochem J* **330 (Pt 1)**:461-468.

Schnabel P, Camps M, Carozzi A, Parker PJ and Gierschik P (1993) Mutational analysis of phospholipase C-β_2: Identification of regions required for membrane association and stimulation by guanine-nucleotide-binding protein $\beta\gamma$ subunits. *EurJBiochem* **217**:1109-1115.

Serunian LA, Haber MT, Fukui T, Kim JW, Rhee SG, Lowenstein JM and Cantley LC (1989) Polyphosphoinositides produced by phosphatidylinositol 3-kinase are poor substrates for phospholipases C from rat liver and bovine brain. *J Biol Chem* **264**(30):17809-17815.

Shao C, Shi X, Wehbi H, Zambonelli C, Head JF, Seaton BA and Roberts MF (2007) Dimer structure of an interfacially impaired phosphatidylinositol-specific phospholipase C. *J Biol Chem* **282**(12):9228-9235.

Shim JO, Shin CY, Lee TS, Yang SJ, An JY, Song HJ, Kim TH, Huh IH and Sohn UD (2002) Signal transduction mechanism via adenosine A1 receptor in the cat esophageal smooth muscle cells. *Cell Signal* **14**(4):365-372.

Shin CY, Lee YP, Lee TS, Je HD, Kim DS and Sohn UD (2002) The signal transduction of endothelin-1-induced circular smooth muscle cell contraction in cat esophagus. *J Pharmacol Exp Ther* **302**(3):924-934.

Shin DM, Dehoff M, Luo X, Kang SH, Tu J, Nayak SK, Ross EM, Worley PF and Muallem S (2003) Homer 2 tunes G protein-coupled receptors stimulus intensity by regulating RGS proteins and PLCbeta GAP activities. *J Cell Biol* **162**(2):293-303.

Shortridge RD, Yoon J, Lending CR, Bloomquist BT, Perdew MH and Pak WL (1991) A Drosophila phospholipase C gene that is expressed in the central nervous system. *J Biol Chem* **266**(19):12474-12480.

Sidhu RS, Clough RR and Bhullar RP (2005) Regulation of Phospholipase C-{delta}1 through Direct Interactions with the Small GTPase Ral and Calmodulin. *J Biol Chem* **280**(23):21933-21941.

Siegel LM and Monty KJ (1966) Determination of molecular weights and frictional ratios of proteins in impure systems by use of gel filtration and density gradient centrifugation. Application to crude preparations of sulfite and hydroxylamine reductases. *Biochim Biophys Acta* **112**(2):346-362.

Singer AU, Waldo GL, Harden TK and Sondek J (2002) A unique fold of phospholipase C-β mediates dimerization and interaction with Gαq. *Nat Struct Biol* **9**(1):32-36.

Singh SM and Murray D (2003) Molecular modeling of the membrane targeting of phospholipase C pleckstrin homology domains. *Protein Sci* **12**(9):1934-1953.

Smrcka AV and Sternweis PC (1993) Regulation of purified subtypes of phosphatidylinositol-specific phospholipase C beta by G protein alpha and beta gamma subunits. *J Biol Chem* **268**(13):9667-9674.

Snyder JT, Singer AU, Wing MR, Harden TK and Sondek J (2003) The pleckstrin homology domain of phospholipase C-beta2 as an effector site for Rac. *J Biol Chem* **278**(23):21099-21104.

Stace CL and Ktistakis NT (2006) Phosphatidic acid- and phosphatidylserine-binding proteins. *Biochim Biophys Acta* **1761**(8):913-926.

Stålberg P, Wang S, Larsson C, Weber G, Öberg K, Gobl A and Skogseid B (1999) Suppression of the neoplastic phenotype by transfection of phospholipase C ? 3 to neuroendocrine tumor cells. *FEBS Letters* **450**(3):210-216.

Stephens L, Anderson K, Stokoe D, Erdjument-Bromage H, Painter GF, Holmes AB, Gaffney PR, Reese CB, McCormick F, Tempst P, Coadwell J and Hawkins PT (1998) Protein kinase B kinases that mediate phosphatidylinositol 3,4,5-trisphosphate-dependent activation of protein kinase B. *Science* **279**(5351):710-714.

Strassheim D, Law PY and Loh HH (1998) Contribution of phospholipase C-beta3 phosphorylation to the rapid attenuation of opioid-activated phosphoinositide response. *MolPharmacol* **53**(6):1047-1053.

Strassheim D and Williams CL (2000) P2Y2 Purinergic and M3 Muscarinic Acetylcholine Receptors Activate Different Phospholipase C-beta Isoforms That Are Uniquely Susceptible to Protein Kinase C-dependent Phosphorylation and Inactivation. *J Biol Chem* **275**(50):39767-39772.

Su X, Smolock EM, Marcel KN and Moreland RS (2004) Phosphatidylinositol 3-kinase modulates vascular smooth muscle contraction by calcium and myosin light chain phosphorylation-independent and -dependent pathways. *Am J Physiol Heart Circ Physiol* **286**(2):H657-666.

Suh P-G, Ryu SH, Moon KH, Suh W and Rhee SG (1988) Cloning and sequence of multiple forms of phospholipase C. *Cell* **54**:161-169.

Tall E, Dorman G, Garcia P, Runnels L, Shah S, Chen J, Profit A, Gu QM, Chaudhary A, Prestwich GD and Rebecchi MJ (1997) Phosphoinositide binding specificity among phospholipase C isozymes as determined by photo-cross-linking to novel substrate and product analogs. *Biochemistry* **36**(23):7239-7248.

Tang W, Tu Y, Nayak SK, Woodson J, Jehl M and Ross EM (2006) Gbetagamma inhibits Galpha GTPase-activating proteins by inhibition of Galpha-GTP binding during stimulation by receptor. *J Biol Chem* **281**(8):4746-4753.

Tang Y, Tang J, Chen Z, Trost C, Flockerzi V, Li M, Ramesh V and Zhu MX (2000) Association of Mammalian Trp4 and Phospholipase C Isozymes with a PDZ Domain-containing Protein, NHERF. *J Biol Chem* **275**(48):37559-37564.

Tappia PS, Yu CH, Di Nardo P, Pasricha AK, Dhalla NS and Panagia V (2001) Depressed responsiveness of phospholipase C isoenzymes to phosphatidic acid in congestive heart failure. *J Mol Cell Cardiol* **33**(3):431-440.

Tolloczko B, Turkewitsch P, Al-Chalabi M and Martin JG (2004) LY-294002 [2-(4-morpholinyl)-8-phenyl-4H-1-benzopyran-4-one] affects calcium signaling in airway smooth muscle cells independently of phosphoinositide 3-kinase inhibition. *J Pharmacol Exp Ther* **311**(2):787-793.

Tsunoda S, Sierralta J, Sun Y, Bodner R, Suzuki E, Becker A, Socolich M and Zuker CS (1997) A multivalent PDZ-domain protein assembles signalling complexes in a G- protein-coupled cascade. *Nature* **388**(6639):243-249.

Ushio-Fukai M, Griendling KK, Akers M, Lyons PR and Alexander RW (1998) Temporal dispersion of activation of phospholipase C-beta1 and -gamma isoforms by angiotensin II in vascular smooth muscle cells. Role of alphaq/11, alpha12, and beta gamma G protein subunits. *JBiolChem* **273**(31):19772-19777.

van Huizen R, Miller K, Chen DM, Li Y, Lai ZC, Raab RW, Stark WS, Shortridge RD and Li M (1998) Two distantly positioned PDZ domains mediate multivalent INAD-phospholipase C interactions essential for G protein-coupled signaling. *Embo J* **17**(8):2285-2297.

Varnai P, Rother KI and Balla T (1999) Phosphatidylinositol 3-kinase-dependent membrane association of the Bruton's tyrosine kinase pleckstrin homology domain visualized in single living cells. *J Biol Chem* **274**(16):10983-10989.

Venkateswarlu K, Oatey PB, Tavare JM and Cullen PJ (1998) Insulin-dependent translocation of ARNO to the plasma membrane of adipocytes requires phosphatidylinositol 3-kinase. *Curr Biol* **8**(8):463-466.

Vlahos CJ, Matter WF, Brown RF, Traynor-Kaplan AE, Heyworth PG, Prossnitz ER, Ye RD, Marder P, Schelm JA, Rothfuss KJ and et al. (1995) Investigation of neutrophil signal transduction using a specific inhibitor of phosphatidylinositol 3-kinase. *J Immunol* **154**(5):2413-2422.

Vlahos CJ, Matter WF, Hui KY and Brown RF (1994) A specific inhibitor of phosphatidylinositol 3-kinase, 2-(4-morpholinyl)-8-phenyl-4H-1-benzopyran-4-one (LY294002). *J Biol Chem* **269**(7):5241-5248.

Walker MB, Miller CT, Swartz ME, Eberhart JK and Kimmel CB (2007) phospholipase C, beta 3 is required for Endothelin1 regulation of pharyngeal arch patterning in zebrafish. *Dev Biol* **304**(1):194-207.

Wang L-P, Lim C, Kuan Y-S, Chen C-L, Chen H-F and King K (1996) Positive Charge at Position 549Is Essential for Phosphatidylinositol 4,5-Bisphosphate-hydrolyzing but Not Phosphatidylinositol-hydrolyzing Activities of Human Phospholipase C delta 1. *J Biol Chem* **271**(40):24505-24516.

Wang T, Dowal L, El-Maghrabi MR, Rebecchi M and Scarlata S (2000) The pleckstrin homology domain of phospholipase C-beta(2) links the binding of gbetagamma to activation of the catalytic core. *J Biol Chem* **275**(11):7466-7469.

Wang T, Pentyala S, Elliott JT, Dowal L, Gupta E, Rebecchi MJ and Scarlata S (1999a) Selective interaction of the C2 domains of phospholipase C-beta1 and -beta2 with activated Galphaq subunits: an alternative function for C2-signaling modules. *Proc Natl Acad Sci U S A* **96**(14):7843-7846.

Wang T, Pentyala S, Rebecchi MJ and Scarlata S (1999b) Differential association of the pleckstrin homology domains of phospholipases C-β1, C-β2, and C-δ1 with lipid bilayers and the βγ subunits of heterotrimeric G proteins. *Biochemistry* **38**:1517-1524.

Wang T, Pentyala S, Rebecchi MJ and Scarlata S (1999c) Differential association of the pleckstrin homology domains of phospholipases C-beta 1, C-beta 2, and C-delta 1 with lipid bilayers and the beta gamma subunits of heterotrimeric G proteins. *Biochemistry* **38**(5):1517-1524.

Weber G, Friedman E, Grimmond S, Hayward NK, Phelan C, Skogseid B, Gobl A, Zedenius J, Sandelin K, Teh BT and et al. (1994) The phospholipase C beta 3 gene located in the MEN1 region shows loss of expression in endocrine tumours. *Hum Mol Genet* **3**(10):1775-1781.

Wojcikiewicz RJH, Tobin AB and Nahorski SR (1994) Muscarinic receptor-mediated inositol 1,4,5-trisphosphate formation in SH-SY5Y neuroblastoma cells is regulated acutely by cytosolic Ca^{2+} and by rapid desensitization. *JNeurochem* **63**(1):177-185.

Wong R, Fabian L, Forer A and Brill JA (2007) Phospholipase C and myosin light chain kinase inhibition define a common step in actin regulation during cytokinesis. *BMC Cell Biol* **8**:15.

Wu D, Jiang H, Katz A and Simon MI (1993a) Identification of critical regions on phospholipase C-beta 1 required for activation by G-proteins. *J Biol Chem* **268**(5):3704-3709.

Wu DW, Jiang H, Katz A and Simon MI (1993b) Identification of critical regions on phospholipase C-β1 required for activation by G-proteins. *JBiolChem* **268**:3704-3709.

Xia C, Bao Z, Yue C, Sanborn BM and Liu M (2001) Phosphorylation and Regulation of G-protein-activated Phospholipase C-beta 3 by cGMP-dependent Protein Kinases. *J Biol Chem* **276**(23):19770-19777.

Xie W, Samoriski GM, McLaughlin JP, Romoser VA, Smrcka A, Hinkle PM, Bidlack JM, Gross RA, Jiang H and Wu D (1999) Genetic alteration of phospholipase C beta 3 expression modulates behavioral and cellular responses to {micro} opioids. *PNAS* **96**(18):10385-10390.

Xie Z, Singleton PA, Bourguignon LY and Bikle DD (2005) Calcium-induced human keratinocyte differentiation requires src- and fyn-mediated phosphatidylinositol 3-kinase-dependent activation of phospholipase C-γ1. *Mol Biol Cell* **16**(7):3236-3246.

Xu A, Suh PG, Marmy-Conus N, Pearson RB, Seok OY, Cocco L and Gilmour RS (2001a) Phosphorylation of nuclear phospholipase C beta1 by extracellular signal-regulated kinase mediates the mitogenic action of insulin-like growth factor I. *Mol Cell Biol* **21**(9):2981-2990.

Xu A, Wang Y, Xu LY and Gilmour RS (2001b) Protein kinase C alpha -mediated negative feedback regulation is responsible for the termination of insulin-like growth factor I-induced activation of nuclear phospholipase C beta1 in Swiss 3T3 cells. *J Biol Chem* **276**(18):14980-14986.

Yamamoto T, Takeuchi H, Kanematsu T, Allen V, Yagisawa H, Kikkawa U, Watanabe Y, Nakasima A, Katan M and Hirata M (1999) Involvement of EF hand motifs in the Ca(2+)-dependent binding of the pleckstrin homology domain to phosphoinositides. *Eur J Biochem* **265**(1):481-490.

Yoko-o T, Matsui Y, Yagisawa H, Nojima H, Uno I and Toh-e A (1993) The putative phosphoinositide-specific phospholipase C gene, PLC1, of the yeast Saccharomyces cerevisiae is important for cell growth. *Proc Natl Acad Sci U S A* **90**(5):1804-1808.

Young KW, Nash MS, Challiss RA and Nahorski SR (2003) Role of Ca2+ feedback on single cell inositol 1,4,5-trisphosphate oscillations mediated by G-protein-coupled receptors. *J Biol Chem* **278**(23):20753-20760.

Yu JW, Mendrola JM, Audhya A, Singh S, Keleti D, DeWald DB, Murray D, Emr SD and Lemmon MA (2004) Genome-wide analysis of membrane targeting by S. cerevisiae pleckstrin homology domains. *Mol Cell* **13**(5):677-688.

Yue C, Dodge KL, Weber G and Sanborn BM (1998) Phosphorylation of serine 1105 by protein kinase A inhibits phospholipase Cbeta3 stimulation by Galphaq. *JBiolChem* **273**(29):18023-18027.

Yue C, Ku CY, Liu M, Simon MI and Sanborn BM (2000) Molecular mechanism of the inhibition of phospholipase C beta 3 by protein kinase C. *J Biol Chem* **275**(39):30220-30225.

Yue C and Sanborn BM (2001) KN-93 inhibition of G protein signaling is independent of the ability of Ca2+/calmodulin-dependent protein kinase II to phosphorylate phospholipase Cbeta3 on 537-Ser. *Mol Cell Endocrinol* **175**(1-2):149-156.

Zhang W and Neer EJ (2001) Reassembly of phospholipase C-beta2 from separated domains: analysis of basal and G protein-stimulated activities. *J Biol Chem* **276**(4):2503-2508.

Zhang X, Wehbi H and Roberts MF (2004) Cross-linking phosphatidylinositol-specific phospholipase C traps two activating phosphatidylcholine molecules on the enzyme. *J Biol Chem* **279**(19):20490-20500.

Zhang Y, Hoon MA, Chandrashekar J, Mueller KL, Cook B, Wu D, Zuker CS and Ryba NJ (2003) Coding of sweet, bitter, and umami tastes: different receptor cells sharing similar signaling pathways. *Cell* **112**(3):293-301.

Zhang Y, Vogel WK, McCullar JS, Greenwood JA and Filtz TM (2006) Phospholipase C-β3 and -β1 form homodimers, but not heterodimers, through catalytic and carboxyl-terminal domains. *Mol Pharmacol* **70**(3):860-868.

Zhong M, Yang M and Sanborn BM (2003) Extracellular Signal-Regulated Kinase 1/2 Activation by Myometrial Oxytocin Receptor Involves GαqGβγ and Epidermal Growth Factor Receptor Tyrosine Kinase Activation. *Endocrinology* **144**(7):2947-2956.